National Library
of Canada

Acquisitions and
Bibliographic Services Branch

395 Wellington Street
Ottawa, Ontario
K1A 0N4

Bibliothèque nationale
du Canada

Direction des acquisitions et
des services bibliographiques

395, rue Wellington
Ottawa (Ontario)
K1A 0N4

Your file Votre référence

Our file Notre référence

NOTICE

The quality of this microform is heavily dependent upon the quality of the original thesis submitted for microfilming. Every effort has been made to ensure the highest quality of reproduction possible.

If pages are missing, contact the university which granted the degree.

Some pages may have indistinct print especially if the original pages were typed with a poor typewriter ribbon or if the university sent us an inferior photocopy.

Reproduction in full or in part of this microform is governed by the Canadian Copyright Act, R.S.C. 1970, c. C-30, and subsequent amendments.

AVIS

La qualité de cette microforme dépend grandement de la qualité de la thèse soumise au microfilmage. Nous avons tout fait pour assurer une qualité supérieure de reproduction.

S'il manque des pages, veuillez communiquer avec l'université qui a conféré le grade.

La qualité d'impression de certaines pages peut laisser à désirer, surtout si les pages originales ont été dactylographiées à l'aide d'un ruban usé ou si l'université nous a fait parvenir une photocopie de qualité inférieure.

La reproduction, même partielle, de cette microforme est soumise à la Loi canadienne sur le droit d'auteur, SRC 1970, c. C-30, et ses amendements subséquents.

Canada

UNIVERSITY OF ALBERTA

HYDROLOGY, SALINITY AND ENVIRONMENT OF ANCIENT WATER MASSES DETERMINED BY C, O, Sr AND Nd ISOTOPES IN CARBONATES, PHOSPHATES AND SILICATES

BY CHRIS HOLMDEN ©

A thesis submitted to the faculty of Graduate Studies and Research in partial fulfilment of the requirements for the degree of Doctor of Philosophy

Department of Earth and Atmospheric Sciences
Edmonton, Alberta
Fall 1995

National Library of Canada
Acquisitions and Bibliographic Services Branch
395 Wellington Street
Ottawa, Ontario
K1A 0N4

Bibliothèque nationale du Canada
Direction des acquisitions et des services bibliographiques
395, rue Wellington
Ottawa (Ontario)
K1A 0N4

Your file Votre référence

Our file Notre référence

THE AUTHOR HAS GRANTED AN IRREVOCABLE NON-EXCLUSIVE LICENCE ALLOWING THE NATIONAL LIBRARY OF CANADA TO REPRODUCE, LOAN, DISTRIBUTE OR SELL COPIES OF HIS/HER THESIS BY ANY MEANS AND IN ANY FORM OR FORMAT, MAKING THIS THESIS AVAILABLE TO INTERESTED PERSONS.

L'AUTEUR A ACCORDE UNE LICENCE IRREVOCABLE ET NON EXCLUSIVE PERMETTANT A LA BIBLIOTHEQUE NATIONALE DU CANADA DE REPRODUIRE, PRETER, DISTRIBUER OU VENDRE DES COPIES DE SA THESE DE QUELQUE MANIERE ET SOUS QUELQUE FORME QUE CE SOIT POUR METTRE DES EXEMPLAIRES DE CETTE THESE A LA DISPOSITION DES PERSONNE INTERESSEES.

THE AUTHOR RETAINS OWNERSHIP OF THE COPYRIGHT IN HIS/HER THESIS. NEITHER THE THESIS NOR SUBSTANTIAL EXTRACTS FROM IT MAY BE PRINTED OR OTHERWISE REPRODUCED WITHOUT HIS/HER PERMISSION.

L'AUTEUR CONSERVE LA PROPRIETE DU DROIT D'AUTEUR QUI PROTEGE SA THESE. NI LA THESE NI DES EXTRAITS SUBSTANTIELS DE CELLE-CI NE DOIVENT ETRE IMPRIMES OU AUTREMENT REPRODUITS SANS SON AUTORISATION.

ISBN 0-612-06227-9

Canada

UNIVERSITY OF ALBERTA

LIBRARY RELEASE FORM

NAME OF AUTHOR: Christopher Eric Holmden

TITILE OF THESIS: Hydrology, Salinity and Environment of Ancient Water Masses Determined by C O, Sr and Nd Isotopes in Carbonates, Phosphates and Silicates

DEGREE: Doctor of Philosophy

YEAR THIS DEGREE GRANTED: 1995

Permission is hereby granted to the University of Alberta Library to reproduce single copies of this thesis and to lend or sell such copies for private, scholarly, or scientific research purposes only.

The author reserves all other publication and other rights in association with the copyright in the thesis, and except as hereinbefore provided, neither the thesis nor any substantial portion thereof may be printed or otherwise reproduced in any material form whatever without the author's prior written permission.

Chris Holmden

Chris Holmden
10950-82 Ave. #309
Edmonton, Alberta
T6G 2R9

Date: Oct 6/95

University of Alberta

Faculty of Graduate Studies and Research

The undersigned certify that they have read, and recommend to the Faculty of Graduate Studies and Research for acceptance, a thesis entitled Hydrology , Salinity and Environment of Ancient Water Masses Determined by C, O, Sr and Nd Isotopes in Carbonates, Phosphates and Silicates by Christopher Eric Holmden in partial fulfillment of the requirements for the degree of Doctor of Philosophy.

K. Muehlenbachs (supervisor)

R. A. Creaser (co-supervisor)

B. D. E. Chatterton

Marvin J. Dudas
M. J. Dudas

Stein B. Jacobsen
S. B. Jacobsen (external)

Date Oct 6/95

ABSTRACT

Radiogenic isotopes (Nd, Sr) and stable isotopes (O, C) are combined to elucidate isotopic compositions, paleoenvironments and paleosalinities of ancient water masses. Isotopic differences between deep oceans and shallow epeiric seas are demonstrated using Nd isotopes in conodonts and C isotopes in limestones sampled proximal to the regionally correlated (454 Ma) Millbrig and Deicke K-bentonites. Evidence that the chemistry of the Mohawkian epeiric sea varied both internally ($\varepsilon_{Nd} = -2$ to -19 : $\delta^{13}C = -2.4$ to $+2.4$) and with respect to the adjacent Iapetus Ocean ($\varepsilon_{Nd} = -2$ to -5) has important implications for interpretation of chemical and isotopic proxies in old marine sediments which are known predominantly from epicontinental deposits. Constraints on the O isotope composition of a deep Proterozoic ocean were obtained from the imprint of seawater preserved in the 2 Ga Purtuniq ophiolite. The magnitude of $\delta^{18}O$ variations is identical to those of younger ophiolites and the modern oceanic crust, implying a constant $\delta^{18}O$ of seawater over time. Claims for secular variation in seawater $\delta^{18}O$ and secular variations in Nd and C isotopes using epeiric sea sediments must consider not only potential alteration effects but local environmental influences.

A detailed study of the isotopic and elemental systematics of Sr and Nd in Ordovician conodonts and other biogenic apatites showed that apatites undergo compositionally dependent, post-depositional Sr-exchange which renders phosphatic brachiopods, conulariids, and many conodonts unreliable recorders of ancient seawater $^{87}Sr/^{86}Sr$. Conodont taxa comprising 100% enamel-like crown material (e.g., *Drepanoistodus suberectus*) have the greatest potential for preserving *in vivo* isotopic signatures. In contrast, all biogenic apatites appear to preserve ancient seawater $^{143}Nd/^{144}Nd$.

The C, O and Sr isotope paleohydrology of brackish water sediments of the Western Canada Sedimentary basin were investigated to gain constraints of paleosalinity in the seawater-freshwater mixing zone. A graphical approach using combined $^{87}Sr/^{86}Sr$ and Sr/Ca ratios enables a brackish water hypothesis to be tested. Strontium isotope paleosalinities are precise and potentially accurate over a 0–20‰ range of salinity and for a variety of depositional settings.

ACKNOWLEDGEMENTS

I would like to thank my thesis supervisors Dr. Karlis Muehlenbachs and Dr. Robert Creaser for welcoming me into their laboratories and for always being available for lively discussions of scientific matters. It has been my great fortune to work so closely with both of them and I have nothing but fond memories to take away with me. In particular I thank Karlis for allowing me the freedom to steer my own course through my doctoral years and for teaching me how to conference (if you retire before 3 a.m.—your not working hard enough!). Thank you Rob for enduring all of my chattering in your ear while you were trying to work, and for giving up so graciously your knowledge of chemistry and mass spectrometry.

Appreciation is expressed to my fellow graduate students many of whom have left before me; Bjarni Gautason, James Farquhar, Jackie Staveley, Agnes Koffyberg, Rob Stevens, Barb Henderson, James Steer, Rob King, Gerard Zaluski, Ed Cloutis, Steve Prevec and Paul Blanchon. Technical support and many conversations with Olga Levner will be fondly remembered. Thanks also to Paul Wagner for probe-magic, Dianne Caird for XRD support and Dragan Krstic in mass spectrometry. I also want to thank Dr. Tom Chacko, Dr. Brian Chatterton and Dr. Larry Heaman for their support of my work. Appreciation is also extended to my external examiners Dr. Stein Jacobsen and Dr. Marvin Dudas. The National Sciences and Engineering Research Council, Graduate Studies and Research and the Canadian Society of Petroleum Geologists are thanked for postgraduate scholarships.

Several people furnished specimens that comprised a large part of this thesis work. Dave Scott is thanked for samples of the Purtuniq ophiolite and Steve Leslie and Stig Bergstrom for supplying conodonts. Mike Ranger is thanked for many discussions of the Mannville Group and for supplying fossil shell locations. Blair Mattison is thanked for supplying fossil shells from the Mannville Group, as is Joseph Hartman for fossils from the Kootenai Formation and Carl Drummond for samples of the Peterson Limestone.

My wife Cathrin Hagey is the lone witness to the multitude of events which have somehow led to this point. Thankyou Cathrin for your encouragement and support through our past 10 years together.

Table of Contents

Chapter 1

Introduction (1–4)
    References (5)

Chaper 2

The ^{18}O/^{16}O Ratio of 2-Billion-Year-Old Seawater Inferred From Ancient Oceanic Crust (6–16)
    References (14–16)

Chapter 3

Isotopic and Elemental Systematics of Sr and Nd in Ordovician Biogenic Apatites: Implications for Paleoseawater Studies (17–45)
    Introduction (17–19)
    Fossil Biogenic Apatites Useed in this Study (19-21)
    Analytical Procedures (21–23)
    Results (25–33)
        Systematics of Sr and ^{87}Sr/^{86}Sr (25–27)
        Systemtatics of Nd and ε_{Nd} (27–28)
        Antithetic distribution of Sr and Nd (28–29)
        Conodont leach experiment (29–33)
    Discussion (33–40)
        Comparitive chemistry and crystallography of modern vertebrate and ancient conodont apatites (33–35)
        Comparative diagenesis of vertebrate and conodont apatites (35–39)
    Conclusions and Implications for Paleoseawater Studies (40–41)
    References 42–45)

Chapter 4

Restricted Marine Setting for Anceint Epeiric Seas: Evidence from ^{143}Nd/^{144}Nd Ratios in 454 Ma Conodonts and ^{13}C/^{12}C Ratios in Limestones (46–59)
    References (57–59)

Chapter 5

Depositional Environment of the Early Cretaceous Ostracode Zone: Paleohydrologic Constraints of O, C and Sr (60–93)
    Introduction (60–61)
    The Ostracode Zone (61–64)

NATERIALS AND METHODS (64–65)

OXYGEN AND CARBON ISOTOPE PALEOHYDROLOGY (65–75)

  Marine waters (65–69)

  Fresh waters (69–74)

  Ostracde, Wabasca and McMurray waters (74–75)

THE OXYGEN ISOTOPE BALANCE (76–78)

STRONTIUM ISOTOPE PALEOHYDROLOGY (78–84)

  Isotopic composition of Sr in marine and fresh waters (78–80)

  Sr isotope paleosalinities (80–84)

DEPOSITIONAL ENVIRONMENT OF THE OSTRACODE ZONE (84–87)

CONCLUSIONS (87–88)

REFERENCES (89–93)

Chapter 6

PALEOSALINITIES IN ANCIENT BRACKISH WATER SYSTEMS DETERMINED BY ^{87}SR/^{86}SR RATIOS IN CARBONATE FOSSILS: A CASE STUDY FROM THE WESTERN CANADA SEDIMENTARY BASIN (94–127)

INTRODUCTION (94–97)

THE MANNVILLE GROUP (97–100)

SAMPLING AND ANALYTICAL TECHNIQUES (100–101)

GENERAL MIXING RELATIONSHIPS (102–106)

ISOTOPE PALEOHYDROLOGY OF THE CRETACEOUS MANNVILLE GROUP (106–112)

  Marine end-member (108-109)

  Freshwater end-member (109–111)

  Strontium isotope paleosalinities for Ostracode, Wabasca and McMurray fossils (111–112)

APPLICATION OF SR/CA RATIOS IN SR ISOTOPE PALEOHYDROLOGY (112–113)

  Application to the L. bituminous suite (McMurray sub-basin) (114–117)

  Application to the G. multicarinata sutie (Group 2 freshwaters) (117–118)

IMPLICATIONS FOR THE DEPOSITIONAL ENVIRONMENT OF THE OSTRACODE, WABASCA AND MCMURRAY SUB-BASINS (118–119)

CONCLUSIONS (120–121)

REFERENCES (122–127)

Chapter 7

CONCLUSIONS (128)

LIST OF TABLES

TABLES

2–1 Purtuniq ophiolite oxygen isotope results (7)

3–1 Sr and Nd isotopic and elemental data for biogenic apatites (24)

3–2 Electron microprobe results for Ca and P contents in biogenic apatites (29).

3–3 *Panderodus gracilis* acetic acid leach results for Nd, Sr and $^{87}Sr/^{86}Sr$ (32).

4–1 Nd isotopic data for conodonts and C and O isotopic data for limestones of the Mohawkian epeiric sea (48).

5–1 Oxygen and carbon isotopic data on fossils and whole-rock carbonates from the Ostracode, Wabasca and McMurray sub-basins (67–68).

5–2 Correlated Sr and O isotope data for Group 1 and 2 fresh waters of the early Cretaceous foreland basin, western North America (79).

6–1 Percentiles for Sr, Ca, Sr/Ca and $^{87}Sr/^{86}Sr$ for world rivers and lakes from literature sources (103).

6–2 $^{87}Sr/^{86}Sr$ and Sr data for fossil molluscs of the Mannville Group and carbonates of the Kootenai Formation, Montana and Peterson limestone, Wyoming (108).

6–3 $^{87}Sr/^{86}Sr$, Sr and Ca contents for present day rivers draining the western North American Cordillera compiled from literature sources (108).

LIST OF FIGURES

FIGURE

2–1 $\delta^{18}O$ profile of 2 Ga Purtuniq ophiolite (8)

2–2 Comparison of Purtuniq $\delta^{18}O$ profile with of those of younger ophiolites and the modern oceanic crust (11).

3–1 Photographs of biogenic apatites analysed in this study including conodonts, phosphatic brachiopods and conulariids (20).

3–2 Hanover, Iowa lithological cross section from which conodonts were obtained (21).

3–3 Plot of $^{87}Sr/^{86}Sr$ *vs.* Sr (ppm) for biogenic apatites (25).

3–4 Plot of $^{87}Sr/^{86}Sr$ *vs.* 1000/Sr (ppm) for biogenic apatites (26).

3–5 Plot of ε_{Nd} *vs.* Nd (ppm) for biogenic apatites (27).

3–6 Plot of Nd (ppm) *vs.* Sr (ppm) for biogenic apatites (28).

3–7 Plot of ε_{Nd} *vs.* $^{87}Sr/^{86}Sr$ for biogenic apatites (28).

3–8 Sr and Nd compositional x-ray maps for the conodont species *Panderodus gracilis* (30).

3–9 Plot of $^{87}Sr/^{86}Sr$ *vs.* Nd/Sr describing 5% acetic acid leach of *Panderodus gracilis* (31).

3–10 Plot of $^{87}Sr/^{86}Sr$ vs. Nd/Sr comparing biogenic apatite fossils and *Panderodus* leach results (37).

4–1 Nd isotopic map of the 454 Ma Mohawkian (epeiric) Sea (50).

4–2 Plots of ε_{Nd} *vs.* Sm/Nd and $\delta^{13}C$ for the Mohawkian Sea (51).

5–1 Paleogeography of the early Cretaceous Seaway of western North America (61).

5–2 Stratigraphic framework for the Lower Cretaceous Mannville Group (62).

5–3 Paleogeography of the Lower Cretaceous Ostracode Zone, Mannville Group (63).

5–4 C and O isotope profile for lacustrine limestones of the Kootenai Formation, Montana (70).

5–5 Range in $\delta^{18}O$ values for early Cretaceous meteoric waters of the western Canada sedimentary basin (72).

5–6 O isotope map for depositional waters of the Ostracode, Wabasca and McMcMurray subbasins inferred from isotopic analyses of fossil molluscs (73).

5–7 C isotope map for depositional waters of the Ostracode, Wabasca and McMurray subbasins inferred from isotopic analyses of fossil molluscs (75).

5–8 $\delta^{18}O$ *vs.* salinity for Ostracode, Wabasca and McMurray depositional waters (76).

5–9 Histogram of Sr contents in world rivers and lakes compiled from literature sources (81).

5–10 Plot of $^{87}Sr/^{86}Sr$ vs. salinity for Ostracode, Wabasca and McMurray depositional waters

5–11 Comparison of Ostracode, Wabasca and McMurray $^{87}Sr/^{86}Sr$ results with the $^{87}Sr/^{86}Sr$ (83).

seawater age curve (83).

5–12 Map showing physiography and δD balance for waters of Lake Maracaibo, Venezuela (86).

6–1 Paleogeography of the early Cretaceous Seaway of western North America showing location of the Mannville Group (98).

6–2 Paleogeography of the Lower Cretaceous Ostracode Zone, Mannville Group (99).

6–3 Hyperbolic mixing curves (^{87}Sr/^{86}Sr *vs.* Salinity) showing relationship ^{87}Sr/^{86}Sr, salinity and modelled parameters for the fresh water end-member (103).

6–4 Plot of Sr *vs.* Ca for world rivers and lakes compiled from literature sources (104).

6–5 Historgram of ^{87}Sr/^{86}Sr for world rivers and lakes compiled from litertature sources (105).

6–6 ^{87}Sr/^{86}Sr *vs.* salinity for inferred depositional waters of the Ostracode, Wabasca and McMurray sub-basins (111).

6–7 (a) ^{87}Sr/^{86}Sr *vs.* 1000Ca/Sr for the fossil gastropod species *Lioplacodes bituminous* of the McMurray sub-basin (114). (b) ^{87}Sr/^{86}Sr *vs.* 1000Sr/Ca (114).

6–8 (a) ^{87}Sr/^{86}Sr *vs.* 1000Ca/Sr for the fossil gastropod species *Goniobasis multicarinata* of the General Petroleums unit, Upper Mannville Group. (b) ^{87}Sr/^{86}Sr *vs.* 1000Sr/Ca (116).

6–9 Remane plot showing relationship between species diversity and salinity in the estuarine setting (120).

Chapter 1

INTRODUCTION

Paleoceanography is a multidisciplinary effort that endeavors to reconstruct aspects of the physics, chemistry and biology of ancient oceans and seas by proxy study of their preserved sediments, or of rocks and minerals that have undergone reaction in the presence of seawater. This dissertation is concerned with advancing this effort through the use of traditional isotopic systems (C, O, Sr and Nd) in novel ways: by judicous combination of stable and radiogenic isotopes in paleohydrology and paleosalinity determination, by investigating the use of bentonites to study horizontal (spatial) as opposed to vertical (temporal) differences in isotopic signatures in old marine sediments, and by testing claims for secular O isotope variation in Precambrian seawater using an ophiolite $\delta^{18}O$ profile. A common theme throughout all of the papers of this dissertation is that isotopes may be used to solve specific problems concerning the paleoceanography and paleohydrology of ancient epicontinental water masses if the scale of inquiry matches the paleoenvironmental context. In Cenozoic paleoceanography, isotopic proxies from deep ocean sediments are interpreted in the context of a deep global ocean; however, marine sediments older than the oldest *in situ* oceanic crust are, by virtue of preservation, epicontinental deposits formed during high relative sea level in epeiric seas. In *Chapter 3* , it is shown that epeiric seas are restricted from mixing with deep contemporaneous oceans. This discovery has profound implications for the nature of the epeiric sea environment and for the context in which isotopic and chemical information from epeiric sea sediments is interpreted.

In the first study (*Chapter 2*) new constraints on the $\delta^{18}O$ value of Proterozoic seawater are obtained through study of the Earth's oldest preserved section of oceanic crust: the 2 Ga Purtuniq ophiolite (Scott et al., 1992). This study reaffirms that ophiolite $\delta^{18}O$ profiles are identical over the past 2 Ga and show no inferred deviation of seawater from the modern isotopic composition of 0‰ (SMOW) (Muehlenbachs and Clayton, 1976; Gregory, 1992). This is a controversial assertion in that marine limestones and carbonate fossils older then 350 Ma (and dolostones, cherts and phosphates in Precambrian sediments) are predominantly depleted of ^{18}O relative to modern equivalents (Perry and Tan, 1972; Veizer et al., 1986; Karhu and Epstein, 1985; Burdett et al., 1990). Ophiolites (which preserve a record of ^{18}O-exchange with hot seawater circulating beneath mid-oceans ridges) are more likely to record the true isotopic composition of past oceans; whereas, Paleozoic and older carbonates formed in epeiric seas are more likely to deviate from the oceans in that epicontinental seas are inherently more susceptible to mixing with ^{18}O-depleted meteoric waters. Consequently, variations in $\delta^{18}O$ values of Paleozoic and older carbonates may reflect mixing between an original seawater source and ^{18}O-depleted meteoric water in a restricted epicontinental environment. This explanation accounts for potential primary aspects of the $\delta^{18}O$ record of carbonates and avoids large temperature increases in ancient oceans, or violation of plate tectonic concepts.

Rapid progress in Cenozoic paleoceanography may in large part be attributed to identification of a suitable substrate for analysis (the foraminiferal test). It follows that progress in the oceanography of older periods in Earth history is likewise contingent on identifying a suitable proxy mineral. Articulate brachiopods composed of low magnesium calcite are widely considered to retain original O, C and Sr isotopic compositions, and a variety of methods have been developed to identify specimens considered to be unaltered (Veizer, 1983). Fossil carbonates may pass all initial screening tests, and still yield isotopic compositions that appear to be altered. Conodont apatite may provide a more reliable substrate than calcite for recording paleoseawater chemistry since apatite is less soluble than calcite in aqueous solution. In *Chapter 3,* a detailed study of the isotopic and elemental systematics of Sr and Nd in pristine 454 Ma conodonts and other biogenic apatites is presented. The fossils analyzed were collected within 18cm of the Millbrig and Deicke K-bentonites (altered volcanic ash beds) to provide a measurable source of contaminant Nd and Sr. It is demonstrated that original seawater $^{87}Sr/^{86}Sr$ ratios are more easily disturbed than $^{143}Nd/^{144}Nd$. This is surprising given that marine apatites have high *in vivo* Sr contents but negligible *in vivo* Nd (which accumulates postmortem at the seawater-sediment interface). If precautions are taken, conodont taxa consisting of 100% enamel-like crown material may provide original seawater $^{87}Sr/^{86}Sr$ signatures, whereas all biogenic apatites appear to preserve seawater $^{143}Nd/^{144}Nd$.

In *Chapter 4*, information learned from the conodont study (*Chapter 3*) is used to test the question of whether the middle-late Ordovician North American epeiric sea was restricted from mixing with the adjacent, deep Iapetus Ocean. Rather than apply conventional isotope stratigraphic techniques, conodonts were collected proximal to the regionally correlated 454 Ma Millbrig and Deicke K-bentonites (Kolata et al., 1986; Huff and Kolata, 1990; Haynes, 1994). Since ash deposition is instantaneous relative to geologic time, sampling close to the bentonites enabled comparison of conodont $^{143}Nd/^{144}Nd$ ratios and limestone $\delta^{13}C$ values from contemporaneous depositional environments separated by more than 1500 km across the Mohawkian epeiric sea. The results clearly show that the Mohawkian epeiric sea was restricted from mixing with the deep Iapetus Ocean, confirming speculations in *Chapter 2* based on the ophiolite evidence. Furthermore, the Mohawkian epeiric sea is itself composed of two major water masses that show very little mixing between them. The implications for the restricted mixing within and between shallow epeiric seas and deep basalt-floored oceans confers upon the epeiric sea a new status in paleoceanographic investigations. The assumption that epeiric sea sediments behave as proxies for deep ocean sediments is shown to be invalid, particularly for elements with short seawater residence times (Nd) and for elements involved in the exogenic cycle (C, O, S). Consequently, the interpretation of chemical and isotopic data from epeiric sea sediments is complicated not only by preservational concerns (that are well recognized) but by regional paleoenvironmental influences that are generally not considered.

One of the consequences of shallow, restricted epeiric seas is that their salinities may deviate from that of the bulk ocean. Epeiric seas situated within the belt of net precipitation (15°N—15°S) may be brackish, whereas those situated within the belt of net evaporation (20-30°N — 20-30°S) may be hypersaline. This simple dichotomy will be complicated by orographic effects, internal barriers to mixing, and the location of major river inputs (influences that may be studied using isotopes). Many of these factors are considered in *Chapter 5* in a study of the O, C and Sr isotope paleohydrology of the early Cretaceous Mannville Group, Western Canada Sedimentary basin (Hayes et al., 1994). The Mannville Group contains numerous examples of brackish water deposits having formed in a complex hydrological setting: between an advancing epicontinental sea and a major freshwater drainage system (e.g., Hayes et al., 1994; Leckie and Smith, 1992). The Ostracode Zone is one of the more prominent units of the Mannville Group which contains pyritic, dark shales and carbonates thought to have been deposited in a large brackish bay. However paleohydrological constraints from O, C and Sr isotopes indicate a predominantly freshwater depositional environment for the Ostracode Zone. Thus it is shown that a paleohydrological perspective can provide important constraints for reconstructing past environments.

The paleohydrology study of *Chapter 5* was undertaken, in part, to explore the use of C, O and Sr isotopes as proxy measures of paleosalinity in the seawater-freshwater mixing zone. Although C and O isotopes are shown to be unreliable because of non-conservative effects, paleosalinities determined using Sr isotopes are both precise and potentially very accurate.

In *Chapter 6*, a detailed account of the Sr isotope paleosalinity method is presented. Paleosalinities in brackish water limestones and fossils are determined by comparison to the ^{87}Sr/^{86}Sr of contemporaneous marine and freshwater sources. Alternatively, combining ^{87}Sr/^{86}Sr and Sr/Ca ratios from a single species of possible brackish dwelling fauna allows the brackish water hypothesis to be tested graphically (rather than assumed) on a plot of ^{87}Sr/^{86}Sr *vs.* Ca/Sr as linear correlations constitute evidence for two-component mixing, To convert shell Sr/Ca to water Sr/Ca ratios, a species specific distribution coefficient ($K_d = 0.24$–0.31) is applied. For seawater-freshwater mixing, *Kd* is fixed by the requirement that seawater must lie on the mixing line. Since seawater and freshwater differ in Sr content by nearly 2 orders of magnitude, paleosalinities are most precisely determined below 20‰. Accordingly, very few depositional basins (or epeiric seas) will have the combined characteristics of high freshwater ^{87}Sr/^{86}Sr and Sr concentration necessary for resolution of paleosalinities in the critical 20–30‰ salinity range.

It is hoped that the studies presented in this dissertation will help lay new foundations for the isotopic study of ancient deep oceans and shallow epeiric seas.

REFERENCES

Burdett J.W., Grotzinger J.P. and Arthur M.A. (1990) Did a major change in the stable-istope composition of Proterozoic seawater occur? *Geology* **18**, 227-230

Gregory R.T. (1991) Oxygen isotope history of seawater revisited: Timescales for boundary event changes in the oxygen isotope composition of seawater. In *Stable Isotope Geochemistry: A Tribute to Samuel Epstein* (H.P. Taylor, J.R. O'Neil and I.R. Kaplan), pp.65-76. The Geochemical Society, Special Publication No. 3.

Hayes B.J.R., Christopher J.E., Rosenthal L., Lus G., McKercher B., Minker D., Trembley Y.M. and Fennell J. (1994) The Mannville Group. In *Geological Atlas of the Western Canada Sedimentary Basin* (Ed. G.D. Mossop and I. Shetsen), pp. 317-334. Canadian Society of Petroleum Geologists.

Haynes J.T. (1994) Yhe Ordovician Deicke and Millbrig K-bentonite beds of the Cincinnati Arch and the souther Valley and Ridge Province. *The Geological Society of America* Special Paper 290.

Huff W.D. and Kolata D.R. (1990) Correlation of the Ordovician Deicke and Millbrig K-bentonites between the Mississippi Vallley and the southern Appalachians. *American Association of Petroleum Geologists Bulletin* **74,** 1736-1747.

Karhu I.R. and Epstein S. (1985) The impication of the oxygen isotope records of coexisting cherts and phosphates. *Geochimica et Cosmochimica Acta* **50,** 1745-1757.

Kolata D.R., Frost J.K. and Huff W.D. (1986) K-bentonites of the Ordovician Decorah Subgroup, upper Missippi Valley: correlation by chemical fingerprinting, III. Department of Energy and Natural Resources, State Geological Survey Division, Circular 537.

Leckie D.A. and Smith D.G. (1992) Regional setting, evolution, and depositional cycles of the Western Canada Foreland Basin. In *Foreland Basins and Foldbelts* (ed. R.W. McQueen and D.A. Leckie), *American Association of Petroleum GeologistsMemoir* **55,** 9-46.

Muehlenbachs K. and Clayton R.N. (1976) Oxygen isotope studies of fresh and weathered submarine basalts. *Canadian Journal of Earth Science* **9,** 172-184

Perry E.C. and Tan F.C. (1972) Significance of oxygen and carbon isotope variations in early Precambrian cherts and carbonate rocks of southern Africa. *Geological Society of America Bulletin* **83,** 647-664.

Scott D.J., Helmstaedt H. and Bickle M.J. (1992) Purtuniq ophiolite, Cape Smith Belt, northern Quebec, Canada: A reconstructed section of early Proterozoic oceanic crust. *Geology* **20,** 173.

Veizer J. (1983) Chemical diagenesis of carbonate rocks: theory and application of trace element technique. In Sedimentary Geology (ed. M.A. Arthur, T.F. Anderson, I.R. Kaplan, J. Veizer and L.S. Land), pp., 1-100. Society of Economic Paleontologists and Mineralogists Short Course Notes 10.

Veizer J, Fritz P. and Jones B. (1986) Geochemistry of brachiopods: Oxygen and carbon isotopic records of Paleozoic oceans. *Geochimica et Cosmochimica Acta* **50,** 1679-1696.

Chapter 2

THE $^{18}O/^{16}O$ RATIO OF 2-BILLION-YEAR-OLD SEAWATER INFERRED FROM ANCIENT OCEANIC CRUST[1]

A long-standing controversy concerns temporal variations in the oxygen isotope composition of Precambrian seawater. It has been suggested that the $\delta^{18}O$[2] record of carbonates (Veizer et al., 1986; Burdett et al., 1990; Veizer et al., 1992) and cherts (Perry and Tan, 1972) over the past 2 billion years reflects variations in the isotopic composition of the seawater in which these sediments were formed. Others argue that pervasive ^{18}O-exchange between seawater and the oceanic crust caused the $\delta^{18}O$ of seawater to remain constant over time (Muehlenbachs and Clayton, 1976; Gregory, 1991; Gregory and Taylor, 1981). Satisfactory resolution of such conflicting views is important in that the oxygen isotope composition of Precambrian seawater bears on the nature of Precambrian plate tectonics and climate.

In this paper we show that the imprint of early Proterozoic seawater is preserved in the $\delta^{18}O$ profile of the 1.998 billion year old Purtuniq ophiolite, situated in the Cape Smith Belt of northern Quebec, Canada (Scott et al., 1991; Scott et al., 1992; Parrish, 1989). The controversy surrounding the true $\delta^{18}O$ value of early Proterozoic seawater is addressed through comparison of the isotopic imprint of 2 billion year old seawater determined for the ophiolite with that in contemporaneous carbonate rocks of the ~1.9 billion year old Rocknest dolostone, situated in the Wopmay orogen, Northwest Territories, Canada (Burdett et al., 1990; Veizer et al., 1992). The opportunity to analyze samples from the lower levels of early Proterozoic oceanic crust distinguishes this work from most

---

[1] A version of this paper was published in *Science (1992)* **259,** 1733-1736, coauthored with K. Muehlenbachs

[2] Defined as $\delta^{18}O$ = (Rsample /Rstandard −1) 1000, where R = $^{18}O/^{16}O$ and the standard is SMOW, standard mean ocean water (Craig, 1966)

Table 2-1 Purtuniq ophiolite oxygen isotope results.

Sample	Type	δ^{18}O*
Basalts		
S-198	MORB	7.0
S-199	MORB	7.4
S-201	MORB	6.3
D-247a	MORB	7.4
B-367	MORB	8.0
Dykes		
C-5	MORB	7.4
C-11	MORB	6.9
B-1	MORB	6.8
B-2	MORB	7.3
B-5	MORB	6.7
E-7	MORB	7.3
D-3	OIB	6.4
E-1	OIB	6.2
E-4	OIB	6.1
E-5	OIB	6.6
E-6	OIB	6.3
Gabbros		
B-407	MORB	5.8
D-143a	MORB	5.5
D-144a	MORB	5.6
D-248f	MORB	5.9
S-212a	MORB	7.0
S-213	MORB	6.7
L-181p	MORB	6.1
L-181m	MORB	5.8
S-315	OIB	4.5
S-316	OIB	3.9
S-317	OIB	5.5
S-326	OIB	6.9
S-345a	OIB	5.9
B-369a	OIB	5.5
B-374	OIB	4.6
B-414a	OIB	6.1

*Isotopic values reported in the standard delta (δ) notation as permil (‰) deviation from Standard Mean Ocean Water (SMOW).

previous studies which have utilized less desirable submarine pillow basalts collected from Precambrian greenstone terranes (Gregory, 1991; Smith et al., 1984).

From their studies of the Rocknest dolostone, Burdett et al. (1990) and Veizer et al. (1992), concluded that the δ^{18}O value of early Proterozoic calcite was nearly 10‰ lower than that of modern marine calcites, which are ~30‰ (SMOW). On the basis of the excellent preservation of original marine fabrics observed in thin section, Burdett et al. argued that dolomitization of the original calcite did not completely overprint the original seawater signature. Using the isotopic composition of the most ^{13}C- and ^{18}O-enriched dolomitized ooid of 22.9‰, and an assumed dolomite-calcite fractionation of +4‰, the authors calculate a δ^{18}O value of 18.9‰ for the original Rocknest calcite. If equatorial seawater temperatures in the early Proterozoic were similar to todays, Burdett *et al.* (1990) suggested, as have others (Veizer et al., 1992; Perry et al., 1972) that lower δ^{18}O values for early Proterozoic sediments may reflect a nearly 10‰ ^{18}O-depletion in early Proterozoic seawater.

Although widely accepted, the above proposal conflicts with predictions that the average δ^{18}O value of the global ocean remained near 0 ±2‰ for most of Earth history (Muehlenbachs and Clayton, 1976; Gregory, 1991). Presently, the δ^{18}O value of seawater is largely determined by its interactions with the oceanic crust. Seawater, which penetrates the oceanic crust at ridges, reacts with newly formed crust ($\delta^{18}O=5.7 \pm 0.3$‰) at both low and high temperatures. In upper crustal levels, low temperature (10° to 150°C) alteration decreases the δ^{18}O value of seawater but increases the δ^{18}O value of the rock (Muehlenbachs and Clayton, 1972a). Deeper in the crustal section, at temperatures of about 350°C, the polarity of exchange reverses and the δ^{18}O value of seawater is increased at the expense of the rock (Muehlenbachs and Clayton, 1972b). The ^{18}O-enrichments balance the ^{18}O-depletions, in effect buffering the δ^{18}O of seawater and imprinting the crustal sec-

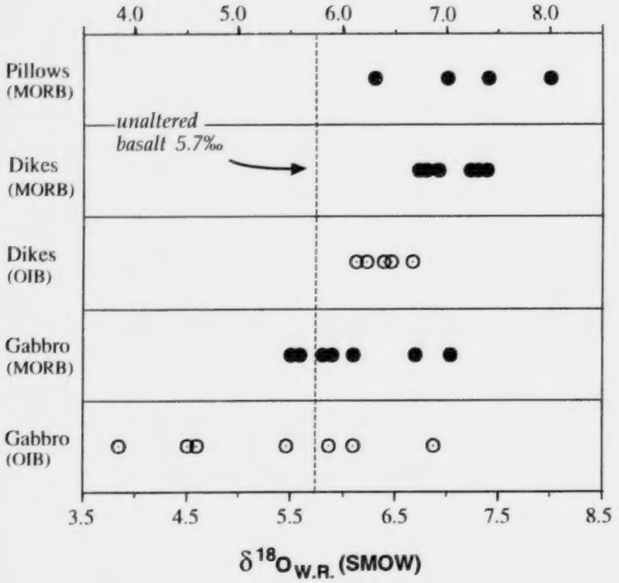

FIGURE 2-1 $\delta^{18}O$ profile of submarine pillows, sheeted dykes and gabbros of the Purtuniq ophiolite presented by suite, (●) MORB and (○) OIB. MORB and OIB suite designations refer to interpretations in (Scott and Hegner, 1990). Powdered whole-rock samples were analyzed by the BrF_5 method (Clayton and Mayeda, 1963). The majority of samples (80%) were analyzed at least in duplicate with a mean pooled variance of 0.14 ±0.1‰. Analytical uncertainties are about the size of the symbols.

tion with a characteristic $\delta^{18}O$ profile (Muehlenbachs and Clayton, 1976; Gregory and Taylor, 1981). The shape of this imposed profile and the magnitude of the $\delta^{18}O$ values reflect the isotopic composition of the circulating seawater. If early Proterozoic seawater was ^{18}O-depleted relative to modern seawater then the 2 billion year old ophiolite would likewise be ^{18}O-depleted compared to modern oceanic crust.

The 2 billion year old Purtuniq ophiolite is part of a package of mafic crustal rocks that were juxtaposed during convergence of early Proterozoic continental and oceanic lithospheric plates (St-Onge and Lucas, 1987; Lucas et al., 1992). Three tectonic settings are inferred for rocks of the belt; a rifted continental margin, an oceanic spreading center, and an island arc-related subduction center. The ophiolitic portion preserves all the requisite components of the modern oceanic crust in a series of thrust bounded sheets that are metamorphosed predominantly to upper greenschist facies (Begin, 1989). This is a slightly higher grade than the lower greenschist conditions prevalent during seawater induced alteration of the deep oceanic crust today. Samples analyzed in this study contain hornblende or actinolite + plagioclase + quartz, ± chlorite, ± epidote, ± calcite and ±sphene (Scott et al., 1991). The belt is argued to be direct evidence for the operation of Phanerozoic-style plate tectonics operating 2 billion years ago (St-Onge et al., 1987).

Field and chemical evidence indicate that two magma sources formed the Purtuniq crustal section (Scott et al., 1992; Scott and Hegner, 1990). An older tholeiitic suite, chemically similar to modern mid-ocean ridge basalts (N-MORB) with $\varepsilon_{Nd}(t)$=4.0-5.3, and, a younger suite chemically similar to ocean island type basalts (OIB) with $\varepsilon_{Nd}(t)$=2.5-3.6, where t= 2 billion years (Scott and Hegner, 1990; Hegner and Bevier, 1991). Most thrust sheets are characterized by rocks of either MORB or OIB affinity with the exception of the sheeted dykes and one example of cross-cutting mafic cumulates (Scott and Bickle, 1991). The composite crustal section (MORB + OIB) is about 9 km thick with roughly equal contributions from each source.[3]

From the pattern observed in Figure 1, it is evident that the Purtuniq ophiolite displays the characteristic isotopic signature that results from seawater ocean-crust interaction, specifically, ^{18}O-enrichment in the pillow and dyke sections in contrast to ^{18}O-depletion in the gabbros. The shape of the profile is evidence that seawater, initially cooler and heating up with depth, penetrated and altered the Purtuniq crustal section. The ~0.7‰ offset between MORB and OIB suites (Fig. 2-1) probably reflects the superposition of the effects of separate hydrothermal circulation cells associated with multiple intrusions. Preservation of the δ^{18}O differences between rock units is evidence against regional-scale isotopic homogenization during later metamorphism. Distinct isotopic signatures for adjacent MORB and OIB dike samples rules out significant isotopic resetting of the whole-rock (Scott and Bickle, 1991).

The δ^{18}O value of 2 billion year old seawater is best inferred from the gabbro section of the ophiolite. Low-temperature alteration products of pillow basalts, as with the low temperature formation and subsequent diagenesis of low temperature carbonate rocks and cherts, involve large mineral-water $\delta^{18}O$ fractionations (for example, $\Delta_{calcite-water} \approx +30‰$, at 15°C). Consequently, the final $\delta^{18}O$ value of the rock is sensitive to the temperature as well as the extent of alteration, and renders sediments and pillow basalts poor monitors of potential changes in the $\delta^{18}O$ value of the oceans. At higher temperatures, isotopic fractionations between interacting water and rock are smaller (for example, $\Delta_{basalt-water} \approx +6‰$, at 350°C) and uncertainty over the exact temperature of *in situ* hydrothermal alteration is less important in determining the final $\delta^{18}O$ value of the rock. Therefore, if seawater were genuinely ^{18}O-depleted to the extreme values suggested (Burdett et al., 1990; Veizer et al., 1992; Perry and Tan, 1972) the gabbros would be significantly depleted of ^{18}O, irrespective of any uncertainty in temperature.

---

[3] Two models have been proposed to account for the bimodal chemistry of the ophiolite (i) a Hawaiian plume model which has the younger OIB suite intruding through an older MORB crust (Scott et al., 1992), or (ii) a plum pudding type model where the two suites are generated by differing degrees of partial melting of a chemically heterogeneous source (Hegner and Bevier, 1991). $\varepsilon_{Nd}(t) = (^{143}Nd/^{144}Nd)_{sample}\,(t) / (^{143}Nd/^{144}Nd)_{CHUR}\,(t) - 1)10^4$ here CHUR is the CHondritic Uniform Reservoir and both CHUR and $^{143}Nd/^{144}Nd_{initial}$ are calculated at some time(t) in the past (DePaolo and Wasserburg, 1976). MORBs are depleted in large ion lithophile elements and originated from mantle sources with higher Sm/Nd ratios than OIBs which are more enriched in large ion lithophiles and originated from mantle sources with lower Sm/Nd ratios.

The $\delta^{18}O$ profile of the Purtuniq ophiolite (Fig. 2-2) overlaps with similar profiles reported for younger ophiolites (Cocker et al., 1982; Stern et al., 1976) and the modern oceanic crust (Muehlenbachs and Clayton, 1972a; Muehlenbachs and Clayton, 1972b; Alt et al., 1986), consistent with an isotopic composition for 2 billion year old seawater near the modern value of 0 per mil. Had the oceans been at -10‰, gabbros with $\delta^{18}O$ values as low as -8‰ would be evident. No such ^{18}O-depleted rocks were observed.

The Purtuniq ophiolite and Rocknest dolostone results may be reconciled through (i) higher equatorial seawater temperatures in the early Proterozoic (ii) diagenetic overprints and (iii) decoupling of the oxygen isotope systematics between epeiric seas and the deep global ocean. Although Burdett *et al.* (1990) argued that they have been able to see through the diagenetic overprint to the imprint of the original seawater, they concede that their data are compatible with either ^{18}O-depleted oceans or higher equatorial seawater temperatures 2 billion years ago; they did not consider the third alternative. Using the criteria outlined in (Burdett et al., 1990), a temperature of 75°C is calculated for precipitation of the original Rocknest calcite if seawater were -1‰[4]. The Rocknest temperature

---

[4] The oceans would attain a $\delta^{18}O$ value of −1‰ if Earth's present day low $\delta^{18}O$ ice caps were melted. Uncertainty over the true $\Delta_{dolomite-calcite}$ equilibrium fractionation limits the degree of precision to which temperatures may be calculated from dolomites. Laboratory experiments suggest a Δ between +4 and +7‰ (Northrop and Clayton, 1966) whereas field studies suggest values of $\Delta \leq 4‰$ (Degens and Epstein, 1964; Friedman and Hall, 1963; Land, 1983).

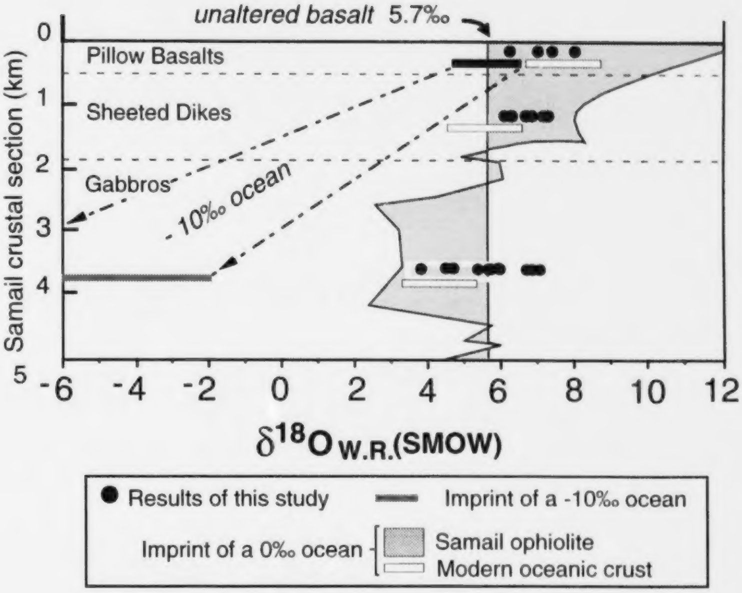

FIGURE 2-2 Composite $\delta^{18}O$ profile of the Purtuniq ophiolite compared to the $\delta^{18}O$ profile of the Samail ophiolite (Gregory and Taylor, 1981) which reflects the characteristic imprint of an ~0‰ ocean. Range of isotopic values for the modern oceanic crust are from (Muehlenbachs and Clayton, 1976; Alt et al., 1986). The hypothetical imprint of a -10‰ ocean on the oceanic crust is also displayed. Conservative estimates for the $\delta^{18}O$ values of pillow basalts reflect modern observations of recent sea floor material and are based on mixtures of 10% clay ($\Delta_{clay-water}$ = +25‰, at temperatures typical of modern seawater) and 90% basalt (+5.7‰). The basalt $\delta^{18}O_{W.R}$ values change by only ~1‰, even though the $\delta^{18}O$ of seawater changes by 10‰. The $\delta^{18}O$ value of a whole-rock gabbro interacting with 0‰ seawater at ~350°C will reflect the modal abundance of metamorphic ^{18}O-enriched quartz ($\delta^{18}O$ @+8‰) and ^{18}O-depleted epidote ($\delta^{18}O$ @ 0‰) which limits the range of expected values. If seawater were -10‰ rather than 0‰, the range of expected values would be -2 to -10‰. The shape of the observed $\delta^{18}O$ profile and the magnitude of the $\delta^{18}O$ values is entirely consistent with an early Proterozoic seawater isotopic composition of 0 ±2‰(SMOW).

falls within the range of temperatures calculated for various phases of the ~2 Ga Gunflint banded iron formation. For example, Winter and Knauth (1990) reported an average chert $\delta^{18}O$ value of 23.2 ±0.08‰ (n=82), which, depending on the silica-water fractionation employed, corresponds to temperatures between 55 and 90°C. From the same formation, Karhu and Epstein (1985) reported paleotemperatures from chert, phosphate and chert-phosphate pairs of 84°, 95° and 66°C respectively, the last determination being independent of the $\delta^{18}O$ value for seawater.

The inferred paleotemperatures are often criticized as unreasonably high in that sedimentary evidence for early Proterozoic glaciations (Crowell, 1982) does not appear to corroborate the idea of hot Precambrian oceans. However, Knauth and Lowe (1978) point out that, on geologic time-scales, glaciations would be short-lived phenomena and not conflicting with an overall hot climate. Furthermore, since it is well established that nearly all post-depositional alteration phenomena lead to ^{18}O-depletion of the original sediment, the lowest calculated temperatures are the most reliable. Alternatively, it may be argued that the original seawater imprint is often not preserved in Precambrian sediments. Diagenesis transforms the primary metastable precipitates of aragonite and high magnesium calcite, hydrous-silica, and dahllite, to the diagenetically stable neomorphs; dolomite, quartz and francolite. Because most isotopic analyses of Precambrian sediments are performed on secondary phases, the high calculated temperatures may reflect the fluid and temperature conditions of diagenesis, including dolomitization, rather than those of the original ocean.

Another potentially important source of uncertainty in carbonate and chert based paleotemperature estimates is the assumption that the δ^{18}O value of the water from which Precambrian sediments precipitated was isotopically identical to that of the deep ocean. Many Precambrian carbonate rocks and cherts probably formed in shallow epeiric or restricted continental shelf seas that are inherently more susceptible to the influx and entrainment of low δ^{18}O meteoric waters. For example, although the δ^{18}O value of the Cretaceous ocean was 0‰, waters of the epicontinental Greenhorn Sea, Cretaceous Western Interior Seaway, were depleted in ^{18}O by as much as 4‰ (Kyser et al., 1993). If the majority of Precambrian sediments formed from ^{18}O-depleted seawater in marginal marine settings, then the temperatures calculated need not be as high as the observed ^{18}O-depletion, that is, for every 1‰ decrease in the δ^{18}O of a marginal marine sea, the inferred paleotemperature decreases by about 4°C.

Although the above considerations hamper a confident interpretation of the δ^{18}O variations observed in Precambrian sediments, the isotopic data garnered from ophiolites are far less equivocal on one important issue, that of the δ^{18}O value of seawater. The imprint of 2 billion year old seawater preserved within the Purtuniq ophiolite clearly shows that the isotopic composition of early Proterozoic seawater was similar to modern seawater. In accordance with model predictions (Muehlenbachs, 1976), the δ^{18}O value of early Proterozoic seawater may be constrained to the range $-2 \leq \delta^{18}O \leq +2$.

Because the $\delta^{18}O$ value of the oceans reflects the cycling of seawater through the oceanic crust, a 0‰ ocean in the early Proterozoic is consistent with widespread sea floor spreading operating in that time. Modern studies have shown that sea floor spreading is the driving force behind the production and maintenance of a 0‰ ocean (Muehlenbachs and Clayton, 1976; Gregory, 1991). Beneath Earth's extensive mid-ocean ridge spreading centers, hot upwelling magmas drive convective circulation of seawater through the oceanic crust and promote pervasive ^{18}O-exchange between water and rock at high temperatures. By removing older altered crust, sea floor spreading provides a mechanism by which new oceanic crust is continually brought into contact with deep convecting seawater. The proposed constancy of the isotopic composition of seawater over time (Muehlenbachs, 1976) reflects the constancy of the grander process of production, alteration, and destruction of the oceanic crust.

This fundamental relation between seawater isotopic composition and sea floor spreading may extend to even older Archean oceans. Archean carbonate rocks (Veizer, et al., 1992) and cherts (Perry and Tan, 1972; Knauth and Lowe, 1978) yield ^{18}O-depleted values similar to, or less than, those of early Proterozoic sediments. In contrast, isotopic studies of proposed Archean oceanic crust, e.g., the Barberton Greenstone Belt (Smith et al., 1984; Hoffman, et al., 1986) and the Pilbara Block (Gregory, 1991), and, of Archean hydrothermal ore deposits (Beaty and Taylor, 1982; Kerrich, 1987), suggest the $\delta^{18}O$ value of the oceans have remained close to 0‰ for the past 3.5 billion years. Isotope budget modelling of the modern oceans (Muehlenbachs and Clayton, 1976; Gregory, 1991; Holland, 1984) suggests that sea floor spreading rates that are at least ~50% of modern average rates are rapid enough to control the $\delta^{18}O$ value of seawater. Because the isotopic composition of seawater reflects, in a fundamental way, plate tectonic processes such as mantle convection and sea floor spreading, global-scale ^{18}O-depleted Precambrian oceans would be possible only if the modern plate tectonic paradigm were considered invalid for most of Earth history.

REFERENCES

Alt J.C., Muehlenbachs K. and Honnerez J. (1986) An oxygen isotope profile through the upper kilometer of oceanic crust, DSDP Hole 504B. *Earth and Planetary Science Letters* **80,** 217-229

Beaty D.W. and Taylor H.P. Jr. (1982) Some petrologic and oxygen isotopic relationships in the Amulet Mine, Noranda, Quebec and their bearing on the origin of Archean massive sulfide deposits. *Economic Geology* **77,** 95-108.

Begin N.J. (1989) P-T conditions of metamorphism inferred from the metabasites of the Cape Smith Belt, northern Quebec. *Geoscience Canada* **16,** 151-154.

Burdett J.W., Grotzinger J.P. and Arthur M.A. (1990) Did a major change in the stable-istope composition of Proterozoic seawater occur? *Geology* **18**, 227-230.

Clayton R.N. and Mayeda T. (1963) The use of bromine pentafluoride in the extraction of oxygen from oxides and silicates for isotopic analysis. *Geochimica et Cosmochimica Acta* **27,** 43-52.

Cocker J.D., Griffin B.J. and Muehlenbachs K. (1982) Oxygen and carbon isotope evidence for seawater-hydrothermal alteration of the Macquarie Island ophiolite. *Earth and Planetary Science Letters* **61,** 112-122.

Craig H. (1961) Standard for reporting concentrations of deuterium and oxygen-18 in natural waters. *Science* **133,** 1833

Crowell J.C. (1982) Continental glaciation through geologic time. In *Climate in Earth History* (Geophysics study committee, National Academy Press), pp. 77-82.

Degens E.T. and Epstein S. (1964) Oxygen and carbon isotope ratios in coexisting calcites and dolomites from recent and ancient sediments. *Geochimica et Cosmochimica Acta* **28,** 23-44.

DePaolo D.J. and Wasserburg G.J. (1976) Nd isotopic variations and petrogenetic models. *Geophysical Research Letters* **3,** 249-252.

Friedman G.M. and Hall W.E. (1963) Fractionation O^{18}/O^{16} between coexisting calcite and dolomite. *Journal of Geology* **71,** 283-243.

Gregory R.T. (1991) Oxygen isotope history of seawater revisited: Timescales for boundary event changes in the oxygen isotope composition of seawater. In *Stable Isotope Geochemistry: A Tribute to Samuel Epstein* (H.P. Taylor, J.R. O'Neil and I.R. Kaplan), pp.65-76. The Geochemical Society, Special Publication No. 3.

Gregory R.T. and Taylor H.P. (1981) An oxygen isotope profile in a section of Cretaceous oceanic crust, Samail ophiolite, Oman: Evidence for ^{18}O buffering of the oceans by deep (≥5km) seawater hydrothermal circulation at mid-oceans ridges. *Journal of Geophysical* Research **86,** 2737-2755.

Hegner E. and Bevier M.L. (1991) Nd and Pb isotopic constraints on the origin of the Purtuniq ophiolite and early Proterozoic Cape Smith Belt, northern Quebec, Canada. *Chemical Geology* **91,** 357-371.

Holland H.D. (1984) *The Chemical Evolution of the Atmosphere and Oceans* (Princeton University Press).

Hoffman S.E., Wilson M. and Stakes D.S. (1986) Inferred oxygen isotope profile of Archean oceanic crust, Onverwacht Group, south Africa. *Nature* **321,** 55-58.

Karhu I.R. and Epstein S. (1985) The impication of the oxygen isotope records of coexisting cherts and phosphates. *Geochimica et Cosmochimica Acta* **50,** 1745-1757.

Kerrich R. (1987) Stable isotope studies of fluids in the crust. In *Stable Isotope Geochemistry of Low Temperature Fluids* (ed. T. Kyser), pp. 258-278. Mineralogical Association of Canada Short Course 13.

Knauth L.P. and Lowe D.R. (1978) Oxygen isotope geochemistry of cherts from the Onverwacht Group (3.4 billion years), Transvaal, South Africa, with implications for secular variations in the isotopic compositions of cherts. *Earth and Planetary Science Letters* **41,** 209-222.

Kyser T.K., Caldwell W.G.E., Whittaker S.G. and Cadrin A.A.J. (1993) Paleoenvironment and geochemistry of the northern portion of the Western Interior Seaway during late Cretaceous time. In *Evolution of the Western Interior Basin* (Ed. W.G.E Caldwell and E.G. Kaufman), Geological Association of Canada Special Paper **39,** 355-378.

Land L.S. (1980) The isotopic and trace element geochemistry of dolomite: The state of the art. In *Stable Isotopes in Sedimentary Geology* (eds, M.A.Arthur, T.F. Anderson), pp. 4-1–4-22. Society of Economic Paleontologists and Mineralogist Short Course 10.

Lohmann K.C. and Walker J.C.G. (1989) The δ^{18}O record of Phanerozoic abiotic marine cements.*Geophysical Research Letters* **16**, 319-322.

Lucas S.B., St-Onge M.R., Parrish R. and Dunphy J.M. (1992) Long-lived continent-ocean interaction in the early Proterozoic Ungava Orogen, northern Quebec, Canada. *Geology* **29,** 113-116

Muehlenbachs K. and Clayton R.N. (1976a) Oxygen isotope studies of fresh and weathered submarine basalts. *Canadian Journal of Earth Science* **9,** 172-184

Muehlenbachs K. and Clayton R.N. (1976b) Oxygen isotope geochemistry of submarine greenstones. *Canadian Journal of Earth Science* **9,** 471-478

Muehlenbachs K. and Clayton R.N. (1976) Oxygen isotope composition of the oceanic crust and its bearing on seawater. *Journal of Geophysical Research* **81**, 4365-4369

Northrop D.A. and Clayton R.N. (1966) Oxygen isotope fractionations in systems containing dolomite. *Journal of Geology* **74,** 174-196.

Parrish R.R. (1989) U-Pb geochronology of the Cape Smith Belt and Sugluk block, northern Quebec. *Geoscience Canada* **16,** 126-130.

Perry E.C. and Tan F.C. (1972) Significance of oxygen and carbon isotope variations in early Precambrian cherts and carbonate rocks of southern Africa. *Geological Society of America Bulletin* **83,** 647-664.

Scott D.J. and Hegner E. (1990) Two mantle sources for the two-billion-year-old Purtuniq ophiolite, Cape Smith Belt, northern Quebec. Annual Meeting, Geological Association of Canada **15,** A118 (abstract).

Scott D.J. and Bickle M.J. (1991) Field relationships in the early Proterozoic Purtuniq ophiolite, Lac Watts and Purtuniq map areas, Quebec. In *Current Research, Part C, Paper 91-1C*, pp. 179-188. Geological Survey of Canada.

Scott D.J., Helmstaedt H. and Bickle M.J. (1992) Purtuniq ophiolite, Cape Smith Belt, northern Quebec, Canada: A reconstructed section of early Proterozoic oceanic crust. *Geology* **20,** 173.

Scott D.J., St-Onge, M.R., Lucas S.B. and Helmstaedt H. (1991) Geology and chemistry of the early Proterozoic Purtuniq ophiolite, Cape Smith Belt, northern Quebec, Canada. In. *Symposium on Ophiolite Genesis and Evolution of Oceanic Lithosphere* (ed. T. Peters), p. 817. Kluwer Academic.

Smith H.S., O'Neil J.R. and Erlank A.J. (1984) Oxygen isotope composition of minerals and rocks and chemical alteration patterns in pillow lavas from the Barberton Greenstone Belt, south Africa. In *Archean Geochemistry* (eds. A. Kroner, G.N. Hanson and A.M. Goodwin), pp. 115-137. Springer-Verlag.

Stern C., de Wit M.J. and Lawrence J.R. (1976) Igneous and metamorphic processes associated with the formation of Chilean ophiolites and their implications for ocean floor metamorphism *Journal of Geophysical Research* **81,** 4370-4380.

St-Onge. M.R. and Lucas S.B. (1987) Evolution of the Cape Smith Belt: Early Proterozoic continental underthrusting, ophiolite obduction, and thick-skinned folding. In *The Early Proterozoic Trans-Hudson Orogen of North America* (eds. J.F. Lewry and M.R. Stauffer), pp. 313-351. Geological Association of Canada, Special Paper 37.

Winter B.L. and Knauth L.P. (1990) Geological Society of America **22,** A263 (abstract)

Veizer J., Clayton R.N., Hinton R.W. (1992) *Geochimica et Cosmochimica Acta* **56,** 875-

Veizer J., Fritz P., and Jones B. (1986) Geochemistry of brachiopods: oxygen and carbon isotopic records of Paleozoic oceans. *Geochimica et Cosmochimica Acta* **50**, 1679-1696.

Veizer J., Plumb K.A., Clayton R.N., Hinton R.W. and Grotzinger J.P. (1986). *Geochimica et Cosmochimica Acta* **56**, 2487.

Chapter 3

ISOTOPIC AND ELEMENTAL SYSTEMATICS OF SR AND ND IN ORDOVICIAN BIOGENIC APATITES: IMPLICATIONS FOR PALEOSEAWATER STUDIES[1]

INTRODUCTION

Conodonts are teeth-like microfossils thought to have comprised the feeding apparatus of an extinct eel-like organism which ranged from Late Cambrian to Late Triassic. They are traditionally studied for the purposes biostratigraphic correlation of sedimentary rocks but are increasingly being used as a proxy for recording past seawater trace element and isotopic compositions. Due to their high rare earth element (REE) contents, conodonts (Wright et al., 1984; Keto and Jacobsen, 1987, 1988; Grandjean-Lecuyer et al., 1993) and other biogenic apatites (Staudigel et al., 1986; Grandjean et al. 1987, 1988) have become the principal substrate for studying the REE chemistry and ^{143}Nd/^{144}Nd variations in ancient seawater. Biogenic apatites also contain high concentrations of Sr providing an alternate substrate to biogenic calcite for recording variations in past seawater ^{87}Sr/^{86}Sr ratio (Staudigel et al., 1986; Keto and Jacobsen, 1987; Bertram et al., 1992; Cummins and Elderfield, 1994).

Despite the low solubility of hydroxyapatite relative to calcite in aqueous solution (Stumm and Morgan, 1981) there is substantial evidence that biogenic apatites are diagenetically reactive. For example, present day vertebrate teeth and bones are dahllite (carbonate hydroxyapatite) whereas apatitic fossils are predominantly francolite (carbonate fluorapatite) (Pietzner et al., 1968). Much of the carbonate (Schoeninger and DeNiro, 1982) and fluorine (McConnell, 1962) in ancient francolites may have accumulated, or was exchanged, during diagenetic modification of a dahllite precursor. The REE contents in old francolites can be several orders of magnitude greater than those in young dahllites (Shaw and Wasserburg, 1985; Elderfield and Paget, 1986), and field (Tuross et al., 1989) and laboratory based studies (Hodge et al., 1946) indicate high potential for uptake of externally derived Sr.

---

[1] A version of this paper has been submitted to *Earth and Planetary Science Letters*–Oct/95– co-authored by R.A. Creaser and K. Muehlenbachs, Dept. of Earth and Atmospheric Sciences, University of Alberta, and S.A. Leslie and S.M. Bergstrom, Dept. of Geological Sciences, The Ohio State University.

Conodonts and ichthyoliths yield conflicting results on whether *in vivo* isotopic signatures are preserved. Bernat (1975) showed that post-mortem REE increase in Cenozoic fish remains occurred rapidly after death of the organism at the sediment water interface. REE profiles and ^{143}Nd/^{144}Nd ratios confirmed that seawater was the source (Shaw and Wasserburg, 1985; Staudigel et al. 1986; Grandjean et al. 1987). Others have shown or deduced that sediment porewaters contribute REE to ichthyoliths (Elderfield and Pagett, 1986; Toyoda and Tokonami, 1990), particularly if they are reducing (Elderfield and Sholkovitz, 1987), and that later diagenetic uptake of REEs can modify the fine structure of original seawater REE profiles. For Sr isotopes, Staudigel et al. (1986) concluded that Cenozoic fish teeth from deep sea sediments accurately recorded the ^{87}Sr/^{86}Sr of contemporaneous seawater provided steps were taken to remove authigenic calcite overgrowths, whereas Nelson et al. (1986) and Koch et al. (1992) could not recover *in vivo* ^{87}Sr/^{86}Sr signatures from the bones of fossil seal and salmon, respectively.

Preservation issues are the most important obstacle to elucidating the chemical and isotopic oceanography of Paleozoic seas. Potentially, biogenic apatites could be used to better resolve Paleozoic sections of the ^{87}Sr/^{86}Sr seawater age curve (Bertram et al., 1992; Cummins and Elderfield, 1994), thus increasing the potential of the curve as a tool in Paleozoic isotope stratigraphy (DePaolo and Ingram, 1985). This application is particularly appealing since conodonts provide their own biostratigraphy. In contrast to Sr which has a long ($5\text{x}10^6$ yrs) residence time in seawater (Taylor and McLennan, 1985) the residence time of Nd (~1000 yrs; Elderfield and Greaves, 1982) is shorter than the mixing time of the oceans (~1000 yrs; Broecker, 1963) resulting in differences in ε_{Nd} between the present day Atlantic and Pacific oceans. The source of Nd in seawater is almost entirely derived from river discharges and so the specific Nd isotopic composition of a water mass reflects the mean age of continental crust comprising the watershed. Keto and Jacobsen (1987;1988), Grandjean et al. (1988), Stille and Fischer (1990) and Stille (1992) have demonstrated the potential of Nd isotopes to trace the evolution of ancient oceans and their surrounding crustal landmasses; an approach that relates oceanography and tectonics. With exceptional stratigraphic control it is possible to trace paleocirculation.

In this paper we present a detailed account of the isotopic and elemental systematics of Sr and Nd in 4 types of pristine biogenic apatite separated from 3 handsamples of Ordovician limestone collected proximal to the Millbrig and Deicke K-bentonites (Huff et al., 1992; Haynes, 1994), dated at 454 ±3 Ma (Kunk and Sutter, 1984). Sampling both within and adjacent to the bentonites provides a measurable source of contaminant Sr and Nd (of contrasting isotopic composition to that of 454 Ma seawater) which persisted throughout the entire depositional history of the fossils.

FOSSIL BIOGENIC APATITES USED IN THIS STUDY

Conodont elements define a wide range of morphological types divisible into 3 components: (1) crown material, which comprises the enamel-like denticles of conodonts, (2) a more variably preserved basal body which comprises the base and and internal cavity, and (3) white matter, so called for its tendency to give an opaque appearance to otherwise translucent crown material in pristine specimens (Sansom et al., 1992). Conodont crown material has been compared to vertebrate tooth enamel (Schmidt and Muller, 1964; Andres, 1988), and the basal bodies to dentine (Schmidt and Muller, 1964; Andres, 1988), bone or cartilage (Stewart and Sweet, 1956). Recent studies on the microstructure of conodont elements provide evidence for histological homology between apatitic components in conodonts and different types of hypermineralized calcium-phosphatic tissues limited to the vertebrates (Sansom et al., 1992). Scanning electron micrographs show that the surface area of white matter contains holes that resemble the lacunae and canaliculi of cellular bone and basal bodies have a spherulitic structure resembling globular calcified cartilage (Sansom et al., 1992).

Two conodont types were chosen for analysis. One type was mono-specific consisting of

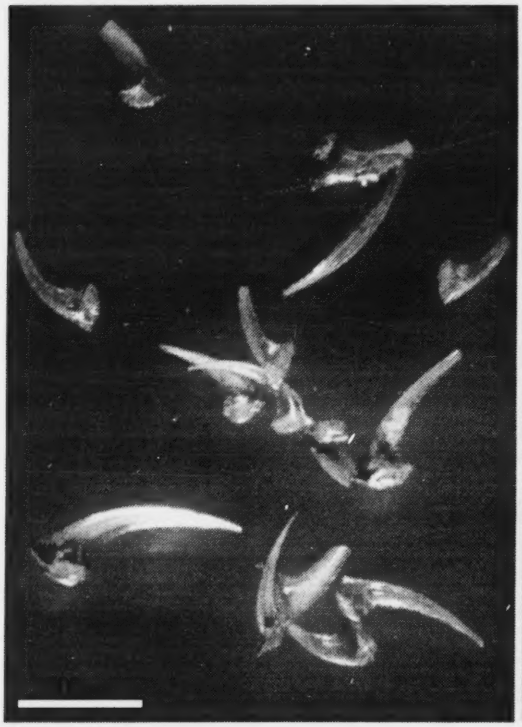

FIGURE 3-1 (a) Coniform conodonts (*Drepanoistodus suberectus*) lacking basal bodies.

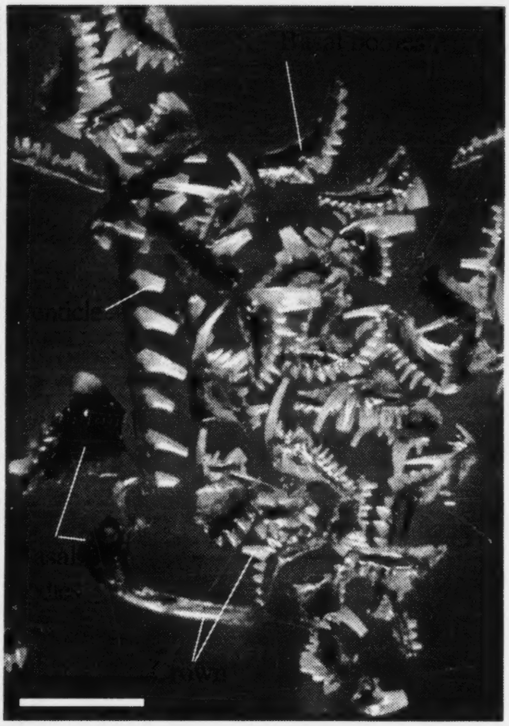
Basal body
Denticle
Basal bodies
Crown

FIGURE 3-1 (b) Ramiform and coniform conodonts with basal bodies

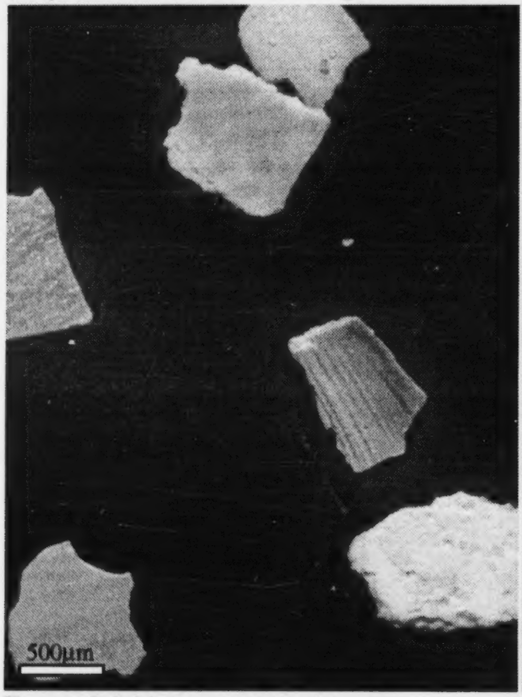

FIGURE 3-1 (c) Phosphatic brachiopods

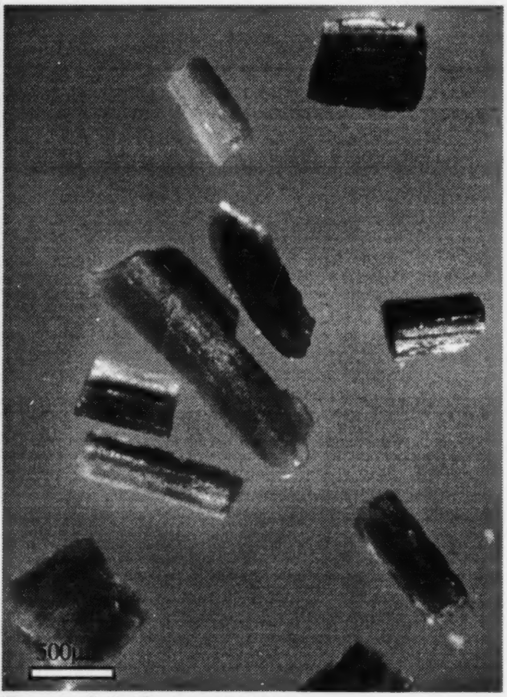

FIGURE 3-1 (d) Conulariids

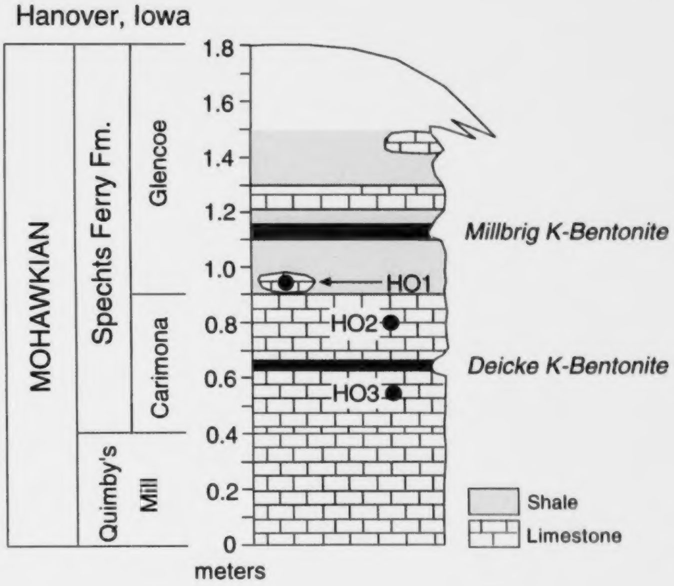

FIGURE 3-2. Carbonate and shale section of the Lower Spechts Ferry Formation, Hanover, Iowa. Shown are the positions of the 3 handsamples used in this study with respect to the Millbrig and Deicke K-bentonites. Biogenic apatites from the Millbrig bentonite bed were also analyzed.

simple cone elements (*Drepanoistodus suberectus*) with crown material and variably developed white matter but no basal body material (Fig. 3-1a). A second type comprised a variety of ramiform and coniform elements with crown material, white matter and visibly preserved basal body material (Fig. 3-1b). Conodonts analyzed in this study have color alteration indices (CAI) of 1.0–1.5, on a scale of 8 (Epstein et al., 1977), indicating diagenetic temperatures <90°C. In addition to conodonts, inarticulate (Ca-phosphatic) brachiopods (Fig. 3-1c) and conulariid fragments (Fig. 3-1d) were analyzed. Our study of brachiopods and conulariids was motivated in part because they are much larger fossils than conodonts and so less effort is required to obtain a quantity sufficient for analysis. Samples were obtained from the lower Spechts Ferry Formation at Hanover, Iowa which contained both the Millbrig and Deicke K-bentonites. A stratigraphic section showing the lithologies and position of the handsamples relative to the bentonites is shown in Fig. 3-2.

ANALYTICAL PROCEDURES

Limestone samples (2 kg) were crushed into fragments smaller than 2.5 cm^3. Conodonts, conulariids and phosphatic brachiopod shells were separated from their enclosing limestone matrix in individual plastic buckets with 10 L of fresh 10% technical-grade acetic acid over a period of 2-

3 days. After reaction was complete, 9 liters of acid were removed and replaced with 9 liters of fresh 10% acetic acid. This step was repeated 2-3 times until complete dissolution of the limestone was achieved. Sample residues with significant clay minerals were soaked in paint thinner overnight, decanted and water added. Clay minerals flocculated and the sample was passed through 20 and 150 mesh sieves. The residue containing biogenic apatites is collected on the 150 mesh sieve and placed in 1,1,2,2, tetrabromoethane (TBE) for 3–5 hours while the apatite sinks. The heavy fraction is washed with acetone to remove TBE and then examined for apatite microfossils.

Using a fine tipped paint-brush, fossils were transferred to polystyrene petri-dishes under binocular microscope and cleaned by brief ultrasonication (3-4 times) in ultrapure water or ethanol to remove potentially adhering non-apatite mineral matter. One brachiopod sample was left overnight in ultrapure NH_4Cl solution to determine whether potentially exchangeable ions on apatite and potential nonapatite crystal surfaces could influence the bulk isotopic composition of the sample. No effects were observed. All samples were weighed in Al-foil boats on a Mettler microbalance with a weighing uncertainty of ±1.4%. Samples were dissolved in 0.2–1.0 M HNO_3 acid in sealed teflon containers until a solution containing only flocculated organic matter was obtained. Occasional heating and ultrasonication aided the dissolution process.

Weighed aliquots of mixed ^{150}Nd-^{149}Sm and ^{84}Sr-^{87}Rb spikes were added to all sample solutions and subsequently evaporated to dryness. Sample-spike equilibration and conversion to the chloride form was achieved by redissolving the residue in a few mls of 1.5 M HCl and then evaporated again. Subsequently, the sample was redissolved in 200 μl of 1.5 M HCl and loaded onto a 10 cm column containing 1.42 ml of 200-400 mesh AG50W-X8 cation exchange resin for separation of Rb, Sr and REE. The Sr cut was passed through the column a second time to ensure low Ca contents. Purified Rb and Sr were redissolved in 1μl of ultrapure water and loaded in the chloride form onto the side Re filament of a double filament assembly. Separation of Sm and Nd from each other and the other REEs was done on a column of di(2-ethylhexyl)phosphoric acid coated biobeads (Biorad). The complete conversion of (Sm, Nd)Cl_3 to (Sm, Nd)HNO_3 was critical to achieving stable intense ion beams during mass spectrometry. The conversion was accomplished using 3.0 ml of 8.0 N HNO_3 acid and evaporated until just dry. Purified Sm and Nd were redissolved in 1.5μl of 0.1 M HNO_3 and loaded onto the side Re filament of a double filament bead.

The isotopic compositions and concentrations of totally spiked Sr and Nd were determined on a VG 354 using dynamic multi-collector routines and in-house software. Raw ratios for Sr isotopes were corrected for variable mass-discrimination effects to $^{86}Sr/^{88}Sr = 0.1194$ using an exponential law, and for the effects of low (non-^{84}Sr) tracer isotopes. Rb isotope ratios were analysed on a single collector instrument. Mass discrimination effects on Nd isotope ratios were corrected to $^{146}Nd/^{144}Nd = 0.7219$ using an exponential law, and also for the effects of low abundance (non-^{150}Nd). Sm was analysed by static multi-collection with corrections for mass fractionation relative to $^{152}Sm/^{154}Sm = 1.17537$ (Wasserburg et al., 1981) applied using an exponential law. Spiked aliquots of the La Jolla Nd standard gave spiked unmixed $^{143}Nd/^{144}Nd=0.511848 \pm 0.000008$. External reproducibility (determined on multiple runs of our in house Nd_2O_3 standard) is ± 0.000016 (2σ) which is taken as the minimum estimate of the uncertainty of the $^{143}Nd/^{144}Nd$ of an unknown sample. As an additional check on the accuracy of spike unmixed $^{143}Nd/^{144}Nd$ determinations, $^{145}Nd/^{144}Nd$ was monitored for all totally-spiked samples yielding 0.348405 ($2\sigma_m$). Multiple runs of the SRM 987 standard gave 0.710232 ± 0.000012 ($2\sigma_m$). A spiked aliquot of SRM 987 (after Rb-Sr separation) gave a spike unmixed ratio of 0.71024, in agreement with our unspiked determinations. A minimum estimate of external reproducibility for $^{87}Sr/^{86}Sr$ is ± 0.00002 (2σ) based on SRM 987 determinations. Nd isotopic analyses are reported in the standard epsilon notation where $\varepsilon_{Nd} = [(^{143}Nd/^{144}Nd)_{sample}(t) / (^{143}Nd/^{144}Nd)_{CHUR}(t) - 1]10^4$, where CHUR is the chondritic uniform reservoir with a present day $^{143}Nd/^{144}Nd = 0.512638$ and $^{147}Sm/^{144}Nd = 0.1967$.

Microprobe analysis of Ca and P contents in conodonts and phosphatic brachiopods were conducted on an ARL SEMQ instrument using a Durango fluorapatite standard with an uncertainty of ± 1.0% (1σ). Compositional X-ray maps were determined on a JEOL 8900R instrument with a 0.3 μm spacing, count times of 100 ms and a beam current of 50 ηA. A modern marine tooth was released from the jaw of a monkfish purchased from the Seattle fishmarket by emaciation in a bucket of distilled water over a period of one month and then mounted directly for probe analysis.

Table 3-1 Sr and Nd isotopic and elemental data for biogenic apatites

Sample	Rb	Sr	$^{87}Rb/^{86}Sr$	$^{87}Sr/^{86}Sr$	$^{87}Sr/^{86}Sr$	Sm	Nd	$^{147}Sm/^{144}Nd$	$^{143}Nd/^{144}Nd$	$^{143}Nd/^{144}Nd$	ε_{Nd}^{+}
	ppm	ppm		t=0	t=454 Ma	ppm	ppm		t= 0	t=454 Ma	t=454 Ma
HO-1 Handsample (Hanover, Iowa, Spechts Ferry Formation, 18 cm below Millbrig K-bentonite)											
Coniform conodonts											
1.	0.895	7454	0.00035	0.708022 (18)	0.708020	37.5	176.8	0.1281	0.511679 (29)	0.511298	-14.7 ±0.6
2.	0.708	6061	0.00034	0.708096 (09)	0.708094	—	—	—	—	—	—
Ramiform and coniform conodonts (with basal bodies)											
3.	0.845	3414	0.00072	0.708100 (10)	0.708095	309.6	1417	0.1321	0.511689 (12)	0.511296	-14.8 ±0.2
4.	0.821	3677	0.00065	0.708246 (24)	0.708242	—	—	—	—	—	—
5.	0.878	3689	0.00069	0.708218 (16)	0.708214	212	1015	0.1263	0.511646 (38)	0.511270	-15.3 ±0.7
6.	0.624	3645	0.00050	0.708176 (24)	0.708173	—	—	—	—	—	—
Inarticulate brachipods											
7.	1.63	2489	0.00189	0.708257 (10)	0.708245	557.1	2383	0.1413	0.511739 (14)	0.511319	-14.3 ±0.3
8. *	1.16	2344	0.00143	0.708295 (15)	0.708286	624.6	2706	0.1396	0.511694 (19)	0.511279	-15.1 ±0.4
9.	2.13	2402	0.00257	0.708361 (17)	0.708344	494.4	2300	0.1300	0.511701 (10)	0.511315	-14.4 ±0.2
Conulariids											
10.	0.704	2139	0.00095	0.708387 (10)	0.708381	531.3	2300	0.1397	0.511738 (18)	0.511323	-14.3 ±0.3
11.	1.12	2222	0.00146	0.708367 (12)	0.708358	—	—	—	—	—	—
Enclosing limestone matrix											
12. HO-1 w.r.	—	—	—	0.708064 (10)	—	—	—	—	—	—	—
HO-2 Handsample (Hanover, Iowa, 13 cm above Diecke and 30 cm below the Millbrig K-bentonite)											
Ramiform and Coniform conodonts (with basal bodies)											
13.	—	—	—	—	—	71.4	333.1	0.1296	0.511667 (14)	0.511282	-15.1 ±0.4
Enclosing limestone matrix											
14. HO-2 w.r.	—	—	—	0.708123 (15)	—	—	—	—	—	—	—
HO-3 Handsample (Hanover, Iowa, 10 cm below Deicke K-bentonite)											
Ramiform and Coniform conodonts (with basal bodies)											
15.	—	—	—	—	—	32.9	169.0	0.1175	0.511779 (22)	0.511430	-12.2 ±0.4
Enclosing limestone matrix											
16. HO-3 w.r.	—	—	—	0.708050 (17)	—	—	—	—	—	—	—
Millbrig K-Bentonite Handsample (Hanover, Iowa)											
Coniform conodonts											
17.	0.453	8956	0.00015	0.708068 (14)	0.708067	—	—	—	—	—	—
Ramiform and coniform conodonts (with basal bodies)											
18.	0.823	6227	0.00038	0.708034 (11)	0.708032	22.2	103.1	0.1304	0.511927 (20)	0.511539	-10.0 ±0.4
Conulariids											
19.	0.893	1984	0.00130	0.708443 (12)	0.708435	439.4	1915	0.1387	0.511943 (12)	0.511531	-10.2 ±0.2

[+] $\varepsilon_{Nd} = [\,(^{143}Nd/^{144}Nd_{SAMPLE} / {}^{143}Nd/^{144}Nd_{CHUR}) - 1\,] \times 10^4$ where CHUR is CHondritic Uniform Reservoir with a $^{143}Nd/^{144}Nd = 0.512638$

* sample treated with NH_4Cl overnight

RESULTS

Systematics of Sr and ^{87}Sr / ^{86}Sr

Contrary to the expectation of a unique seawater ^{87}Sr/^{86}Sr at 454 Ma, no single ^{87}Sr/^{86}Sr is preserved among the fossils analysed (Table 3-1) (Fig. 3-3). Rather, ^{87}Sr/^{86}Sr ratios correlate strongly with Sr contents. Coniform conodonts lacking basal body material have the highest Sr and lowest ^{87}Sr/^{86}Sr whereas brachiopods and conulariids have the highest ^{87}Sr/^{86}Sr and the lowest Sr contents. Basal-body-containing ramiform and coniform conodonts yielded intermediate ^{87}Sr/^{86}Sr and Sr contents. Rubidium contents are characteristically low in the analyzed apatites. All ^{87}Sr/^{86}Sr analyses are plotted as initial ratios corrected to 454 Ma, the age of the bentonite (Kunk and Sutter, 1984). Therefore the observed trends do not result from time dependent *in situ* decay of ^{87}Rb.

On the inverse Sr plot (^{87}Sr/^{86}Sr – 1000/Sr), linearly correlated data constitutes evidence of 2 component mixing (Fig. 3-4). The covariance displayed by the HO1 fossils indicates that some form of mixing relationship between contemporaneous Ordovician seawater and a diagenetic fluid is preserved. The most likely source of diagenetic Sr are the adjacent Millbrig and Deicke K-bentonites. The Millbrig bentonite has been correlated throughout eastern North America by geochemical

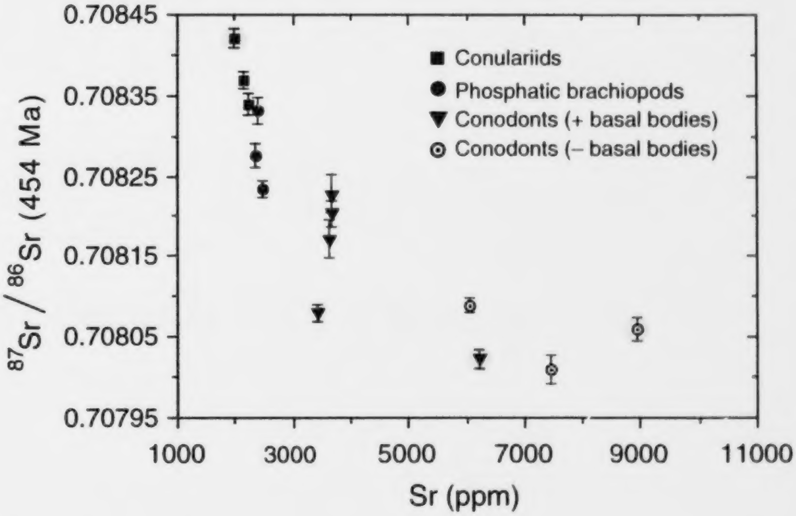

Figure 3-3. Relationship between initial ^{87}Sr/^{86}Sr and Sr concentration of coeval biogenic apatites. Contrary to the expectation of a unique seawater ^{87}Sr/^{86}Sr signature, no single value of ^{87}Sr/^{86}Sr is preserved among the fossil taxa. Eleven of the 14 samples were separated from one 2 kg handsample (HO1). The remaining three analyses (designated by grey background) were obtained from within the Millbrig bentonite layer .

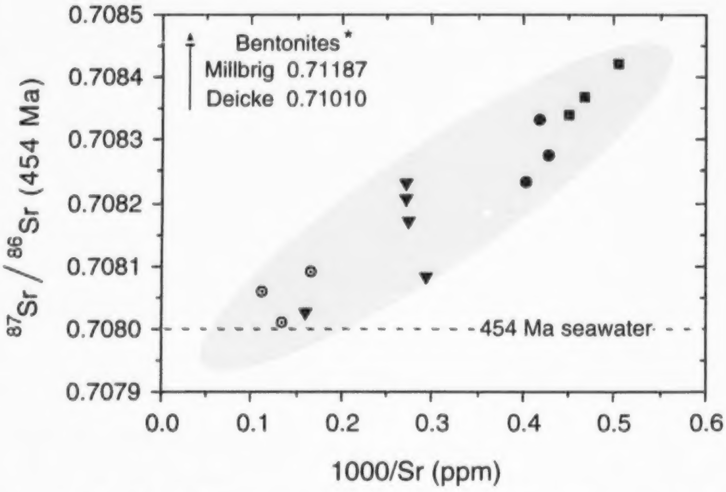

Figure 3-4. Linearly correlated data on the inverse Sr plot indicates potential 2 component mixing. The probable mixing end-members are 454 Ma seawater (~0.7080) and diagenetic Sr leached from the more radiogenic Millbrig and Deicke ash layers during alteration of their original glass constituents. Fossil taxa plot in distinct groups indicating a combination of potentially different original Sr contents and differing susceptibilities to post-mortem Sr-exchange. Phosphatic brachiopods and conulariids are the most susceptible to diagenetic modification of their original seawater signatures and conodonts consisting of 100% crown material are the most resistant. Conodonts (P) with intermediate ^{87}Sr/^{86}Sr and Sr concentrations differ from the other conodonts (O) in having attached basal body material which is deduced to be diagenetically unstable relative to crown material. Initial strontium isotope ratios for Millbrig and Deicke bentonites are from Samson et al., (1989) performed on igneous apatite phenocrysts, and corrected to 454 Ma for this study. Symbols are described in Fig. 3-3.

fingerprinting, wireline logs and phenocryst mineralogy (Kolata et al., 1986; Huff and Kolata, 1990; Haynes, 1994). The original ^{87}Sr/^{86}Sr of the unaltered ash was determined by Samson et al. (1989) on apatite phenocrysts from the Millbrig (0.71188 ±0.00021, 2σ) and Deicke (0.71010 ±0.00008, 2σ). Both ash layers were originally more radiogenic than contemporaneous Ordovican seawater.

The different types of biogenic apatite plot in distinct fields along the mixing trend indicating differing susceptibilities to alteration. It is observed that fossils with the highest Sr concentrations have the most seawater-like ^{87}Sr/^{86}Sr. Generally, these are the basal-body-absent coniform elements. Conulariids and phosphatic brachiopods were consistently more radiogenic than other fossils (and closer to the bentonite in ^{87}Sr/^{86}Sr ratio) indicating they are the most easily altered. The only difference between conodonts with intermediate and high Sr contents is the presence or absence of basal body material, respectively, and so it is deduced that basal body material contains proportionately more radiogenic Sr than crown material. The same diagenetic pattern is evident in fossils analyzed from the Millbrig bentonite (Table 3-1). Basal-body-absent coniform conodonts gave less radiogenic ^{87}Sr/^{86}Sr (0.70807) than conulariids (0.70844). Fragments of ramiform elements with basal bodies mostly broken off (which likely occurred during washing and sieving procedures) yielded higher Sr (6227 ppm) and and lower ^{87}Sr/^{86}Sr (0.70802) than ramiform elements with basal bodies (3606 ppm, 0.708185) from the HO1 handsample, thus confirming that basal bodies are a reservoir of radiogenic Sr (Table 3-1). Interestingly, the magnitude of Sr disturbance is similar for fossils both within and proximal to the ash layer.

Systematics of Nd and ε_{Nd}

The fossil apatites display a range in Nd concentrations (100–2700 ppm) that is 6 times larger than for Sr, but no analogous correlation of Nd and ε_{Nd} is observed (Table 3-1) (Fig. 3-5). Seven analyses of conodonts, conulariids and inarticulate brachiopods from the HO1 handsample yield a mean ε_{Nd} (454) = –14.7±0.3 ($2\sigma_m$), corrected for *in situ* decay of ^{147}Sm to 454 Ma. These values contrast markedly with the initial ε_{Nd}(454) of the original Millbrig (–4.1 ±0.2, $2\sigma_m$) and Deicke (–3.6 ±0.2, $2\sigma_m$) ash (Samson et al. 1989). Ramiform conodonts and conulariids from the

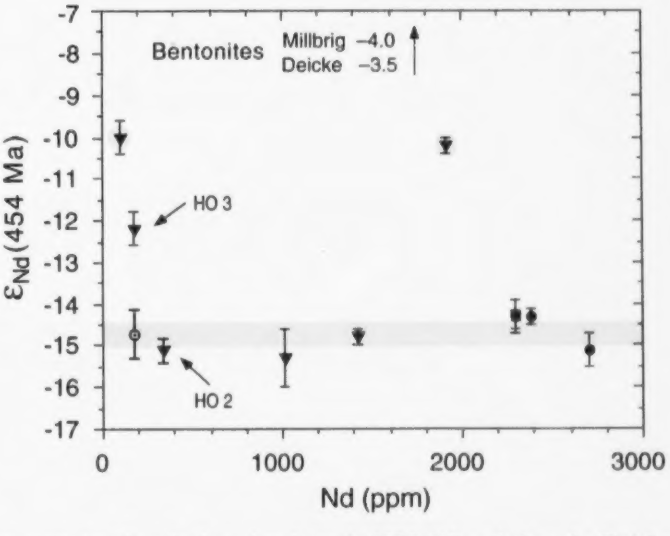

FIGURE 3-5. Relationship between initial ε_{Nd} and Nd concentration in coeval biogenic apatites. In contrast to Sr, the majority of Nd analyses (and all fossils from HO1) yielded the same initial isotopic composition within the analytical uncertainty of each analysis [ε_{Nd} (454)= -14.7 ±0.3; $2\sigma_m$], which is interpreted as the ε_{Nd} of 454 Ma seawater overlying the HO1 depositional site. Two analyses of fossils from within the Millbrig bentonite (gray background) yielded uniformly less radiogenic ε_{Nd} values despite varying greatly in Nd concentration. Fossils from handsample HO3 (10cm below the Deicke bentonite) yielded an intermediate ε_{Nd} value whereas fossils from handsample HO2 (13cm above the Deicke bentonite) yielded an ε_{Nd} value identical to the HO1 fossils. The ε_{Nd} (454) values for the Millbrig and Deicke bentonites are from igneous apatite phenocrysts in Samson et al. (1989). Symbols are described in Fig. 3-3.

FIGURE 3-6 Biogenic apatites have an antithetic distribution of Sr and Nd. Conodonts without basal bodies have the highest Sr and lowest Nd concentrations and brachiopods and conulariids have the highest Nd and lowest Sr. Conodonts with basal bodies have intermediate Sr and Nd concentrations. Data points with gray background are samples from within the Millbrig bentonite.

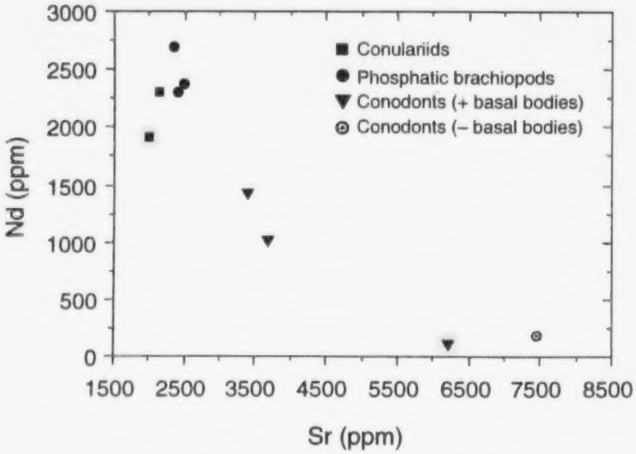

within the Millbrig bentonite yielded less radiogenic but uniform ε_{Nd} values of –10.1, indicating significant incorporation of bentonite-derived Nd. Conodonts from the HO3 handsample (10 cm below the Deicke) gave $\varepsilon_{Nd} = -12.2$, indicating only slight contamination from the bentonite, whereas conodonts from HO2 (13 cm above the Deicke and 30 cm below the Millbrig) yielded an ε_{Nd} value of –15.1, within analytical uncertainty of the HO1 fossils (Table 3-1).

Antithetic distribution of Sr and Nd

The concentration of Sr and Nd display a strong negative correlation within and between the fossil taxa (Fig. 3-6). Conulariids and phosphatic brachiopods have low Sr and high Nd contents whereas basal-body-absent coniform conodonts have low Nd and high Sr. Ramiform and coniform conodonts possessing basal bodies have nearly identical Sr and Nd contents. There is no correlation

FIGURE 3-7. The uniformity in ε_{Nd} values for the majority of fossil taxa contrasts markedly with the spread in $^{87}Sr/^{86}Sr$. Our best estimate for the $^{87}Sr/^{86}Sr$ of 454 Ma seawater is 0.7080, and -14.7 for ε_{Nd} of seawater overlying the HO1 depositional site. The bentonites plot far outside the frame of this plot with $^{87}Sr/^{86}Sr$ ratios of ~0.711 and ε_{Nd} values of -4 to -5.

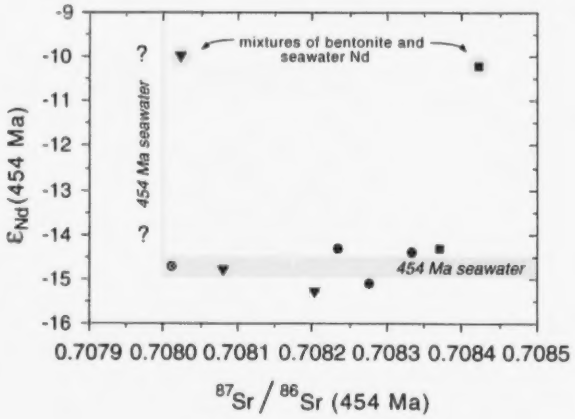

Table 3-2. Electron microprobe results for Ca and P contents in biogenic apatites

Type	Ca (wt.%)	P (wt.%)	Ca/P (atom)
Conodont crowns			
1.	37.03	17.67	1.62
2.	38.09	17.99	1.64
3.	37.92	17.65	1.66
4.	37.35	17.56	1.64
Average (1σ)	37.59 ±0.5	17.72 ±0.2	1.64 ±0.02
Conodont basal bodies			
1.	34.24	14.00	1.89
2.	35.00	14.41	1.88
3.	34.03	14.16	1.86
4.	32.25	13.33	1.87
5.	34.26	13.82	1.92
Average (1σ)	33.0 ±1	13.94 ±0.4	1.88 ±0.02
Phosphatic brachiopod shells			
1.	35.39	14.65	1.87
2.	35.87	14.65	1.89
3.	36.15	14.81	1.89
4.	32.20	13.23	1.88
5.	28.47	11.76	1.87
6.	28.38	11.42	1.92
Average (1σ)	32.7 ±3.6	13.42 ±1.5	1.89 ±0.02

between $^{87}Sr/^{86}Sr$ and ε_{Nd} (Fig. 3-7). Compositional x-ray maps of the simple cone conodont *Panderodus gracilis* show that this antithetic distribution of Sr and Nd contents also exists within single conodonts, specifically those with basal bodies (Fig. 3-8). Crown material is high in Sr but low in Nd whereas basal body material has low Sr and high Nd, consistent with Pietzner (1968) who analysed Sr-Y distributions. The distribution of Sr in conodont basal body material is uniform, as is the distribution of Sr and Nd in brachiopods and conulariids.

Differing Ca/P (atom) between conodont crown (1.64) and basal body (1.88) material (Table 3-2) suggests that the observed antithetic distribution of Sr and Nd reflects a compositional difference between crown and basal body apatite. The Ca/P ratio in phosphatic brachiopods (1.89) is identical to that of conodont basal bodies. Backscattered electron imaging and absence of microprobe burn scars indicates that basal body material is less dense but more refractory than crown material. Phosphatic brachiopod fragments are the least refractory biogenic apatite analysed. Microprobe analysis of a modern monkfish tooth showed no gradient in Sr analogous to that observed in the conodont crown material.

Conodont leach experiment

Since the microprobe results suggest that basal body material is more refractory than crown material, leaches were undertaken to determine whether diagenetic Sr is contained in the basal body, crown, or uniformly distributed throughout the element. A one-milligram sample of *Panderodus*

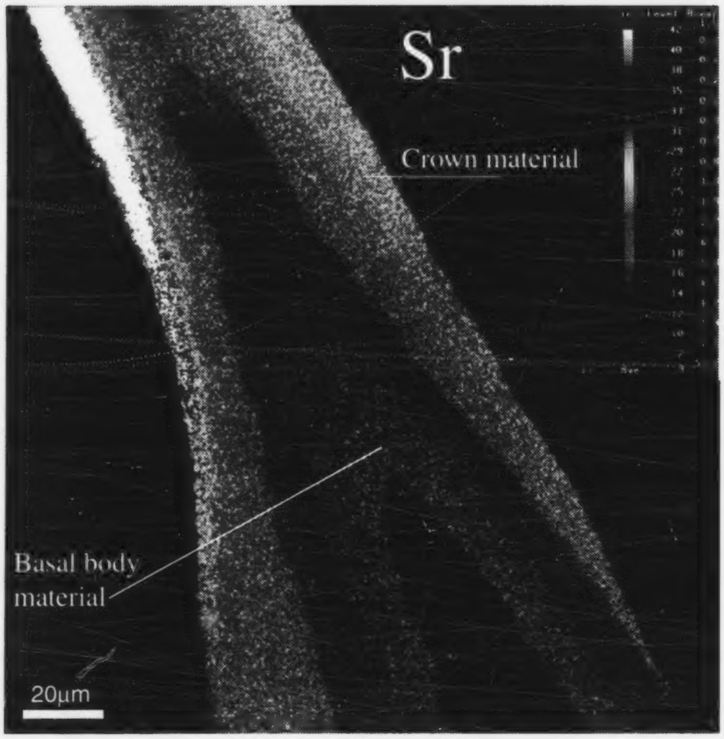

Figure 3-8. Sr and Nd X-ray maps of the conodont *Panderodus gracilis* which has a simple cone in cone structure. The outer cone is enamel like crown material and the inner cone is basal body material, shown here in section. **(a)** Antithetic distribution of Sr in *Panderodus* showing high Sr in crown material and low Sr in basal bodies. In addition, conodont crowns display a gradient of increasing Sr contents towards the rim. Sr contents in basal bodies are uniform

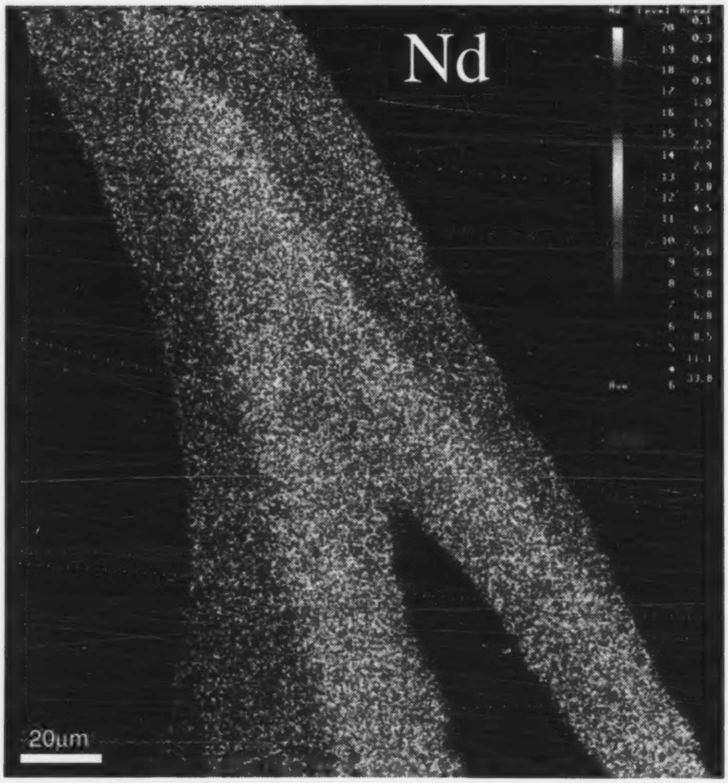

(b) Antithetic distribution of Nd in *Panderodus* showing high Nd in basal bodies and low Nd in crown material. The opposite of Sr.

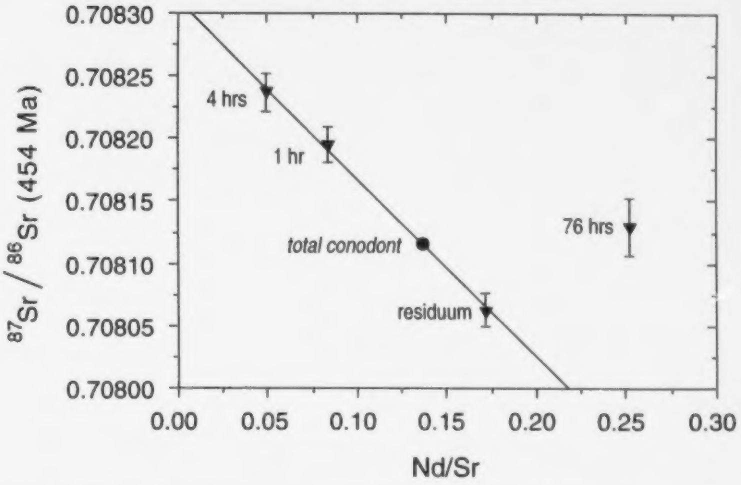

FIGURE 3-9. Leaching of *Panderodus gracilis* in 5% unbuffered acetic acid. Cumulative leach times are indicated on the plot. Dissolution begins with the crown material. The first leach was stopped just as crown material began to whiten. At 4 hrs, most crown material was visibly whitened and denticles tips showed evidence of dissolution. At the end of the long 3rd leach, about 1/3 to 1/2 of the tip of each denticle was dissolved away and basal bodies also appeared to be thinning and disaggregating. Basal bodies (which have a translucent brown appearance under the light microscope) did not appreciably whiten. The first two leaches and the residuum fall on a mixing line. The long third leach falls off the line, containing an excess of Nd. Table 3 shows that during leach 3, 62% of the total Nd was released indicating that significant basal body material dissolved during the long leach. The mixing line is interpreted as mixing between Sr and Nd in successively deeper layers of crown material. Therefore the residuum consisted of mostly inner layers of crown material. The 3rd leach falls off the mixing line because the Nd/Sr and ^{87}Sr/^{86}Sr systematics are different, potentially indicating different diagenetic histories for conodont crown and basal body material.

gracilis was leached in 5% unbuffered acetic acid. *Panderodus gracilis* has a cone in cone structure; an outer cone of crown material and an inner cone of basal body material. Three leaches were obtained with cumulative leach times of 1hr, 4 hrs and 76 hrs. The residuum was also analyzed. Leach progress was monitored using a binocular microscope. Initially, crown material appeared more susceptible to acid dissolution than basal body material as evidenced by whitening of the denticles followed by denticle thinning from tip to base. As crown material was leached away, brown translucent basal body material was increasingly exposed. Basal body material did not appreciably whiten during the leach suggesting greater resistance to acid dissolution, however, after 2-3 days the basal bodies appeared to be thinning and disaggregating even though significant crown material remained.

The 3 leaches and residuum were analyzed for Sr and Nd contents and ^{87}Sr/^{86}Sr ratios (Table 3-3). On a plot of ^{87}Sr/^{86}Sr–Nd/Sr, linearly correlated data constitute potential mixing lines.

Table 3.3 *Panderodus* leach results for Nd, Sr and $^{87}Sr/^{86}Sr$

Sample	$^{87}Rb/^{86}Sr$ (measured)	$^{87}Sr/^{86}Sr$ (measured)	$^{87}Sr/^{86}Sr$ t=454 Ma)	Nd (nmole)	Sr (nmole)	Nd/Sr (atom)	Mole % Sr	Mole % Nd
Leach 1	0.00289	0.708214 (14)	0.708195	0.8544	10.209	0.084	17.5	10.7
Leach 2	0.00244	0.708253 (15)	0.708237	1.0586	21.769	0.049	37.2	13.2
Leach 3	0.00264	0.708146 (23)	0.708129	4.9586	19.711	0.252	33.8	61.8
Residuum	0.00969	0.708126 (13)	0.708063	1.1504	6.6920	0.172	11.5	14.3
Total	——	——	0.708115	8.022	58.381	0.137	100	100

Initial weight of sample = 0.000924 g   Total: Nd = 1252.3 ppm , Sr = 5534.8 ppm

If dissolution progressed from the crown rim to the core of the basal body, solution Nd/Sr should increase with successive leaches. Such a pattern is not observed (Fig. 3-9). Leach 1 has higher Nd/Sr than leach 2 and the residuum has lower Nd/Sr than leach 3. Examination of % Nd and %Sr leached in each leach aliquot (Table 3-3) reveals that the first 2 leaches contained more Sr than Nd (consistent with dissolution of the high Sr rim in crown material). The high Nd/Sr ratio of the 3rd leach indicates significant dissolution of basal body material. For example, the first 3 leaches contain 89% of total conodont Nd whereas total dissolution of an identical amount of crown material containing 200 ppm Nd would yield only 16% of this amount. It is concluded that basal bodies dissolved throughout the leach experiment with most of the dissolution occurring in the long 72 hr leach.

The covariance observed between $^{87}Sr/^{86}Sr$ and Nd/Sr reflects some form of mixing relationship between two Nd/Sr reservoirs within *Panderodus*. Since leach 3 falls off the mixing line crown and basal body material cannot be the mixing end-members. Rather the mixing observed is like between successive layers of crown material with decreasing Nd/Sr ratios. The fact that the residuum lies on the mixing line indicates that mostly crown material remained after the third leach.

The results of the leach experiment indicate that the high Sr rim of *Panderodus gracilis* contains radiogenic Sr and that progressively less radiogenic Sr is encountered deeper within the enamel-like crown material. Indeed the residuum (upon correction of a significant quantity of ^{87}Rb relative to the other leaches) yielded a $^{87}Sr/^{86}Sr$ of 0.70806, within analytical uncertainty of conodonts without basal bodies. We have no explanation for the high Rb in the residuum, but the trend towards decreased $^{87}Sr/^{86}Sr$ with increased leaching is well established.

DISCUSSION

The susceptibility to diagenetic disturbance of conodonts, phosphatic brachiopods and conulariids has been clearly demonstrated. The result that ε_{Nd} is better preserved than $^{87}Sr/^{86}Sr$ is surprising because Nd is acquired almost entirely post-mortem whereas teeth and bones in living marine vertebrates contain relatively high *in vivo* Sr contents (Schmitz, et al., 1991). If increasing Nd concentration is considered an index of diagenetic reactivity then phosphatic brachiopods, conulariids and conodont basal bodies are diagenetically more reactive than conodont crown material. This interpretation is supported by the more radiogenic $^{87}Sr/^{86}Sr$ in brachiopods and conulariids relative to conodonts lacking basal bodies and the intermediate $^{87}Sr/^{86}Sr$ and Sr contents of conodonts with basal bodies. The leaching of *Panderodus* suggests that crown material may also contain diagenetic-Sr which may be removed through progressive leaching. Therefore subtle differences exist in conodont crown material that causes some crowns (*Panderodus*) to be more susceptible to diagenetic disturbances than others (*Drepanoistodus*). This observation may reflect the abundance of white matter in conodont crowns which is characterized by numerous unconnected holes and relatively smaller crystallites than the bulk of crown material (Pietzner et al. 1968; Barnes et al., 1973). Although, *Drepanoistodus* and *Panderodus* both contain white matter, its distribution, relative abundance or uniformity from one element to another is difficult to ascertain. The main difference is that *Drepanoistodus* consists of 100% crown material that is relatively thick and robust compared to *Panderodus* whose crown material forms an external sheath and thin tip. Evidence of histological homology between conodont mineralized tissue types and vertebrate enamel, dentine and bone prompts a review of the dental literature to gain additional insight into diagenetic effects observed in conodonts.

Comparative chemistry and crystallography of modern vertebrate and ancient conodont apatites

All biogenic apatites in vertebrates are composed of small crystals of dahllite in a matrix of collagen. Enamel contains substantially less collagen and larger more densely packed crystallites (0.13–0.03 μm) than dentine or bone (0.02–0.004 μm) (LeGeros and LeGeros, 1984). Enamel crystallites are long and rod-shaped whereas those of dentine and bone are equidimensional. Conodont crowns and basal bodies show similar differences in crystal sizes and morphologies. At 8000 times magnification, scanning electron micrographs reveal that conodont crown material is composed of elongate crystals of francolite oriented with respect to a lamellar organic framework (Burnett and Hall, 1992). Observed crystallite diameters are ~0.5 μm with a length to width ratio >10, but may represent bundles of crystals rather than individual crystallites (Barnes et al. 1973). Basal bodies contain most of the visible organic matter in conodonts which is often spongy in appearance. At 8000 times magnification, basal bodies consist of botryoidal masses in a closed or open framework (Burnett and Hall, 1992). Although crystallites are too small to be seen, a decrease in the *a* lattice-constant for basal bodies relative to crown material (Pietzner, 1968) indicates more equidimensional crystallites (McClellan and Lehr, 1969) in basal bodies.

In vertebrate dahllites, crystal morphology is linked to CO_3^{-2} contents (LeGeros and LeGeros, 1984; Grunner et al., 1937). Substitution of CO_3^{-2} for PO_4^{-3} leads to destabilization of the dahllite lattice resulting in smaller more equant crystallites (Okazaki et al., 1981). At CO_3^{-2} contents greater than 8–10 wt.%, the lattice cannot form (McClellan and Lehr, 1969). Teeth with their large rod-shaped crystallites contain less CO_3^{-2} (3.5 wt.%) than dentine or bone (5–6 wt.%) which have small equant crystallites. Okazaki et al., (1981) showed that the *crystallinity* of dahllites (determined by X-ray diffraction as the inverse of the measured half-peakwidth of the (002) reflection) decreased and solubilities increased in precipitates with increasing CO_3^{-2}/PO_4^{-3} ratios. A temperature effect was also observed wherein the *crystallinity* of precipitates formed at increasing temperatures (40°, 60° and 80°C) and constant CO_3^{-2} contents also increased. The crystallinity/solubility behavior of crystals formed at 80°C was nearly constant over the entire range of natural CO_3^{-2} substitution in dahllite.

Pietzner et al. (1968) determined by wet chemical methods that conodont crown material contained 1.84 wt.% CO_3^{-2}. Although basal body CO_3^{-2} was not measured, the decrease in the *a* lattice-constant for basal body francolite (9.35 Å) relative to crown francolite (9.37 Å)(as measured by Pietzner, 1968) is consistent with greater CO_3^{-2} contents in the former (McClellan and Lehr, 1969). Likewise the higher Ca/P (atom) of basal bodies (1.88) relative to crown material (1.64) is also consistent with increased substitution of CO_3^{-2} for PO_4^{-3} (Table 3-2). The corresponding Ca/P of vertebrate teeth and bones is 1.6 and 1.8, respectively (LeGeros and LeGeros, 1984). To obtain a Ca/P of 1.88 for conodont basal bodies (and phosphatic brachiopods) requires ~3 times more substituted CO_3^{-2} than that occurring in the crown material analyzed by Pietzner (1968), for a total of 5–6 wt.% CO_3^{-2} , similar to vertebrate bone. Crystallochemically, conodont crowns and basal bodies are analogous to vertebrate teeth and bones, respectively.

Comparative diagenesis of vertebrate and conodont apatites

Post-mortem increase in the Sr content of bone is established in both field (Nelson et al., 1986; Tuross et al., 1989; Koch et al., 1992) and laboratory (Hodge et al., 1946; Gedalia et al., 1976; Lambert et al., 1985) based studies. Tuross et al., (1989) showed that the uptake of Sr in taphonomic bone can occur rapidly in a natural weathering environment. A ten year collection of bone samples from a wildebeest carcass showed correlated increases in both Sr/Ca and *crystallinity* (measured by X-ray diffraction as growth in the c-axis direction of bone crystallites). Attempts to remove diagenetic Sr by rinsing in buffered acetic acid showed that some Sr was adsorbed and therefore easily leached. A second fraction was unleachable indicating Sr-Ca exchange in the dahllite lattice, possibly facilitated by Ostwald ripening; a process of simultaneous dissolution and recrsytallization of aggregates of very small crystals in the presence of a fluid (Eberl et al., 1990). During Ostwald ripening mean crystallite size increases (the smallest crystals dissolving preferentially) until all crystals are the same size. The largest crystals in the population do not dissolve but may become zoned by progressively younger mineral overgrowths.

Since the apatite lattice strongly discriminates against Sr (favouring Ca) in both biological and abiological systems, a positive chemical potential is required to effect Sr–Ca exchange. However the distribution coefficient (K_d), defined as

$$(\mathrm{Sr/Ca})_{\mathrm{apatite}} = K_d\ (\mathrm{Sr/Ca})_{\mathrm{water}}$$

is poorly constrained. Odum compiled apparent K_ds between 0.21–0.26 for teeth and bones of marine vertebrates (Odum, 1955a; Table 7). In a study of Ca-Sr solid solution in inorganically precipitated hydroxyapatite, Collin (1959) showed that the precipitate Sr/Ca is correlated with solution Sr/Ca. The curve is nearly linear at low solution Sr/Ca (closer to natural waters) yielding a K_d =0.30, similar to biogenic apatites. Choosing a median K_d of 0.25 and assuming a seawater 1000Sr/Ca (atom) ratio of 8.5, modern fish apatites should have have 1000Sr/Ca ratios of ~2.1. If teeth and bones are considered ideal hydroxyapatite $[\mathrm{Ca_{10}(PO_4)_6OH)_2}]$ then stoichiometric Ca contents of 39.89 wt.% yield a Sr concentration of ~1800 ppm for marine biogenic apatites. However, biogenic apatites are rarely stoichiometric with Ca contents ranging from 36.5 (enamel) to 24.5 wt.% (bone) (LeGeros and LeGeros, 1984), yielding Sr concentrations between 1676 and 1125 ppm, respectively. These concentrations are consistent with those reported in Schmitz et al. (1991) for a modern cod bone (1100 ppm) and shark tooth (1630 ppm), and Sr contents for Recent seafloor phosphorites (McArthur, 1978).

The Sr contents of fossil apatites analyzed in this study are higher than in vivo Sr contents in modern living fish apatite. Using average Ca concentrations from Table 3-2 and assuming a marine 1000Sr/Ca (atom) ratio of 8.5 for Ordovician seawater, Sr/Ca for phosphatic brachiopods ranges from 3.3–3.5 and conodont crowns range from 7.4 to 10.9, much higher than the predicted marine value of 2.1.

All biogenic apatites in this study increased their Sr contents post-mortem with conodont crown material gaining substantially more Sr than basal body material, conulariids or phosphatic brachiopods. The Sr gradient in conodont crowns has a precedent in gradients of Sr and F observed in human dental enamel. Little and Barret (1976) documented Sr gradients in erupted human tooth enamel with up to 4 times higher Sr in surface enamel than in bulk enamel. The Sr gradient is not established in the enamel of young pre-erupted molars (Frank et al., 1989) indicating that Sr is being

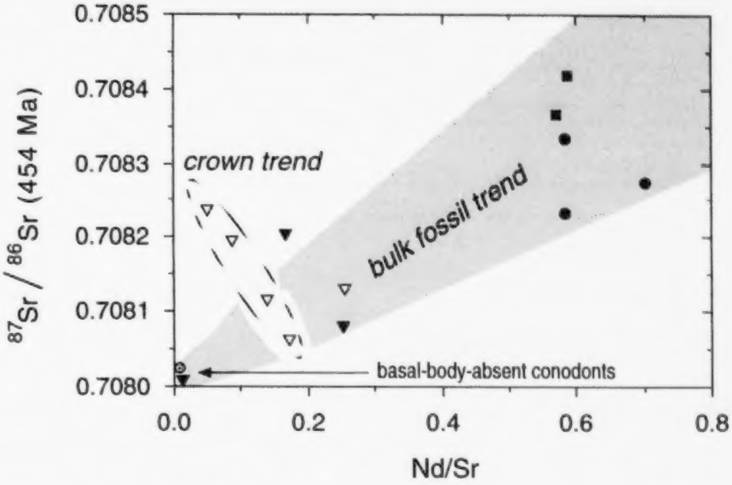

Figure 3-10. All samples for which there is both Sr and Nd isotopic data are plotted, along with the leaches. This is essentially the same plot as Fig. 5-4, normalized to Sr, but enables comparison of the leach data with other samples. The negative slope displayed by the leach data contrasts with the positive slope observed for whole fossil data. The difference is attributed to compositional differences between conodont crowns and conodont basal bodies, brachiopods and conulariids which we interpret to reflect different diagenetic histories for these materials.

sequestered from the external environment through water and food (Little and Barret, 1976). A reverse gradient in dentine (demonstrating potential uptake of Sr from body fluids) is not observed. Relative to enamel, dentine has lower more uniform Sr concentrations (Frank et al., 1989).

The tooth from the marine monkfish showed no Sr gradient analogous to conodont crowns or human teeth. Indeed, a Sr-gradient in marine fish teeth will only develop if the Sr/Ca of the external fluid is higher than seawater. In terrestrial environments the external Sr/Ca of fluids which may come in contact with teeth can range widely (Odum, 1955b) whereas in the marine environment the Sr/Ca of the seawater is very uniform (De Villiers et al., 1993). Conditions for uptake of Sr in marine apatites will occur post-mortem because marine sediment pore fluids generally have higher Sr/Ca ratios (Stout, 1985) than seawater because of dissolution of metastable biogenic carbonates and precipitation of carbonate cement which incorporates less Sr (Baker et al., 1982). Degradation of volcanic ash is another major contributor of Sr to sediment pore fluids (Elderfield and Gieskes, 1982). Consequently, the most likely environment to develop the Sr gradient observed in conodont crowns is during early marine diagenesis in sediments dominated by carbonate lithologies. If there are no volcanics in the section and clastic detritus is low, early marine diagenesis should reinforce the original seawater ^{87}Sr/^{86}Sr signature in biogenic apatites because most of the pore fluid Sr originates from dissolution of marine biogenic carbonates. This process of isotopic buffering explains the observed correlation between high Sr contents and increasingly marine-like $^{87}Sr/^{86}Sr$ in Figure 3-4.

Isotopic buffering does not appear to operate in conodont basal bodies, phosphatic brachiopods or conulariids. If conodont basal bodies are diagenetically more reactive than conodont crown material, then why doesn't Sr follow Nd in being more concentrated in basal bodies? A possible explanation is that the compositional differences between conodont crowns and basal bodies imply different diagenetic histories. Different apparent mixing trajectories are exhibited by the leaching of predominantly crown material in *Panderodus* compared to the apparent mixing array represented by bulk fossils consisting of crystallochemically similar brachiopods, conulariids and basal-body-containing conodonts (Fig. 3-10). It is possible that basal bodies, conulariids and brachiopods remain diagenetically reactive over a longer period of time, perhaps due to their smaller crystal sizes, but to explain their relatively low Sr contents a recrystallization step is required which would release Sr to pore waters. Several authors have noted that the organic lamellae of basal bodies sometimes appear to outgrow the mineralized portion indicating an apparent shrinkage of the basal body (Lindstrom and Ziegler 1971;1981). We suggest that the basal bodies have been extensively recrystallized by Ostwald ripening, and that their low Sr/Ca reflects the Sr/Ca of the last equilibrated fluid. Since trivalent Nd has a greater ionic potential than divalent Sr, Nd is predictably less mobile in the confined pore fluid environment and therefore less responsive to changes in fluid chemical potentials throughout the course of diagenesis. Therefore the Nd contents may remain elevated during recrystallization even though Sr is lost.

The low mobility of Nd in pore fluids is implied in the results of Bernat (1975) showing that the Nd content of deep sea ichthyoliths did not increase with increasing depth in the sediment. The lack of a Sr gradient, or conversely the uniform distribution of Sr and Nd in conodont basal bodies, is consistent with recrystallization. The preservation of a Sr gradient in conodont crown material suggests that Ostwald-type effects are less developed and that crown material is less recrystallized. If correct, a corresponding gradient in Nd should also exist in crown material but probably lies below the detection sensitivity of our methods. Although the low Nd contents of crown material, have been empasized, they are low relative to basal bodies. Compared to Nd contents in modern fish teeth (0.006 ppm; Shaw and Wasserburg, 1985), conodont crowns are 55,000 times more enriched, whereas Sr is about 5 times enriched. Indeed, partitioning of Sr and Nd in high temperature apatite-igneous-melt systems show that Nd is much more compatible in the apatite lattice than Sr (Watson and Green, 1981). Therefore the low Nd contents of conodont crowns (and their greater resistance to alteration) probably reflects the denser enamel-like structure of crown material which inhibits diffusion of seawater through intercrystalline spaces.

The last aspect of diagenesis that merits discussion is the possibility of diagenetic artefacts introduced into apatitic fossils during their acid extraction from limestone. The effect is probably negligible for Sr, because even if the $^{87}Sr/^{86}Sr$ of the limestone were very different from the conodonts, the 1000Sr/Ca (atom) ratio in limestone is ~0.5, and therefore not high enough to promote uptake of significant Sr from the solution. Shaw and Wasserburg (1985) showed that conodont surfaces could adsorb Nd from an external solution. During conodont extraction, the Nd most likely to be released into solution is from the carbonate, which is probably similar in isotopic composition to the Nd in the conodonts. A possible blank contribution from the reagents used is likely negligible considering the high Nd contents of biogenic apatites and the reproducibility of our analyses which range widely in Nd contents.

CONCLUSIONS AND IMPLICATIONS FOR PALEO-SEAWATER STUDIES

Phosphatic brachiopods, conulariids and basal-body-containing conodonts are unreliable recorders of past seawater $^{87}Sr/^{86}Sr$ whereas conodonts consisting of 100% crown material appear well suited for this purpose. Cummins et al. (1994) likewise showed that the bulk of undifferentiated biogenic apatites were more radiogenic in $^{87}Sr/^{86}Sr$ than coexisting calcitic brachiopods and Bertram et al. (1992) correctly suggested that the difference in $^{87}Sr/^{86}Sr$ ratios between *Ozarkodina* and *Dendacodina* is due to the presence of basal bodies in the latter conodont species. The crystallochemical basis for these observations is: (1) enamel is denser than other apatitic components which slows the diffusion of pore waters through intercrystalline spaces, and (2) enamel crystallites are larger and therefore less susceptible to modification by Ostwald-type effects. A pattern observed in this study is that apatites with the highest Sr contents have the most seawater-like ^{87}Sr/^{86}Sr signatures. This may be generally true of all conodonts separated from marine limestones because of isotopic buffering by high Sr/Ca pore waters accompanying early carbonate diagenesis.

Our best estimate for the ^{87}Sr/^{86}Sr of 454 Ma seawater is 0.7080 based on analyses of conodont crown material and the enclosing HO1 limestone which were identical within the analytical uncertainty. Since the leach experiment showed that crown material may also contain diagenetic-Sr, the true ^{87}Sr/^{86}Sr of 454 Ma seawater may have been slightly lower. The lowest limestone value obtained by Burke et al. (1982) for 454 Ma seawater is 0.7079 (after adjustment for an interlaboratory difference in SRM 987). The results of this study indicate that if conodont crown material is used, and if a leaching protocol is adopted, the Paleozoic portion of the seawater ^{87}Sr/^{86}Sr curve can be better resolved than at present.

Suggestions by Bertram et al. (1992) and Cummins et al. (1992) that there exists a threshold color alteration index (2.5) below which conodonts may be considered unaltered is not supported by this work since the conodonts analysed in this study have the lowest possible CAI values (1.0–1.5). Compositional differences and the Sr/Ca of diagenetic fluids are more important than temperature as a diagenetic variable and so the positive covariance shown by Bertram et al. (1992) between conodont ^{87}Sr/^{86}Sr and CAI cannot be interpreted because the influence of conodont composition was not considered and the samples come from different diagenetic environments.

In contrast to Sr, all biogenic apatites appear to record the ε_{Nd} value of past seawater presumably because the initial uptake of Nd at the sediment-water interface is so large, and subsequently, Nd has limited mobility in pore fluids. Even conodonts deposited within the Millbrig bentonite preserve a component of seawater-derived Nd. In general, the occurrence of bentonites in a stratigraphic section will impact significantly on fossil apatite ^{87}Sr/^{86}Sr, but will be negligible for ε_{Nd}. The suggestion by Bertram et al. (1992) that conodont ε_{Nd} values may be as equally prone to diagenetic disturbance as ^{87}Sr/^{86}Sr is not supported by this study. Their plot showing positive covariance between $^{87}Sr/^{86}Sr$ and Nd contents results from the general antithetic distribution of Sr and Nd in compositionally diverse apatitic fossils and has no direct bearing on the preservation of seawater Nd isotopic compositions. Bertram et al., (1992) also discovered that leaching their conodonts in weak 0.2 HNO_3 acid provided more reproducible $^{87}Sr/^{86}Sr$ results than when stronger acids were used. They attributed this observation to the presence of basal body material and correctly predicted that it may be more refractory than crown material. Our attempts to leach conodonts with HNO_3 acid were unsuccessful as both crown and basal body material readily dissolved. A possible explanation for the observations of Bertram and Elderfield (1992) may exist in the experiments of Okazaki et al. (1981) who showed that the solubility of high carbonate-containing dahllites decreased with increasing temperature of precipitation. Likewise, conodont basal bodies may become more refractory with increasing thermal maturation. Accordingly, conodonts with basal bodies should be avoided in studies involving $^{87}Sr/^{86}Sr$.

We conclude, as have others (Shaw and Wasserburg, 1985; Staudigel et al. 1986; Grandjean et al. 1987) that the bulk of the Nd in biogenic apatites is acquired at the sediment water interface, and that isotopic composition recorded in most ancient apatites is likely to be that of seawater overlying the depositional site. These conclusions are consistent with Jones et al. (1994) who showed that Nd from isotopically distinct hemipelagic sediment, volcanic ash and eolian dust on the Pacific sea floor does not contribute to the ε_{Nd} signature of overlying Pacific bottom waters. Biogenic apatites are therefore suitable material for investigating variations in past seawater ε_{Nd}.

REFERENCES

Andres D. (1988) Strukturen, apparate und Phylogenie primitiver Conodonten. *Palaeontographica Abeteilung A* **200,** 105-152.

Baker P.A., Gieskes J.M. and Elderfield H. (1982) Diagenesis of carbonatesin deep-sea sediments—evidence from Sr/Ca ratios and interstitial dissolved Sr^{+2} data. Journal of Sedimentary Petrology **52,** 71-82.

Barnes C.R., Sass D.B. and Monroe E.A. (1973) Ultrastructure of some Ordovician conodonts. *Geological Society of America* Special Paper 141.

Bertram C.J., Elderfield H., Aldridge R.J. and Morris S.C. (1992) $^{87}Sr/^{86}Sr$, $^{143}Nd/^{144}Nd$ and REEs in Silurian phosphatic fossils. *Earth and Planetary Science Letters* **113**, 239-249.

Bernat R.T. (1975) Les isotopes de l'uranium et du thorium et les terres rares dans l'environment marin. *Cahiers Ostrom Ser. Geol.* **7,** 68-83.

Burke W.H., Denison E.A., Hetherington R.B., Koepnick R.B., Nelson H.F. and Otto J.B. (1982) Variation of seawater $^{87}Sr/^{86}Sr$ ratio throughout Phanerozoic time. Geology **10,** 516-519.

Broecker W. (1963) Radioisotopes and large-scale oceanic mixing. In *The Sea* (ed. M.N. Hill), pp. 88-108. Interscience.

Burnett R.D. and Hall J.C. (1992) Significance of ultrastructural features in etched conodonts. *Journal of paleontology* **66,** 266-276.

Collin R.L. (1959) Stontium-calcium hydroxyapatite solid solutions: Preparation and lattice constant measurements. *Journal of the American Chemical Society* **81,** 5275-5278.

Cummins D.I. and Elderfield H. (1994) The Strontium isotope composition of Brigantian (late Dinantian) seawater. *Chemical Geology* **118,** 255-270.

DePaolo D.J., Ingram B.L (1985) High-resolution stratigraphy with strontium isotopes. *Science* **227,** 938-941.

DeVilliers S., Shen G.T., Nelson B.K. (1993) The Sr/Ca-temperature relationship in coralline aragonite: Influence of variability in $(Sr/Ca)_{seawater}$ and skeletal growth parameters. *Geochimica et Cosmochimica Acta* **58,** 197-208.

Elderfield H. and Gieskes J.M. (1982) Sr isotopes in interstitial waters of marine sediments from Deep Sea Drilling Project cores. *Nature* **300,** 493-497.

Elderfield H. and Greaves G.J. (1982) The rare earth elements in seawater. *Nature* **296,** 214-219.

Elderfield E.R. and Sholkovitz E.R. (1987) Rare earth elements in pore waters of reducing nearshore sediments. *Earth and Planetary Science Letters* **82**, 280-288.

Elderfield E.R. and Pagett R. (1986) REE in ichthyoliths: variations with redox conditions and depositional environment. *The Science of the Total Environment* **49,** 175-197.

Eberl D.D., Srodon J., Kralik M., Taylor B.E. and Peterman Z.E. (1990) Ostwald ripening of clays and metamorphic minerals. *Science* **248,** 474-477.

Epstein A.G., Epstein E.B., Harris L.D. (1977) Conodont color alteration—and index to organic metamorphism. United States Geological Survey Professional Paper 995.

Frank R.M., Sargentini-Maier M.L., Turlot J.C. and Leroy M.J.F. (1989) Zinc and strontium analyses by energy dispersive x-ray fluorescence in human permanent teeth. *Achives of Oral Biology* **34,** 593-597.

Gedalia I., Yariv S., Brayer L. and Greenbaum M. (1976) Strontium uptake by powdered and intact human root dentine. *Archives of Oral Biology* **21,** 413-416.

Grandjean P., Cappetta H., Michard A. and Albarede (1987) The assessment of REE patterns and ^{143}Nd/^{144}Nd ratios in fish remains. *Earth and Planetary Science Letters* **84**, 181-196.

Grandjean P., Cappetta H., Michard A. and Albarede (1988) The REE and ε_{Nd} of 40-70- Ma old fish debris from the West-African platform. *Geophysical Research Letters* **15,** 389-392.

Grandjean-Lecuyer P., Feist R. and Albarede F. (1993) Rare earth elements in old biogenic apatites. *Geochimica et Cosmochmica Acta* **57,** 2507-2514.

Gruner J.W., McConnell D. and Armstrong W.D. (1937) The relationship between crystal structure and chemical composition of enamel and dentin. *Journal of Biological Chemistry* **121,** 771-781.

Haynes J.T. (1994) The Ordovician Deicke and Millbrig K-bentonite beds of the Cincinnati Arch and the Southern Valley and Ridge Province. *Geological Society of America Special Paper* **290.**

Huff W.D. and Kolata D.R. (1990) Correlation of the Ordovician Deicke and Millbrig K-bentonites between the Mississippi Valley and the southern Appalachians. *American Association of Petroleum Geologists Bulletin* **74,** 1736-1747.

Huff W.D., Bergstrom S.M. and Kolata D.R. (1992) Gigantic Ordovician volcanic ash fall in North America and Europe: Biological, tectonomagmatic, and event-stratigraphic significance. *Geology* **20,** 875-878.

Hodge H.C., Gavett E., Thomas I. (1946) The adsorption of Sr at forty degrees by enamel dentin, bone and hydroxyapatite as shown by the radioactive isotope. *Journal of Biological Chemistry* **163,** 1-6.

Jones C.E., Halliday A.N., Rea D.K. and Owen R.M. (1994) Neodymium isotopic variations in North Pacific silicate sediment and the insignificance of detrital REE contributions to seawater. *Earth and Planetary Science Letters* **127,** 55-66.

Keto L.S. and Jacobsen S.B. (1987) Nd and Sr isotopic variations of early Paleozoic oceans. *Earth and Planetary Science Letters* **84**, 21-41.

Keto L.S. and Jacobsen S.B. (1988) Nd isotopic variations in Phanerozoic paleoceans. *Earth and Planetary Science Letters* **90**, 395-410.

Koch P.L., Halliday A.N., Walter L.M., Stearly R.F., Huston T.J. and Smith G.R. (1992) Sr isotopic composition of hydroxyapatite from recent and fossil salmon: the record of lifetime migration and diagenesis. *Earth and Planetary Science Letters* **108**, 277-287.

Kolata D.R., Frost J.K. and Huff W.D. (1986) K-bentonites of the Ordovician Decorah Subgroup, upper Mississippi Valley: correlation by chemical fingerprinting, III. Department of Energy and Natural Resources, State Geological Survey Division, Circular 537.

Kunk M.J. and Sutter J.F. (1984) ^{40}Ar/^{39}Ar age spectrum dating of biotites from Middle Ordovician bentonites, eastern North America. In *Aspects of the Ordovician System* (ed. D.L. Bruton), pp. 11-22. Paleontological contributions from the University of Oslo, no. 295.

Lambert J.B, Simpson S.V., Weiner S.G. and Buikstra J.E. (1985) Induced metal-ion exchange in excavated human bone. *Journal of Archaeological Science* **12,** 85-92.

LeGeros R.Z. and LeGeros J.P. (1984) Phosphate Minerals. In *Phosphate Minerals in Human Tissue* (ed J.O. Nriagu and P.B Moore), pp. 351-386. Springer-Verlag.

Lindstrom M. and Ziegler W. (1971) Feinstrukturelle Untersuchungen an Conodonten. 1 Die Uberfamilie Panderodontacea. Geol. et Palaeont. **5,** 9-33.

Lindstrom M. and Ziegler W. (1981) Surface micro-ornamentation and observations on internal composition. In *Treatise on Invertebrate Paleontology Part W, supplement 2 Conodonta* (ed. R.A. Robinson), pp. W41-W52. Geological Society of America and University of Kansas Press.

Little M.F. and Barrett K. (1976) Strontium and fluoride content of surface and inner enamel versus caries prevalence in the Atlantic Coast of the United States of America. *Carries Research* **10,** 297-307.

McArthur J.M. (1978) Systematic variations in the contents of Na, Sr, CO_3 and SO_4 in marine carbonate-fluorapatite and their relation to weathering. *Chemical Geology* 21, 89-112.

McClellan G.H. and Lehr J.R. (1969) Crystal chemical investigation of natural apatites. *The American Mineralogist* **54,** 1374-1391.

McConnell D. (1962) Dating of fossil bones by the fluorine method. *Science* **136,** 241-244.

Nelson B.K., DeNiro M.J., Schoeninger, M.J. and DePaolo D.J. (1986) Effects of diagenesis on strontium , carbon, nitrogen and oxygen concentration and isotopic composition of bone. *Geochimica et Cosmochmica Acta* **50,** 1941-1949.

Odum H.T. (1955a) Biogeochemical deposition of strontium. *Institute for Marine Science* **4,** 38-114.

Odum H.T. (1955b) Strontium in natural waters. Institute for Marine Science **4,** 22-37.

Okazaki M., Moriwaki Y., Aoba T., Doi Y. and Takajashi J. (1981) Solubility of CO3 apatites in relation to crystallinity. *Carries Research* **15,** 477-483.

Pietzner H., Vahl J., Werner H. and Ziegler W. (1968) Zur chemischen zusammensetzung und mikromorphologie der conodonten. *Palaeontographica* **128,** 115-152.

Samson S.D., Patchett P.J., Roddick J.C. and Parrish R.R. (1989) Origin and tectonic setting of Ordovician bentonites in North America: Isotopic and age constraints. *Geological Society of America Bulletin* **101,** 1175-1181.

Sansom I.J., Smith M.P., Armstrong H.A. and Smith, M.M. (1992) Presence of the Earliest Vertebrate hard Tissues in Conodonts. *Science* **256,** 1308-1311.

Schmidt H. and Muller K.J. (1964) Weitre Funde von Conodonten-Gruppen aus dem oberen Karbon des Sauerlandes. *Palaontologische Zeitschrift.* **38,** 105-135.

Schmitz B., Aberg G., Werdelin L., Forey P. and Bendix-Almgreen S.E. (1991) $^{87}Sr/^{86}Sr$, Na, F, Sr and La in skeletal fish debris as a measure of the paleosalinity of fossil-fish habitats. Geological Society of America

Bulletin **103,** 786-794.

Schoeninger M.J., DeNiro M.J. (1982) Carbon isotope ratios of apatite from fossil bone cannot be used to reconstruct diets of animals. Nature **297,** 577-578.

Shaw H.F. and Wasserburg G.J. (1985) Sm-Nd in marine carbonates and phosphates: Implications for Nd isotopes in seawater and crustal ages. *Geochimica et Cosmochmica Acta* **49,** 503-518.

Staudigel H., Doyle P. and Zindler A. (1986) Sr and Nd isotope systematics in fish teeth. Ear*th and Planetary Science Letters* **76**, 45-56.

Stewart G.A., and Sweet W.C. (1956) Conodonts from the Middle Devonian bone beds of central and west-central Ohio. *Journal of Paleontology* **30,** 261-273.

Stille P. (1992) Nd-Sr evidence for dramatic changes of paleocurrents in the Atlantic Ocean during the past 80 m.y.. *Geology* **20,** 387-390.

Stille, P. and Fischer H. (1990) Secular variation in the isotopic composition of Nd in Tethys seawater. *Geochimica et Cosmochmica Acta* **54,** 3139-3145.

Stout P.M. (1985) Interstitial water chemistry and diagenesis of biogenic sediments from the eastern equatorial Pacific, deep sea drilling project 85. In *Initial Reports of the Deep Sea Drilling Project* **85,** 805-820.

Stumm W. and Morgan J.J. (1981) *Aquatic Chemistry.* John Wiley and Sons.

Taylor S.R. and McLennan S.M. (1985) *The Continental Crust: Its isotopic composition and evolution.* Blackwell Scientific Publications.

Toyoda K. and Tokonami M. (1990) Diffusion of rare earth elements in fish teeth from deep sea sediments. *Nature* **345,** 607-609.

Tuross N., Behrensmeyer A.K. and Eanes E.D. (1989) Strontium increases and crystallinity changes in taphonomic and archaeological bone. *Journal of Archaeological Science* **16,** 661-672.

Wasserburg G.J., Jacobsen S.B., De Paolo D.J., McCulloch M.T. and Wen T. (1981) Precise determination of Sm/Nd ratios, Sm and Nd isotopic abundances in standard solutions. *Geochimica et Cosmochimica Acta* **45,** 2311-2323.

Watson E.B. and Green T.H. (1981) Apatite/liquid partition coefficients for the rare earth elements and strontium. *Earth and Planetary Science Letters* **56**, 405-421.

Wright J., Seymour R.S.Shaw H.F. (1984) REE and Nd isotopes in conodont apatite: Variations with geological age and depositional environment. *Geological Society of America Special Paper* **196,** 325-340.

Chapter 4

RESTRICTED MARINE SETTING FOR ANCIENT EPEIRIC SEAS: EVIDENCE FROM ^{143}ND/^{144}ND RATIOS IN 454 MA CONODONTS AND ^{13}C/^{12}C RATIOS IN LIMESTONES [1]

Viewed in the perspective of geologic time, ocean basins are ephemeral features. Consequently, the record of marine sediments older than the oldest *in situ* oceanic crust is predominantly known from epicontinental deposits, formed during periods of high relative sea level in epeiric seas. Although only a small part of the total volume of the oceans was entrained within the epicontinental environment at any time, there is a tendency in paleoceanographic and paleoclimatologic investigations to treat isotopic and trace element proxies from epeiric sea sediments as representative of whole ocean processes or events. This practice ignores the possibility that epeiric seas were restricted from mixing with their original deep ocean sources and that chemical and isotopic differences may develop both within epeiric seas and between them and the dominant basalt-floored ocean. Local environmental influences are difficult to resolve in very old rocks because establishing sufficiently precise contemporaneity between deposits is beyond the capacity of biostratigraphic (±10.5 Ma) and geochronologic techniques (±1–3 Ma).

In this paper, we present isochronous isotopic variations of Nd in conodont microfossils, and of C in limestones, sampled proximal to the Millbrig and Deicke K-bentonites which are correlated by geochemical fingerprinting, wire line logs and phenocryst mineralogy (Kolata et al., 1986; Huff and Kolata, 1990; Haynes et al., 1994). Since bentonites are altered volcanic ash beds their deposition over a period of days to weeks provides unprecedented time resolution in rocks of this age. Furthermore, the Millbrig is recognized as the most voluminous and widespread ashfall in the Phanerozoic rock record enabling precise correlation over distances exceeding 1500 kms in Laurentia (Huff et al., 1992). The isotopic variations observed across the Mohawkian epeiric sea are as large as those commonly reported by isotope stratigraphic methods at any site. This is the first clear evidence that the chemistry of epeiric seas varied both internally and with respect to contemporaneous deep oceans and has profound implications for the interpretation of chemical and isotopic variations in pre-Cretaceous marine fossils and sediments, and may have important bearing on patterns of faunal distribution, evolution and extinction.

---

[1] A version of this paper has been submitted to *Science* co-authored by R.A.Creaser and K. Muehlenbachs, Dept. of Earth and Atmospheric Sciences, University of Alberta, and S.A. Leslie and S.M. Bergstrom, Dept. of Geological Sciences, The Ohio State University.

Nd isotopes ratios are ideally suited to studying paleocirculation in ancient seas because trivalent Nd has a short seawater residence time compared to oceanic mixing times (Piepgras and Wasserburg, 1980; Elderfield and Greaves, 1982), and an isotopic composition that reflects inputs from continental weathering by way of the riverine transport (Piepgras et al., 1979; Piepgras and Wasserburg, 1980). Since the ε_{Nd} value of continental crust is age-dependent, differences in ε_{Nd} exist between different world oceans because the mean age of continental crust comprising the watershed to each ocean is different. Negative ε_{Nd} values for present day Atlantic waters (–10 to –13) reflects old crustal ages surrounding the Atlantic passive margin (1.9–3.8 Ga) whereas the more positive ε_{Nd} values for Pacific waters (–3 to –1) is due to contributions from weathering of young island arcs situated over subduction zones (Piepgras et al., 1979). The isotopic balance of Nd in the oceans is also affected by mixing of temperature-salinity defined water masses with distinct ε_{Nd} (Piepgras and Wasserburg, 1987). For example, salty bottom waters exiting the Mediterranean have $\varepsilon_{Nd} = -9.8$, compared to –12 for overlying and underlying Atlantic Ocean waters (Piepgras and Wasserburg, 1983), and the Indian Ocean has an intermediate ε_{Nd} value of –8 that originates through mixing of isotopically distinct Atlantic (–13) and Pacific (–3) water masses by the Antarctic circumpolar current (Piepgras and Wasserburg, 1982).

Conodonts are mineralized elements (carbonate-fluorapatite) of the feeding apparatus of an extinct, small, laterally compressed eel-like animal (Aldridge et al., 1993). Along with other bio-

Table 4-1 Nd isotope data for conodonts and C and O isotope data from limestones of the Mohawkian Epeiric Sea.

Sample^A	Position^B (cm)	Sm (ppm)	Nd (ppm)	Sm/Nd (atom)	$^{147}Sm/^{144}Nd$ (measured)	$^{143}Nd/^{144}Nd$ (measured)	T_{DM2}^{C} (Ga)	CAI^D	$\delta^{18}O$ (PDB)	$\delta^{13}C$ (PDB)	ε_{Nd}^{E} (454 Ma)
Iapetus water mass											
1. 7–5 (35)	25 M ↑	58.9	279.6	0.20	0.1273	0.512315 (49)	1.4	3.5	–5.2	1.3	–2.3 ±1.0
2. 7–6 (35)	1200 M ↓	35.7	179.3	0.19	0.1206	0.512159 (48)	1.6	3.5	–5.4	1.5	–4.9 ±0.9
Taconic water mass											
3. ST–8 (36)	34 M ↑	33.2	121.7	0.26	0.1648	0.512180 (29)	1.8	1.5	–4.9	1.4	–7.1 ±0.6
4. UF–9	1430 M ↑	17.5	66.6	0.25	0.1594	0.512110 (236)	1.9	4.5–5	–6.4	2.0	–8.1 ±4.6
5. FF–7 (19)	2006 D ↑	12.3	53.2	0.22	0.1397	0.512044 (29)	1.9	1-1.5	–4.7	0.9	–8.3 ±0.6
6. MB–1 (30)	1000 M ↓	18.7	78.8	0.23	0.1434	0.512012 (26)	1.9	5	–8.0	2.3	–9.1 ±0.5
7. HA–21 (1300)	38 M ↑	31.8	131.5	0.20	0.1460	0.511875 (17)	2.2	2.5-3	–4.7	2.4	–12.0 ±0.3
Midcontinent water mass											
8. NL–17 (—)	38 M ↑	18.6	87.6	0.20	0.1281	0.511838 (12)	2.1	1-1.5	–7.6	–0.4	–11.6 ±0.2
9. HO–3 (6)	10 D ↓	32.9	169.0	0.19	0.1175	0.511779 (22)	2.2	1-1.5	–7.3	–2.3	–12.1 ±0.4
10. P–287 (40)	2480 D ↑	18.0	89.3	0.19	0.1221	0.511681 (31)	2.3	1-1.5	–5.3	–0.3	–14.4 ±0.6
11. HO1–C (6)	18 M ↓	37.5	176.8	0.20	0.1281	0.511679 (29)	2.4	1-1.5	–5.3	–0.3	–14.7 ±0.6
12. HO1–P (6)	18 M ↓	309.6	1416.7	0.21	0.1321	0.511689 (12)	2.4	1-1.5	repeat	repeat	–14.8 ±0.2
13. HO–2 (4)	10 D ↑	71.4	333.1	0.21	0.1296	0.511667 (14)	2.4	1-1.5	–5.7	–1.8	–15.1 ±0.3
14. CB–6 (9)	5320 D ↑	19.0	97.1	0.19	0.1184	0.511564 (55)	2.5	3.5-4	–7.6	0.4	–16.4 ±1.1
15. SP–8 (4)	86 M ↓	73.2	384.6	0.18	0.1150	0.511529 (34)	2.5	1-1.5	–5.9	–2.3	–16.9 ±0.7
16. 24–7 (2)*	3400 D ↑	90.6	513.4	0.17	0.1067	0.511400 (20)	2.7	1-1.5	–4.8	1.1	–18.9 ±0.4
17. B50–8 (7)*	87 D ↑	45.9	229.9	0.19	0.1207	0.511431 (12)	2.7	1.5-2	–7.4	0.7	–19.2 ±0.2

A. Sample name followed by bentonite thickness (cm) in parentheses.

B. Distance of sample above (↑) or below (↓) the Millbrig (M) or Deicke (D) K-bentonites

C. $T_{DM2} = 1/\lambda \, Ln \, [\, ((^{143}Nd/^{144}Nd)_{Sample\ 454\ Ma} - 0.512528 \,) \, / \, (0.1163 - 0.2137) + 1 \,] + 454 \times 10^{6}$ yrs. $\lambda = 6.54 \times 10^{-12}\ y^{-1}$

D. CAI = Conodont Color Alteration Index; condodonts become progressively darker with increasing burial temperature CAI=1–1.5

E. $\varepsilon_{Nd} = [\, (^{143}Nd/^{144}Nd)_{SAMPLE} \, / \, (^{143}Nd/^{144}Nd)_{CHUR} - 1 \,] \times 10^{4}$ where CHUR is CHondritic Uniform Reservoir which today = 0 .512638

* Tentative correlation based on conodont biostratigraphy (Leslie, 1995).

genic apatites, conodonts contain high concentrations of Nd, which modern studies show must have been acquired almost entirely post-mortem, at or near the sediment water interface (Wright et. al., 1984; Shaw and Wasserburg, 1985). Despite the secondary nature of Nd incorporation, there is strong evidence that conodont ε_{Nd} values accurately record the isotopic composition of seawater originally overlying the depositional site (Shaw and Wasserburg, 1985; Staudigel et al., 1986; Grandjean et al., 1987; Grandjean and Albarede, 1989; Holmden et al., submitted). Once covered by sediment, biogenic apatites cease taking in large amounts of Nd (Bernat, 1975) indicating that Nd contributed from pore waters and late diagenetic fluids is insignificant (Grandjean et al., 1987; Grandjean and Albarede, 1989). In contrast to ε_{Nd}, the $\delta^{13}C$ value of the dissolved oceanic C reservoir is very uniform (±1‰) (Kroopnick, 1979). Isotopic differences between water masses result from differences in primary productivity, carbon burial/oxidation rates or mixing with ^{13}C-depleted continental freshwaters.

Carbon isotope analyses were determined on the same limestone from which conodonts were separated. Potential Nd-contamination from the altering ash ($\varepsilon_{Nd} = -5$; Samson et al., 1989) was assessed by detailed study of three whole-rock samples (SAL92 HO1, HO2, HO3) situated <18 cm from either the Millbrig or Deicke K-bentonites. Only one sample showed evidence of contamination yielding an $\varepsilon_{Nd} = -12$, rather than the expected seawater value of -14.7 (Table 6-1). To further minimize potential contamination most samples were collected between 0.35 and 2.5 meters from either K-bentonite. The Nd isotopic data (Table 4-1) are displayed on a map (Fig. 4-1) and the C isotope data listed in Table 4-1.

The isotopic map (Fig. 4-1) represents a single time-frame in the evolution of the Mohawkian epeiric sea and its surrounding crustal mass, which included low relief islands of old Precambrian shield in the north and younger uplifted crust of the Taconic Orogen to the east (Rowley and Kidd, 1981; Rodgers, 1987). Variations in ε_{Nd} spanning 17 parts in 10,000 are observed. This is the range

---

[2] For the majority of Nd analyses analytical uncertainty is less than ±0.6 epsilon units (2σ) (Table 4-1). Quoted ε_{Nd} values are corrected for *in situ* decay of ^{147}Sm to 454 ±3 Ma, the mean age of the Millbrig and Deicke bentonites (Kunk and Sutter, 1984). Reproducibility for $\delta^{18}O$ and $\delta^{13}C$ is ± 0.2 and ±0.1‰, respectively, based on repeat analyses of internal and international standards.

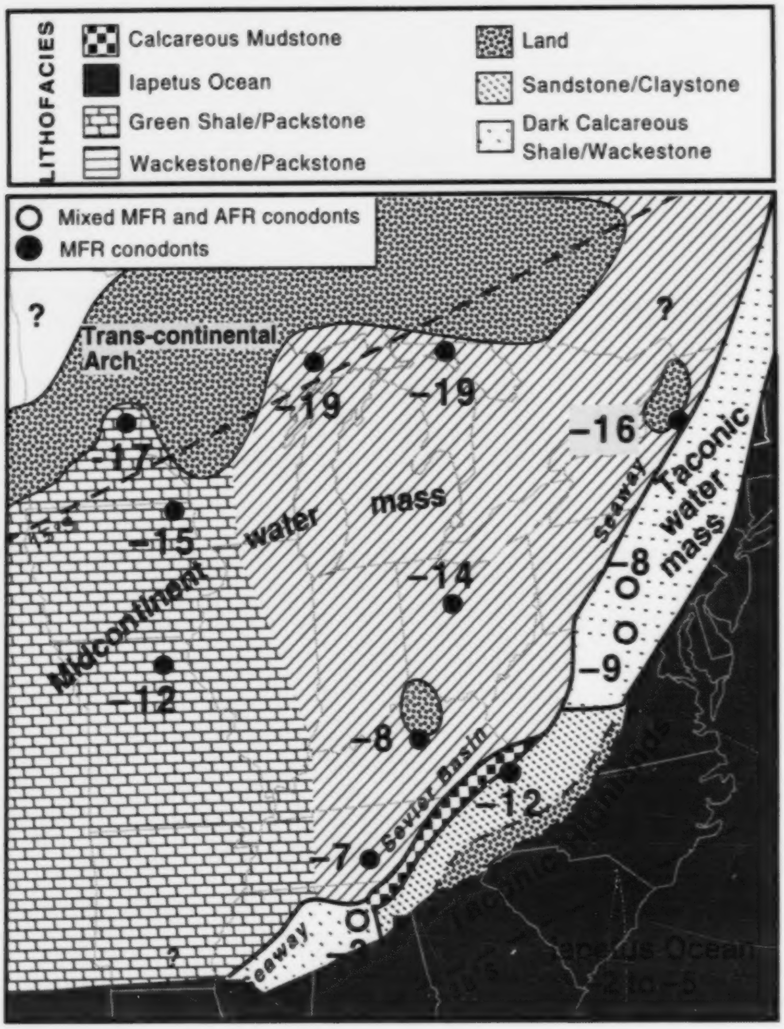
LITHOFACIES
Calcareous Mudstone
Iapetus Ocean
Green Shale/Packstone
Wackestone/Packstone
Land
Sandstone/Claystone
Dark Calcareous Shale/Wackestone
○ Mixed MFR and AFR conodonts
● MFR conodonts
?
Trans-continental Arch
−19
−19
?
−16
−17
Midcontinent water mass
Taconic water mass
Seaway
−15
−8
−14
−9
−12
−8
Sevier Basin
−12
Taconic Highlands
−7
Seaway
?
Iapetus Ocean −2 to −5

FIGURE 4-1. Nd isotopic map of the 454 Ma Mohawkian Epeiric Sea. The ε_{Nd} values for the Mohawkian epeiric sea range from −2 to −19 and are mostly very different from those characterizing the deep Iapetus Ocean (−2 to −5). Emergent islands in the north part of the sea include portions of the Transcontinental Arch and Canadian Shield which are composed of Precambrian crust in this area. The Taconic foreland basin spans the eastern margin of Laurentia during Millbrig-time, formed in response to tectonic loading of the cratonal margin during continent-arc collision (Rowley and Kidd, 1981; Rodgers 1987). Coarse clastic sediments of the Sevier Basin were already being deposited during Millbrig-time suggesting that arc collision in the south predated collision farther north (Ettensohn, 1991). The wide range of εNd values observed within the Mohawkian Sea reflects the diverse ages of the surrounding continental crust. Rivers discharging into the Mohawkian Sea carry Nd that reflects the isotopic age of bedrock in the watershed. The shallow Midcontinent water mass overlies the western carbonate platform whereas the Taconic water mass occupies the Taconic Foreland basin, referred to as the Taconic Seaway. Mixing of Iapetus Ocean waters onto the craton occurs in the extreme south and probably also in the north (outside the frame) based on conodont distribution patterns (Bergstrom, 1990). MFR = Midcontinent Faunal Region AFR = Atlantic Faunal Region

of variation previously reported for the evolution of paleoceans over the entire Phanerozoic eon (Shaw and Wasserburg, 1985; Keto and Jacobsen, 1987;1988). Although a systematic decrease in ε_{Nd} from north to south is evident, on closer inspection three potential water masses may be identified: (1) a water mass occupying the deep Taconic foreland basin with ε_{Nd} values –7 to –9 and mean of Sm/Nd = 0.23 ±0.02 ($2\sigma_m$), (2) a midcontinent water mass overlying shallow water platform carbonates in the interior and western portions of the sea with ε_{Nd} values –12 to –19 and mean Sm/Nd = 0.19 ±0.01 ($2\sigma_m$), and (3) and an Iapetus water mass in the extreme southern reaches of the Mohawkian Sea with ε_{Nd} = –2.3 to –5.3. An independent measure of Iapetus Ocean water (Fig. 4-1) utilizing metaliferous crusts on seafloor submarine pillow lavas (Leggett and Smith, 1980)

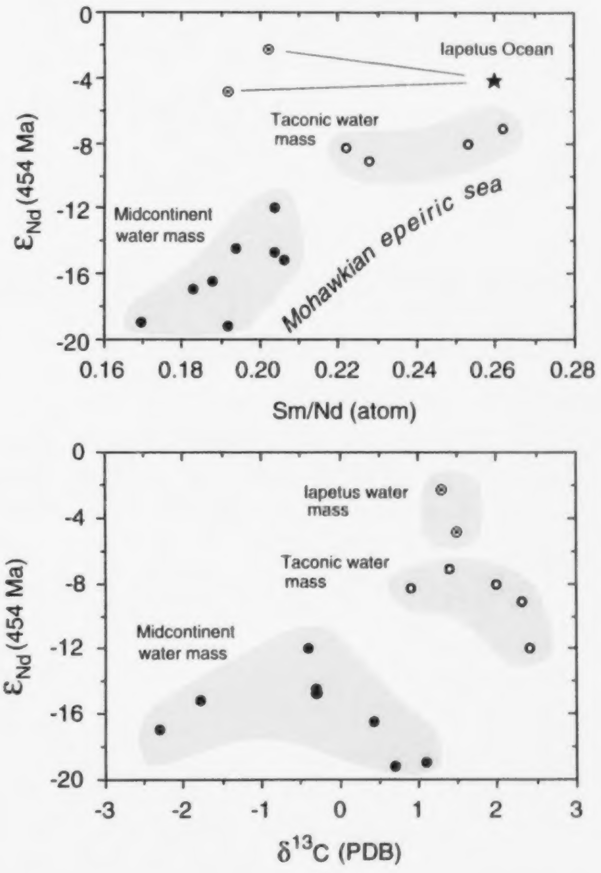

FIGURE 4-2 (a) The ε_{Nd} and Sm/Nd ratios of conodonts from the Mohawkian (epeiric) Sea plot in two distinct fields denoting two epicontinental water masses; a Taconic water mass which occupied the Taconic Seaway (foreland basin) and a Midcontinent water mass that overlay the western Mohawkian carbonate platform. Values for the Iapetus Ocean are from Hooker et al. (1981) determined from metaliferous crusts on middle Ordovician, mid-ocean-ridge pillow lavas from a former Iapetus Ocean-floor spreading center. Two samples from a site in the extreme southern reaches of the Mohawkian Sea have ε_{Nd} values indistinguishable from Iapetus seawater but lower Sm/Nd ratios. (**b**) The Taconic and Midcontinent water masses also have differing $\delta^{13}C$ values. The more ^{13}C-enriched Taconic water mass may be due to enhanced organic carbon burial in low oxygen bottom waters of a salinity stratified seaway. The ^{13}C-depleted values of the Midcontinent water mass may reflect a larger terrestrial component of ^{12}C-enriched organic matter (e.g., bacterial) in fresh water runoff from the Transcontinental Arch.

yielded consistent ε_{Nd} values of -3 to -6 (Hooker et al., 1981).

Analogous to modern oceans, ε_{Nd} differences between Mohawkian water masses reflect differences in the age of the surrounding continental crust. The geochemical coherence of parent (Sm) and daughter (Nd) isotopes during weathering and fluvial transport allow us to calculate crustal-source model ages from the Sm-Nd data in each water mass (Keto and Jacobsen, 1987). The Midcontinent water mass yields model ages from 2.3–2.7 Ga, consistent with fluvial transport of Nd from the Transcontinental Arch (T_{DM} = 2.0–2.3 Ga) and the Canadian Shield (2.7 Ga) (Fig. 4-1) (Bennett and DePaolo, 1987). Model ages for Nd in the Taconic water mass range from 1.8–2.2 Ga, consistent with 1.9–2.1 Ga model ages for Ordovician sediments of the Sevier basin (Gleason et al., 1994) which are the erosional products of the Taconic Orogen (Rowley and Kidd, 1981; Rodgers, 1987) deposited in a margin parallel foreland basin (Ettensohn, 1991).

The excellent correspondence between Sm-Nd systematics in Mohawkian Sea water masses and adjacent continental crust suggests that little of the isotopic variation across the Mohawkian Sea is due to internal mixing between water masses. In addition, there is a strong association between ε_{Nd}, lithofacies (the sum of all rock attributes) and basin physiography. For example, the Taconic water mass overlays the Dark Calcareous Shale/Wackestone Facies which is confined to the trough-like foreland basin, whereas the Midcontinent water mass overlays the Wackestone/Packstone (±Green Shale) Facies of a shallow water carbonate platform (Fig. 4-1). Most striking is the difference in $\delta^{13}C$ values (Fig. 4-2b) between water masses. Although the total variation is 4‰ across the Mohawkian Sea, smaller differences characterize individual Midcontinent (-0.6 ±0.9, $2\sigma_m$) and Taconic (+1.8 ±0.6, $2\sigma_m$) water masses.

Conodonts of Laurentia show distinct provincialism into a group of shallow water species indicative of the Midcontinent Faunal Region (MFR) and a group of cooler water species indicative of the Atlantic Faunal Region (AFR), which includes Scotland in the Mohawkian (Bergstrom 1990). The AFR fauna is found on both eastern (Laurentian) and western (Baltican) shores of the Iapetus Ocean, whereas the MFR fauna is largely restricted to the interior of Laurentia. The distribution of AFR and MFR conodont faunas within the Mohawkian Sea is consistent with the distribution of

Taconic and Midcontinent water masses, respectively. Some mixing of MFR and AFR faunas occurs within the Dark Calcareous Shale/Wackestone Facies of the Taconic foreland basin but mixing of AFR conodonts onto the shallow western carbonate platform is rare. Conodont faunal patterns suggest that the Taconic foreland basin was an interior seaway with southern and northern connections to the Iapetus Ocean. The northern connection is beyond the area covered by this study but the southern connection shows up clearly in the ε_{Nd} values of mixed MFR–AFR conodonts in the extreme southern reaches of the Mohawkian sea (Fig. 4-1).

The evolution of the Mohawkian Sea and the fate of its two major water masses may be described with additional data from Keto and Jacobsen (1987). The contrasting ε_{Nd} signatures between the Iapetus Ocean and Mohawkian Sea date to at least the middle Cambrian (528 Ma), prior to demonstrable arc-continent interaction, and therefore prior to development of a mountainous hinterland which provided an obvious physical barrier to mixing. Similarly, a mixing barrier is not evident between Taconic and Midcontinent water masses of the Mohawkian Sea. We therefore conclude that water depth alone is sufficient to restrict mixing. Development of the Taconic Seaway by Millbrig-time enabled Iapetus Ocean waters less restricted access into the continental interior. Although the Taconic water mass has an ε_{Nd} value distinct from Iapetus in its middle reaches (Fig. 4-1), the salinity, temperature and nutrient characteristics were evidently suitable for AFR conodonts. To avoid potentially unfavorable waters in the surface mixed layer of the seaway (which were likely warmer and less saline due to freshwater runoff from the Taconic highlands; Hay and Cisne, 1988), AFR conodonts may have inhabited deeper, cooler and more saline waters. This suggests a nektobenthic mode of life for AFR conodonts and a plausible explanation for their absence from sediments of the shallow Midcontinent water mass. On the basis of ε_{Nd} data the salinity of the Midcontinent water mass was even lower than surface waters of the Taconic Seaway, otherwise Midcontinent waters (with their distinct ε_{Nd} signature) along the platform edge would sink to form the bottom waters of the Taconic Seaway. If such a circulation pattern existed within the Mohawkian Sea, no contrast in ε_{Nd} values between MFR and AFR conodonts would be expected since conodonts record the ε_{Nd} values of their post-mortem environment, not their living environment. This interpretation conflicts with a model for warm saline deep water formation in Ordovician Oceans (Railsback et al. 1990) which suggests Ordovician epeiric seas (like the Mohawkian Sea) supplied high salinity waters to deep oceans. A warmer, less saline Midcontinent water mass is consistent with its closer proximity to the paleoequatorial convergence (the zone of net precipitation ~15° N-S latitude), and possible sources of freshwater discharging from the Transcontinental Arch and Canadian Shield.

Carbonate lithologies, clastic input, and faunal distributions changed markedly in post-Millbrig time. Nearly 80% of brachiopods became extinct or migrated westward along with calcareous algae and corals (Patzkowsky and Holland, 1993). Conodont biofacies also changed with AFR conodonts appearing for the first time in sediments of the western carbonate platform (Leslie, 1995). Since faunal migration and extinction occurred during a rise in sea level, these events have been related to the circulation of cooler more nutrient-rich Iapetus Ocean waters over the east Laurentian margin (Patzkowsky and Holland, 1993). In the context of the Mohawkian Sea and its two major water masses, we attribute these events to westward expansion of the Taconic water mass over the shallow western carbonate platform. Data from Keto and Jacobsen (1987) are in agreement, showing ε_{Nd} values in North American biogenic apatites becoming more positive after 454 Ma, and Gleason et al (1994) note that all Ordovician clastic sediments deposited in eastern Laurentia post-454 Ma, define a narrow range of ε_{Nd} (-6 to -10), indicating an exclusively western source of sediment (and associated fluvial discharges) from the Taconic highlands, which is consistent with demise of the Midcontinent water mass.

The evidence that epeiric seas are restricted marine enviroments challenges traditional methods of obtaining and interpreting geochemical information from pre-Cretaceous marine sediments, since the majority of these sediments were precipitated from epeiric seawater. A well known dictum in sedimentology is Walther's Law, which states that a vertical succession of strata in a sedimentary column represents a former horizontal array of adjacent depositional environments. Similarly, geochemical signatures denoting once contemporaneous water masses may also become stacked in the rock record, and so the common practice of generating isotope stratigraphies in old marine sediments will be complicated not only by preservational concerns, but by regional paleoenvironmental influences that are generally not considered. A review C isotope stratigraphies associated with extinction horizons (Wang et al., 1991) or purported late Proterozoic biotic events (e.g., Knoll et al., 1986; Kaufman et al., 1991) shows that many $\delta^{13}C$ excursions are associated with changes in lithofacies, indicating potential changes in *geochemical facies* that may originate from shifting water masses within the restricted epeiric sea environment. Indeed, the westward expansion of the Taconic water mass in post-Millbrig time shows up in a C isotope stratigraphy of limestones and kerogen performed near the Transcontinental Arch (Fig. 4-1) (Hatch et al., 1987). Pre-Millbrig limestone $\delta^{13}C$ values are –2‰ (PDB), rising to +2‰ for a brief interval in post-Millbrig time. The magnitude and timing of this positive $\delta^{13}C$ anomaly is consistent with westward expansion of the Taconic water mass in post-Millbrig time.

It is likely that restricted mixing characterizes epeiric seas of all ages and as such may help to explain a wide variety of geochemical enigmas in old marine sediments. In a study of amorphous marine kerogens, Lewan (1986) showed that those extracted from epeiric sea carbonates were significantly ^{13}C-depleted relative to modern deep ocean equivalents and attributed the difference to recycling of ^{13}C-depleted organic carbon in a restricted marine environment. Differences in dissolved CO_2 content of epeiric seawater may influence abiotic carbonate mineralogy (Sandberg, 1983; Given and Wilkinson, 1985) and so it is conceivable that aragonite could be the primary precipitate in one basin, and calcite in another. Restricted marine environments are also required to explain positive $\delta^{34}S$ excursions in ancient marine sediments (Holser, 1971). Goodfellow and Jonasson (1984) showed that the epicontinental Selwyn basin (Laurentia) was restricted from mixing with the deep ocean SO_4 reservoir over much of its early Paleozoic history. A provocative explanation for the prevalence of low $\delta^{18}O$ carbonates in Paleozoic and older strata (Veizer et al., 1986; Lohmann and Walker, 1989; Qing and Veizer, 1992) that does not conflict with constraints derived from seawater-ocean-crust isotope exchange (Muehlenbachs and Clayton, 1976; Gregory, 1992), is that carbonate producing epeiric seas were both warm (25–30 °C) and brackish (29–18‰ salinity)[3] compared to deep oceans. The $\delta^{18}O$ values of brackish water are low because of mixing with ^{18}O-depleted meteoric waters, and so changing circulation patterns and mixing relations with the deep ocean (which remains constant in $\delta^{18}O$ and salinity) can account for secular aspects of the marine sediment record that are otherwise difficult to explain (Gregory, 1992; Holmden and Muehlenbachs, 1992). However no systematic variation in $\delta^{18}O$ values is observed in Mohawkian Sea limestones (Table 4-1), suggesting either incipient alteration of epeiric sea sediments or some other mechanism that can influence epeiric seawater isotopic composition, but which remains to be determined.

Given the high continentality, variable bathymetry and close proximity to freshwater sources, epeiric seas are best viewed as a collage of microenvironments characterized by water masses with differing nutrients, turbidities, temperatures and especially salinities. Such internal variability results from restricted mixing of water masses both within the epeiric sea environment and between epeiric seas and contemporaneous deep oceans. Since the majority of old marine sediments and fossils are from epeiric seas, we suggest that great care must be taken to discriminate local environmental influences from global influences when interpreting chemical, isotopic and faunal information in ancient marine sediments.

---

[3] Salinities are calculated by mass balance (see *Chapter 5*) based on a bulk ocean $\delta^{18}O$ of -1‰ (SMOW) and a meteoric water isotopic composition of -7 ‰ (SMOW) as determined in goethite from an Ordovician weathering profile (Neda Formation) developed on the Transcontinental Arch (Yapp, 1992)

REFERENCES

Aldridge R.J., Briggs D.E.G., Smith M.P., Clarkson E.N.K. and Clark, N.D.L. (1993) The anatomy of conodonts. *Philosophical Transactions of the Royal Society of London* **B 340,** 405-421.

Bennet V.C. and DePaolo D.J. (1987) Proterozoic crustal history of the western United States as determined by neodymium isotopic mapping. *Geological Society of America Bulletin* **99,** 674-685.

Bergstrom S.M. (1990) Relations between conodont prvincialism and the changing palaeogeography during the Early Paleozoic. In Palaeozoic Palaeogeography and Biogeography (ed. W.S. McKerrow and C.R. Scotese), pp. 105-121.

Bernat R.T. (1975) Les isotopes de l'uranium et du thorium et les terres rares dans l'environment marin. *Cahiers OSTROM Ser. Geol.* **7,** 68-83.

Elderfield H. and Greaves M.J. (1982) The rare earth elements in seawater. *Nature* 296, 214-219.

Ettensohn F.R. (1991) Flexural interpretation of relationships between Ordovician tectonism and stratigraphic sequences, central and southern Appalachians, U.S.A. In *Advances in Ordovician Geology* (ed. C.R. Barnes and S.H. Williams), pp. 213-224. Geological Survey of Canada, Paper 90-9.

Gleason J.D., Patchett P.J., Dickinson W.R. and Ruiz J. (1994) Nd isotopes link Ouachita turbidites to Appalachian sources. *Geology* **22,** 347-350.

Goodfellow W.D. and Jonasson I.R. (1984) Ocean stagnation and ventilation defined by $\delta^{34}S$ secular trends in pyrite and barite, Selwyn basin, Yukon. *Geology,* **12,** 583-586.

Grandjean P., Cappetta H., Michard A. and Albarede (1988) The REE and ε_{Nd} of 40-70- Ma old fish debris from the West-African platform. *Geophysical Research Letters* **15,** 389-392.

Grandjean P. and Albarede F. (1989) Ion probe measurement of rare earth elements in biogenic phosphates. *Geochimica et Cosmochmica Acta* **53,** 3179-3183.

Gregory R.T. (1991) In *Stable Isotope Geochemistry: A tribute to Samuel Epstein* (ed. H.P TaylorJr. J.R. O'Neil and I.R. Kaplan) pp. 65-76. Geochemical Society Special Publication No. 3.

Hay B.J. and Cisne J.L. (1988) Deposition in the Oxygen-Defficient foreland basin, Late Ordovician. In *The Trenton Group (Upper Ordovician Series) of Eastern North America, Deposition, diagenesis and Petroleum* (ed. B.D. Keith), pp. 113-134. *American Association of Petroleum Geologists* Studies in Geology #29.

Hatch J.R., Jacobsen S.R., Witzke B.J., Risatti J.B. Anders D.E., Watney W.L., Newell K.D. and Vuletich A.K. (1987) Possible Late Middle Ordovican organic carbon isotope excursion: evidence from Ordovician oils and hydrocarbon source rocks, mid-continent and east-central United States. *American Association of Petroleum Geologists Bulletin* **71,** 1342-1345.

Haynes J.T. (1994) Yhe Ordovician Deicke and Millbrig K-bentonite beds of the Cincinnati Arch and the souther Valley and Ridge Province. *The Geological Society of America* Special Paper 290.

Holmden C., Creaser R.A., Muehlenbachs, K., Leslie S.A. and Bergstrom S.M. Isotopic and elemental systematics of Sr and Nd in Ordovician biogenic apatites: Implications for paleoseawater studies. submitted to *Earth and Planetary Science Letters.*

Holser W.T. (1971) Catastrophic chemical events in the history of the ocean. *Nature* **267,** 403-408.

Hooker P.J., Hamilton P. J. and O'Nions R.K. (1981) An estimate of the Nd isotopic composition of Iapetus seawater from ca. 490 Ma metalliferous sediments. *Earth and Planetary Science Letters* **56,** 180-188.

Huff W.D. and Kolata D.R. (1990) Correlation of the Ordovician Deicke and Millbrig K-bentonites between the Mississippi Vallley and the southern Appalachians. *American Association of Petroleum Geologists Bulletin* **74,** 1736-1747.

Huff W.D., Bergstrom S.M. and Kolata D.R. (1992) Gigantic Ordovician volcanic ash fall in North America and Europe: Biological, tectonomagmatic, and event-stratigraphic significance. *Geology* **20,** 875-878.

Kaufman A.J., Hayes J.M., Knoll A.H. and Germs G.J.B. (1991) Isotopic compositions of carbonates and organic carbon from upper Proterozoic successions in Namibia: stratigraphic variation and the effects of diagenesis and metamorphism. *Precambrian Research* **49,** 301-327.

Keto L.S. and Jacobsen S.B. (1987) Nd and Sr isotopic variations of early Paleozoic oceans. *Earth and Planetary Science Letters* **84,** 21-41.

Keto L.S. and Jacobsen S.B. (1988) Nd isotopic variations in Phanerozoic paleoceans. *Earth and Planetary Science Letters* **90,** 395-410.

Kolata D.R., Frost J.K. and Huff W.D. (1986) K-bentonites of the Ordovician Decorah Subgroup, upper Missippi Valley: correlation by chemical fingerprinting, Ill. Department of Energy and Natural Resources, State Geological Survey Division, Circular 537.

Knoll A.H., Hayes J.M., Kaufman A.J., Swett K. and Lambert I.B. (1986) Secular variations in carbon isotope ratios from Upper Prtoterozoic successions of Svalbard and east Greenland. *Nature* **321,** 832-838.

Kroopnick P. (1980) The distribution of ^{13}C in the Atlantic Ocean. *Earth and Planetary Science Letters* **49,** 469-484.

Kunk M.J. and Sutter J.F. (1984) 40Ar/39Ar age spectrum dating of biotites from Middle Ordovician bentonites, eastern North America. In *Aspects of the Ordovician System* (ed. D.L. Bruton), pp. 11-12, Paleontological contributions from the University of Oslo, no. 295.

Leggett J.K. and Smith T.K. (1980) Fe-rich deposits associated with Ordovician basalts in the southern uplands of Scotland: Possible lower Paleozoic equivalents of modern active ridge sediments. *Earth and Planetary Science Letters* **47,** 431-440.

Leslie S.A. (1995) Upper Middle Ordovician conodont biofacies distribution patterns in eastern North America and nortwestern Europe: Evaluations using the Deicke, Millbrig and Kinnekulle K-bentonite beds as time planes. Unpublished PhD dissertation, The Ohio State University, 450 p.

Lewan M.D. (1986) Stable carbon isotope of amorphous kerogens from Phaerozoic sedimentary rocks. *Geochimica et Cosmochimica Acta* **50,** 1583-1591.

Lohmann K.C. and Walker J.C.G. (1989) The δ^{18}O record of abiotic marine calcite cements. *Geophysical Research Letters* **16,** 319-322.

Muehlenbachs K. and Clayton R.N. (1976) Oxygen isotope composition of oceanic crust and its bearing on seawater. *Journal of Geophysical Research* **81,** 4365-4369.

Patzkowsky M.E. and Holland S.M. (1993) Biotic response to a middle Ordovician paleoceanographic event in eastern North America. *Geology* **21,** 619-622.

Piepgras D.J., Wasserburg G.J. and Dasch E.J. (1979) The isotopic composition of Nd in different ocean masses. *Earth and Planetary Science Letters* **45,** 223-236.

Piepgras D.J. and Wasserburg G.J. (1980) Neodymium isotopic variations in seawater *Earth and Planetary Science Letters* **50,** 128-138.

Piepgras D.J. and Wasserburg G.J. (1982) Isotopic composition of neodymium in waters from the Drake Passage *Science* **217,** 207-214.

Piepgras D.J. and Wasserburg G.J. (1983) Influence of the Mediterranean outflow on the isotopic composition of neodymium in waters of the North Atlantic. *Journal of Geophysical Research* **88,** 5997-6006.

Piepgras D.J. and Wasserburg G.J. (1987) Rare earth element transport in the western North Atlantic inferred from Nd isotopic observations. *Geochimica et Cosmochmica Acta* **51,** 1257-1271.

Qing H. and Veizer J. (1994) Oxygen and carbon isotopic composition of Ordovician brachiopods: Implications for coeval seawater. Geochimica et Cosmochimica Acta **58,** 4429-4442.

Railsback L.B., Ackerly S.C., Anderson T.F. and Cisne J.L. (1990) Palaeontonlogical and isotope evidence for warm saline deep waters in Ordovician Oceans. *Nature* **343,** 156-159.

Rodgers J. (1987) The Appalachian-Ouachita orogenic belt. *Episodes* **10,** 259-266.

Rowley D.B. and Kidd W.S.F. (1981) Stratigraphic relationships and detrital composition of the medial Ordovician flysch of western New England: Implications for the Tectonic evolution of the Taconic Orogeny. *Journal of Geology,* **89,** 199-218.

Samson S.D., Patchett P.J., Roddick J.C. and Parrish R.R. (1989) Origin and tectonic setting of Ordovician bentonites in North America: Isotopic and age constraints. *Geological Soceity of America Bulletin* **101,** 1175-1181.

Sanberg P.A. (1983) An oscillating trend in Phanerozoic non-skeletal carbonate mineralogy. Nature **305,** 19-22.

Shaw H.F. and Wasserburg G.J. (1985) Sm-Nd in marine carbonates and phosphates: Implications for Nd isotopes in seawater and crustal ages. *Geochimica et Cosmochmica Acta* **49,** 503-518.

Staudigel H., Doyle P. and Zindler A. (1986) Sr and Nd isotope systematics in fish teeth. *Earth and Planetary Science Letters* **76,** 45-56.

Veizer J., Fritz P. and Jones B. (1986) Geochemistry of brachiopods: Oxygen and carbon isotopic records of Paleozoic oceans. *Geochimica et Cosmochimica Acta* **50,** 1679-1696.

Wilkinson B.H. and Given R.K. (1986) Secular variation in abiotic marine carbonatesL Constraints on Phanerozoic Atmospheric carbon dioxide contents and oceanic Mg/Ca ratios. *Journal of Geology* **94,** 321-333.

Wang K., Orth C.J., Attrep M. Jr., Chatterton B.D.E., Hou H., Geldsetzer H.H.J. (1991) Geochemical evidence for a catastrophic biotic event at the Frasnian/Famennian boundary in south China. *Geology* **19,** 776-779.

Wright J., Seymour R.S.Shaw H.F. (1984) REE and Nd isotopes in conodont apatite: Variations with geological age and depositional environment. *Geological Society of America Special Paper* **196,** 325-340.

Yapp, C.J. (1992) Paleoenvironment and the oxygen isotope geochemistry of ironstone of the Upper Ordovician Neda Formation, Wisconsin, U.S.A. *Geochimica et Cosmochmica Acta* **57,** 2319-2327.

Chapter 5

DEPOSITIONAL ENVIRONMENT OF THE EARLY CRETACEOUS OSTRACODE ZONE: PALEOHYDROLOGIC CONSTRAINTS FROM O, C AND SR ISOTOPES

INTRODUCTION

The early Cretaceous Mannville Group, Western Canada Sedimentary Basin, contains numerous examples of brackish water deposits formed in a complex hydrological system at the interface between northerly flowing rivers of the early Cretaceous foreland basin drainage system and southerly transgressing waters of the Moosebar-Clearwater epicontinental sea (Fig. 5-1). Assessing the relative contributions of marine and fresh waters in brackish water depositional systems is beyond the scope of most sedimentological investigations, and yet assumptions concerning relative paleosalinity can greatly influence the ultimate choice of depositional environment. Carbonate fossils from Mannville Group sediments can be used to gain isotopic constraints on the paleosalinity of Mannville Group depositional waters because: (1) trace element and isotopic variations in fossil shells reflect those of the original waters, and (2) the salinity of brackish waters is governed by mixing of contemporaneous marine and fluviatile sources. Studies of modern estuarine systems show that natural isotopic contrasts between marine and fresh waters for O and C (Mook, 1970), and Sr (Ingram and Sloan, 1992; Andersson et al., 1992), may be used to infer salinities in the mixing zone. Therefore, isotopic analyses of fossil shells from ancient brackish water deposits may be converted to proxy salinity values with knowledge of the isotopic compositions and concentrations

---

[1] A version of this chapter has been submitted for publication in a forthcoming C.S.P.G. Memoir, 05/ '95 coauthored with K. Muehlenbachs and R.A. Creaser

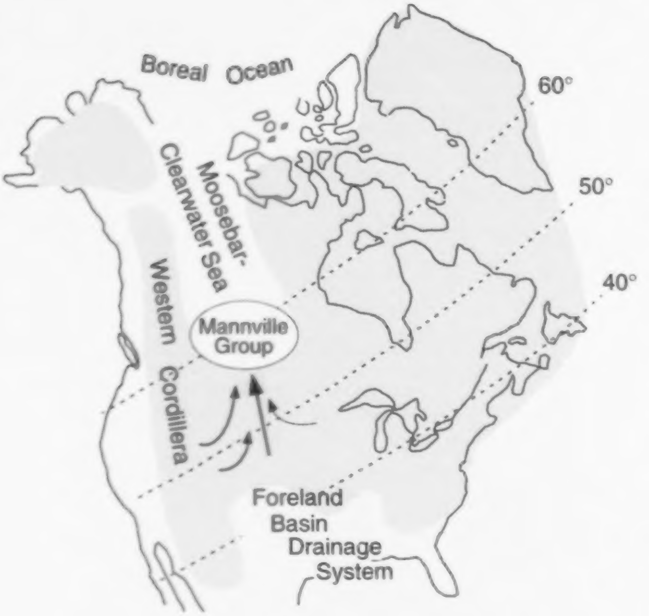

FIGURE 5-1. Reconstructed paleogeography of Cretaceous North America showing the northern arm of the Interior Seaway developing in the early Cretaceous. The Mannville Group was deposited under the influence of northward flowing rivers of the foreland basin drainage system and southerly transgressing waters of the Moosebar-Clearwater sea and contains the whole spectrum of marine, brackish and fresh water depositional environments. Modified from Kauffman (1984) and Koke and Stelck (1984). Middle Cretaceous paleolatitudes from Irving et al. (1993).

of the fluviatile and marine mixing end-members. To determine paleosalinities in Mannville Group depositional waters, it is first necessary to reconstruct the paleohydrology of the Mannville Group with respect to C, O and Sr isotopes, which is one of the main objectives of this study. Following this, the isotopic paleohydrology is applied to assessing the paleosalinity and depositional environment of the Ostracode Zone.

THE OSTRACODE ZONE

The Ostracode Zone (Hunt, 1950), located in the sub-surface of central and southern Alberta, is a conspicuous interval within the overall siliciclastic Mannville Group comprising up to 15 m of thin limestones, pyritic dark shales and coquinas of gastropods and pelecypods. So unique are these occurrences that the Ostracode Zone provides a useful stratigraphic reference point for correlating Mannville sediments in the subsurface. In outcrop locations along the Rocky Mountain foothills, the Ostracode Zone is stratigraphically equivalent to the Calcareous Member of the Blairmore Group, which in turn overlaps calcareous deposits of the lower Kootenai Formation, Montana (Fig. 5-2). The Kootenai Formation has long been regarded as fluvial/lacustrine in origin (Yen, 1951; Hopkins, 1985), but there is little agreement among sedimentologists and paleontologists as to the specific paleoenvironment recorded by the Ostracode Zone and Calcareous Member (Glaister, 1959; McLean and Wall, 1981; Farshori, 1983; Finger, 1983; Wanklyn, 1985; Hayes, 1986; Mattison, 1987; Banerjee, 1990; Banerjee and Kidwell, 1991; McPhee, 1994).

As with the Kootenai formation, earliest studies of the Ostracode Zone concluded that deposition occurred in a predominantly lacustrine paleoenvironment on the basis of fossil ostracodes, charophytes and fresh water gastropods (Loranger, 1951; Glaister, 1959; McLean and Wall, 1981). Uncertainty regarding the salinity tolerances of the various fossil taxa did permit brackish water environments; an idea bolstered by the closer proximity of the Ostracode Zone and Calcareous member to contemporaneous marine waters (Fig. 5-1). Recent studies continue to document an increasing number of marine and brackish water indicators in Ostracode and Calcareous member strata, including bioturbation (Wanklyn, 1985; Banerjee, 1990), echinoid spines, trace fossils of the *cruziana* ichnofacies (Banerjee, 1990), syneresis cracks and dinoflagellates (Banerjee and Davies, 1988) and wavy-bedded heterolithic structures indicative of tides (Banerjee and Kidwell, 1991). Other studies have developed or supported depositional models promoting brackish waters that rely heavily on the assumption that molluscs of the Ostracode Zone constitute a mixed assemblage of

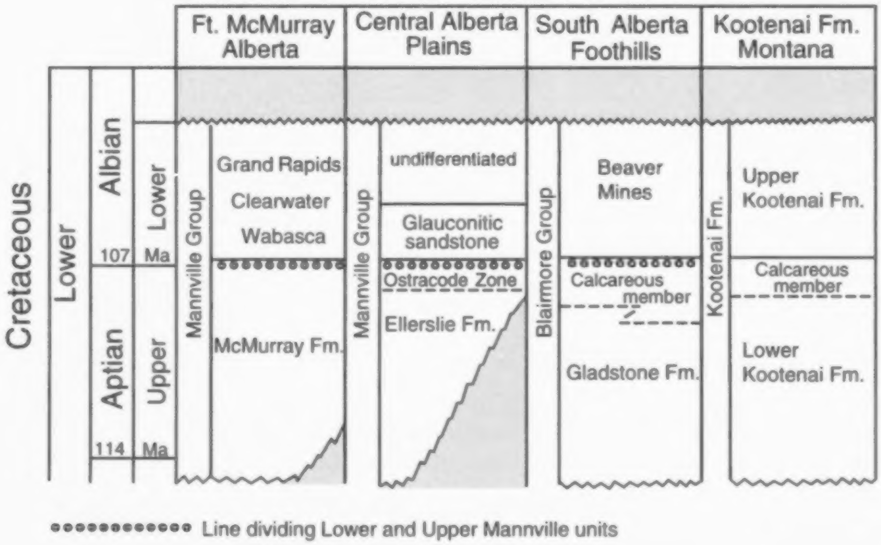
Ft. McMurray Alberta
Central Alberta Plains
South Alberta Foothills
Kootenai Fm. Montana
Cretaceous
Lower
Albian
Aptian
Lower
Upper
107 Ma
114 Ma
Mannville Group
Grand Rapids
Clearwater
Wabasca
McMurray Fm.
Mannville Group
undifferentiated
Glauconitic sandstone
Ostracode Zone
Ellerslie Fm.
Blairmore Group
Beaver Mines
Calcareous member
Gladstone Fm.
Kootenai Fm.
Upper Kootenai Fm.
Calcareous member
Lower Kootenai Fm.
Line dividing Lower and Upper Mannville units

FIGURE 5-2 Stratigraphic correlations relevant to this study. Modified from Hayes (1986) and Hayes et al. (1994).

fresh and brackish water types (Finger, 1983; Wanklyn, 1985; Mattison, 1987; McPhee, 1994).

The erosional limits of the Ostracode Zone have not been mapped and consequently there is confusion (Banerjee, 1990) as to what constitutes Ostracode Zone strata and how these strata fit within the wider context of lower Mannville, McMurray Formation stratigraphy. Isopach maps of Mannville sediment thicknesses show sedimentation occupying three paleovalleys (McMurray, Edmonton and Spirit River channels) incised into older Paleozoic lime/dolostones of the pre-Mannville unconformity surface (Jackson, 1984; Ranger et al., 1994). The paleovalleys are in some cases outlined by paleohighs, ridges of Devonian (and minor Mississippian) carbonates which focused drainage and sediment into 3 sub-basins. Relevant to this study are the McMurray sub-basin (east of the Wainwright Ridge), the Wabasca sub-basin which developed in a pocket of the Wainwright Ridge west of the Grosmont High (Ranger et al., 1994) and the Ostracode sub-basin west of the Wainwright Ridge (Fig. 5-3). Upper McMurray deposits on both sides of the ridge are stratigraphically

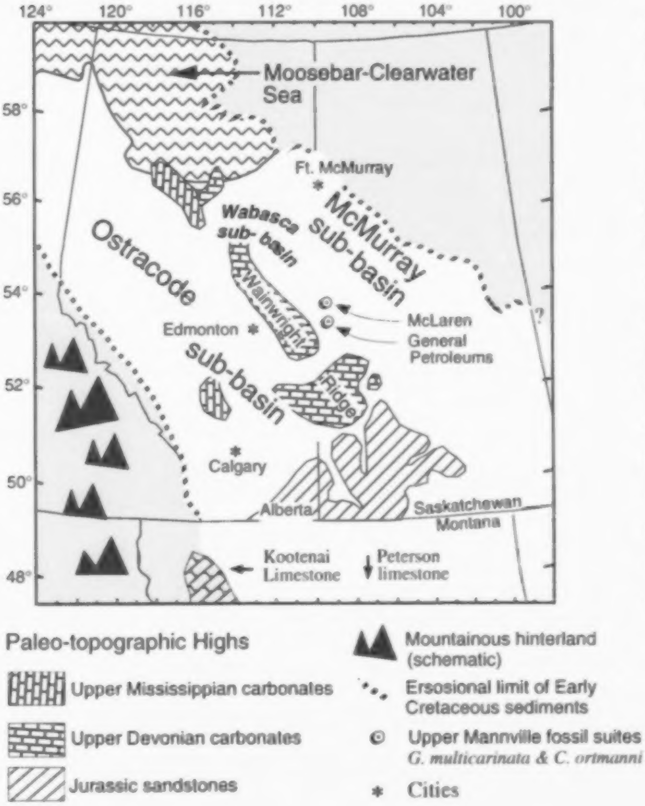
124°
120°
116°
112°
108°
104°
100°
58°
56°
54°
52°
50°
48°
Moosebar-Clearwater Sea
Ft. McMurray
Wabasca sub-basin
McMurray sub-basin
Ostracode sub-basin
Wainwright Ridge
Edmonton
McLaren
General Petroleums
?
Calgary
Alberta
Saskatchewan
Montana
Kootenai Limestone
Peterson limestone
Paleo-topographic Highs
Upper Mississippian carbonates
Upper Devonian carbonates
Jurassic sandstones
Mountainous hinterland (schematic)
Ersosional limit of Early Cretaceous sediments
Upper Mannville fossil suites
G. multicarinata & C. ortmanni
Cities

Figure 5-3 Paleogeography of the Western Canada Sedimentary Basin during Ostracode Zone time. The Wainwright Ridge is a prominent paleotopographic high representing the eastern wall of the incised Spirit River Valley System (Ranger et al., 1994). Locations of the McMurray and Wabasca sub-basins (Ranger et al., 1994) and Ostracode sub-basins are shown. The Ostracode sub-basin includes Ostracode Zone strata from the subsurface of central and southern Alberta and Calcareous member strata of the Blairmore formation, Rocky Mountain foothills. Figure modified from Leckie and Smith (1992).

equivalent but it is not known whether sediment deposition within the Ostracode, McMurray and Wabasca sub-basins was precisely contemporaneous (McPhee, 1994). Therefore, isotopic results on fossils from the three sub-basins are documented separately but discussed as a whole. The most recent dating places the Ostracode Zone near the Aptian-Albian boundary (Pocock, 1980; Banerjee and Davies, 1988).

MATERIALS AND METHODS

Aragonitic fossils were analyzed wherever possible to minimize diagenetic effects. Aragonite mineralogy was confirmed for many of the samples analyzed for stable isotopes and all of the samples for Sr isotopic analyses by X-ray diffraction. Marine waters were characterized using aragonite from two ammonite specimens of *Beudenticeras* collected from marine shales of the Loon River formation, stratigraphically equivalent to the Moosebar and Clearwater shales. Data from several sources were compiled to constrain the isotopic composition of fluviatile waters. Included are: (1) O isotope data on Upper Mannville, aragonitic gastropods *Goniobasis multicarinata* and *Circamelania ortmanni* of the General Petroleums and McLaren units, respectively (this study), (2) Whole-rock O isotope data on lacustrine limestones of the Kootenai formation, Montana (this study), and the Peterson lime/dolostone, Wyoming (Drummond and Wilkinson, 1993), (3) Hydrogen isotope data on preserved Upper Mannville coal, Athabasca tar sands (J. Steer, unpublished data), and (4) Hydrogen isotope data on fluid inclusion waters in Cretaceous and Tertiary quartz veins and ore deposits of the North American Cordillera (Nesbitt and Muehlenbachs, 1989). Aragonitic fossils from the Ostracode Zone were collected from two subsurface cores in central Alberta (Williams, 1960). Fossils from the McMurray sub-basin comprising a single species, *Lioplacodes bituminous,* were collected from outcrops of the upper McMurray formation exposed along the Hangingstone River near Ft. McMurray, Alberta (Russell, 1932; Kramers, 1973), and aragonitic shells from upper McMurray deposits of the Wabasca sub-basin were collected from two subsurface cores (M. Ranger, unpublished data).

Shell material was prepared for analysis by physically removing adhering detritus and diagenetic overgrowths, followed by brief sonication in ultradistilled water or ethanol. The shells were then powdered in an agate mortar. Samples for stable isotope analysis were bleached for at least 1 week to remove organic matter, then rinsed and dried prior to sample digestion in 100% phosphoric acid following the method of McCrea (1950). The CO_2 produced was analyzed on a VG 602 mass spectrometer. Oxygen and hydrogen isotope data are reported relative to Standard Mean Ocean Water (SMOW) and carbon isotope analyses relative to Pee Dee Belemnite (PDB) in the standard delta (δ) notation defined as $(R_{sample}/R_{standard} - 1)1000$, where $R={}^{18}O/{}^{16}O$, D/H or ${}^{13}C/{}^{12}C$. Stable isotope analyses were monitored using internal and international standards. Uncertainty on stable isotope analyses is 0.3‰ for O and 0.2‰ for C, based on reproducibility of samples and international standards.

Separate aliquots of powder were weighed out for Sr isotope dilution and isotope abundance analysis and dissolved in 0.25 M HCl for 8-14 hrs, with the exception of the Peterson lime/dolostone which was dissolved in 0.4 M HCl. A weighed aliquot of mixed ${}^{87}Rb$-${}^{84}Sr$ spike was added to the solution intended for isotope dilution analysis and left overnight to equilibrate. Residues were removed by centrifugation and both solutions evaporated to dryness. Rb and Sr were separated and purified by standard cation chromatography and loaded onto the side filament of double rhenium filament assembly for mass spectrometric analysis. Isotope dilution analyses were done using a Micromass 30 instrument and precise ${}^{87}Sr/{}^{86}Sr$ ratio determinations were done on a VG 354 by multidynamic peak-hopping using VG-software. All analyses are normalized for variable mass-dependent isotope fractionation to a ${}^{86}Sr/{}^{88}Sr$ ratio of 0.1194. Repeat analyses of NBS 987 over the course of this work gave a ratio of 0.71028 ± 0.00001 $(2\sigma_m)$.

OXYGEN AND CARBON ISOTOPE PALEOHYDROLOGY

Marine Waters

Modern seawater has an O isotopic composition near 0‰ (SMOW). The $\delta^{18}O$ values for carbonates formed in isotopic equilibrium with modern seawater range from 33.3 to 27.2 ‰ (SMOW) reflecting a temperature range of 4 to 30 °C. Two specimens of the ammonite *Beudenticeras* from the Loon River Formation (stratigraphically equivalent to the Moosebar shales) have $\delta^{18}O$ values of 30.8 and 30.7‰ (SMOW), within the range of modern marine carbonates. These results are similar to those of McKay and Longstaffe (1993) for ammonites of the Clearwater shales (29.1 ±1.0‰) and together the data support normal marine salinities for the Albian, Moosebar-Clearwater epicontinental sea. This is an important consideration if the natural contrast in isotopic composition between marine and fresh waters is to be used as the basis for semi-quantifying paleosalinity of potential brackish water deposits such as the Ostracode Zone. For example, by the early Cenomanian, ammonites from this part of the Western Interior Seaway had $\delta^{18}O$ values as low as 21‰ (Kyser et al., 1993) which are thought to reflect decreased marine salinities (Barron et al., 1985; Wright, 1987; Glancy, et al., 1993; Pratt et al., 1993).

The ammonite $\delta^{18}O$ values may be used to estimate the paleotemperature of the Moosebar-Clearwater sea provided the isotopic composition of its waters is known. Early Cretaceous seawater was likely lower in $\delta^{18}O$ than modern seawater due to the absence of ^{18}O-depleted polar ice caps in the warmer, more equable Cretaceous climate (Barron, 1983). The isotopic shift imparted to modern seawater if the ice caps are melted has been estimated at -0.5 ‰ (Dansgaard and Tauber, 1969). This is close to the semi-empirical value of -0.4 ±0.3‰ for the isotopic composition of Cretaceous seawater maintained in steady-state isotopic equilibrium with the alteration of Cretaceous oceanic crust (Gregory and Taylor, 1981). For the calculations that follow, a $\delta^{18}O$ value of -0.5‰ is adopted for the isotopic composition of seawater in warm ancient climates.

Using the temperature dependent carbonate-water equilibrium fractionation relation of O'Neil et al. (1969), a +0.6 ‰ correction for the aragonite-calcite equilibrium fractionation (Tarutani et al., 1969), and a $\delta^{18}O$ value of -0.5‰ for early Cretaceous seawater, a mean paleotemperature of 14.5 °C is calculated. The relatively high $\delta^{18}O$ values obtained for the ammonites minimizes the uncertainty in the paleotemperature determination. If the Moosebar-Clearwater sea had a lower $\delta^{18}O$ value of -2.0 ‰, then a mean paleotemperature of 8.3 °C would be calculated. This lower temperature is outside the range of temperatures predicted for 60° N latitude using Cretaceous latitudinal temperature gradients of -0.14 (Spicer and Corfield, 1992) and -0.21 (Barron, 1983) °C per degree

Table 5-1 Oxygen and Carbon Isotope Data on Fossils and Whole-rock Carbonates

Sample Name	Phase	$\delta^{13}C$ (PDB)	$\delta^{18}O$ (SMOW)	Sample Description
I. Marine Waters				
1. Ammonites (U. of Alberta collection, Dr. Stelck personal collection)				
BEUD-26-46-34F	A	1.3	30.8	thin fragments, nacreous lustre
BEUD-38081	A	2.1	30.7	thick fragment, nacreous lustre
II. Ostracode Sub-basin				
2. 1-18-64-26W4 (866.2-869.5 m) (G.D.C. Williams, 1960)				
Hand Sample 1 (866.2 m.)				
1-Mtrx	C,S,D	0.4	19.0	black shale
1-F1	nd	2.5	20.4	pelecypod shell fragments
1-W1	nd	1.2	20.3	single pelecypod shell fragment
Hand Sample 2 (869.5 m)				
2-Mtrx	D	0.3	24.6	black shale
2-F1	A	3.0	19.9	pelecypod shell fragments
2-W1	nd	3.3	20.8	single pelecypod shell fragment
3. 7-21-56-27W4 (G.D.C. Williams, 1960)				
Handsample 1 (1154.3-1157.3 m)				
1-mtrx	D	0.4	22.4	black shale matrix
1-F1	A	2.4	21.0	composite of shell fragments
1-W1	nd	2.1	20.4	single pelecypod shell fragment
Hansample 2 (1154.3-1157.3 m)				
2-mtrx	D	0.2	23.1	black shale matrix
2-F1	A,S	3.4	21.3	pelecypod shell fragments
2-F2	nd	2.6	20.4	pelecypod shell fragments
Handsample 3 (1154.3-1157.3 m)				
3-F1	A	2.5	21.1	shell composite A
3-F2	A	2.1	21.0	shell composite B
3-F3	A	2.5	22.6	single pelecypod shell fragment
Hand Sample 4 (1157.8 m)				
W.R.	A,C,S	2.5	19.8	gastropod & pelecypod limestone
4. 10-12-25-20W4 (1421.3 m)				
W.R.	C	-2.5	21.2	whole-rock black shale
F1	nd	1.7	23.2	recrystallized shell composite
W1	C	1.2	21.7	single recrystallized shell fragment
II. Wabasca Sub-basin				
5. 7-11-82-20W4 (429.1 m) (M. Ranger, unpublished core descriptions)				
W.R.	nd	-2.7	22.6	whole rock fossiliferous siltstone
6. 6-17-76-23W4 (795.8-798.6 m) (M. Ranger, unpublished core descriptions)				
W.R.	A,C	5.6	20.8	cemented pelecypod coquina
F1	A	4.2	22.5	recrystallized shell fragments
7. 11-6-76-22W4 (611.1-611.4 m) (M. Ranger, unpublished core descriptions)				
W.R.	A,C	3.9	21.0	coquina
F1	A	3.9	20.8	composite of shell fragments
III. McMurray Sub-basin				
8. Hangingstone River, Ft. McMurray, Alberta (Kramers, 1971)				
Hand-sample B				
B-G1	A,C	4.8	20.3	single gastropod shell fragment
B-G2	A	4.9	20.7	single gastropod shell fragment
B-G3	A	3.8	20.4	single gastropod shell fragment
B-G6	A	4.5	20.6	single gastropod shell fragment
B-G7	A	4.7	20.0	single gastropod shell fragment
B-D1	C	-0.2	19.8	infilling chamber cement
B-D2	C	0.2	19.9	infilling chamber cement
B-D3	C	0.5	22.1	infilling chamber cement
B-D6	C	0.7	22.1	infilling chamber cement
Hand-sample C				
C-P1	A	3.5	19.4	single pelecyod shell fragment
C-P2	A	4.1	20.1	single pelecyod shell fragment

Table 5-1 Oxygen and Carbon Isotope Results on Fossils and Carbonate Whole-rock (continued)

Sample Name	**Phase**	$\delta^{13}C$ (PDB)	$\delta^{18}O$ (SMOW)	**Sample Description**
Hand-sample D				
D-G1	A	4.3	21.3	single gastropod shell fragment
D-G2	A	4.3	21.0	single gastropod shell fragment
D-G3	A	5.7	19.9	single gastropod shell fragment
D-G4	A,C	4.5	20.3	single gastropod shell fragment
D-G5	A,C	4.6	21.0	single gastropod shell fragment
D-G6	A	4.8	20.6	single gastropod shell fragment
D-G7	A,C	4.9	20.8	single gastropod shell fragment
D-G8	A,C	4.1	20.6	single gastropod shell fragment
D-D1	nd	4.8	21.5	infilling chamber cement
D-D4	nd	4.2	21.5	infilling chamber cement
Measured Section (cm)				
FM 330 cm	nd	3.8	21.0	gastropod shell composite
FM 285 cm	nd	4.2	20.7	gastropod shell composite
FM 250 cm	A	4.9	21.0	gastropod shell composite
FM 205 cm	nd	4.4	21.6	gastropod shell composite
FM 190 cm	nd	4.0	21.2	gastropod shell composite
FM 145 cm	nd	4.9	22.0	gastropod shell composite
FM 120 cm	nd	4.3	21.1	gastropod shell composite
FM 105 cm	nd	3.5	21.4	gastropod shell composite
FM 70 cm	A	3.5	20.7	gastropod shell composite
FM 30 cm	nd	3.9	21.1	gastropod shell composite
FMG 0 cm	nd	2.8	21.5	gastropod shell composite
FMP 0 cm	A	5.3	22.3	gastropod shell composite
IV. Upper Mannville, Cold Lake (B. Mattison, 1991)				
9. McLaren Unit (13-1-65-4W4 383-386 m)				
C. ortmanni	A	0.21	24.1	single gastropod shell fragment
C. ortmanni 1	A	0.54	22.9	single gastropod shell fragment
C. ortmanni 2	A	0.19	22.6	single gastropod shell fragment
C. ortmanni 3	A	0.08	23.1	single gastropod shell fragment
V. murraiensis	A	1.3	23.2	single gastropod shell fragment
L. bituminous	A	0.53	23.9	single gastropod shell fragment
L. bituminous	A	0.21	22.6	single gastropod shell fragment
10. General Petroleums Unit (16-13-58-5W4 505 m)				
G. multicarinata 1A	A	1.0	16.6	single gastropod shell fragment
G. multicarinata 1A	C	7.9	21.4	infilling chamber cement
G. multicarinata 2	A	0.9	16.5	single gastropod shell fragment
G. multicarinata 4	A	0.9	16.2	single gastropod shell fragment
G. multicarinata 5	A	0.5	17.3	single gastropod shell fragment
G. multicarinata 7	A	1.0	17.2	single gastropod shell fragment
G. multicarinata 9	A	0.1	16.4	single gastropod shell fragment
V. Kootenai Formation, Montana				
11. Harlowton, Montana (Yen, 1951)				
F2	C	-4.3	20.7	single recrystallized shell fragment
F3	nd	-7.2	19.9	single recrystallized shell fragment
F4	nd	-8.7	19.0	single recrystallized shell fragment
F5	nd	-6.2	19.0	single recrystallized shell fragment
12. Drummond, Montana				
Measured section (cm)				
Drum 1010 cm	nd	0.7	16.1	marl
Drum 960 cm	nd	0.7	16.3	marl
Drum 880 cm	nd	0.3	17.5	gastropod limestone
Drum 770 cm	nd	1.5	17.5	gastropod limestone
Drum 703 cm	nd	1.6	17.8	gastropod limestone
Drum 620 cm	C	0.6	15.4	gastropod limestone
Drum 604 cm	nd	1.9	18.4	marl
Drum 602 cm	nd	1.3	16.9	gastropod limestone
Drum 600 cm	C	-0.3	14.2	black shale
Drum 598 cm	nd	0.3	13.2	gastropod limestone
Drum 596 cm	nd	0.6	16.3	gastropod limestone
Drum 594 cm	nd	1.3	16.9	gastropod limestone
Drum 475 cm	nd	1.4	17.5	gastropod limestone
Drum 335 cm	C	-0.8	17.6	gastropod limestone
Drum 235 cm	nd	2.1	15.8	gastropod limestone
Drum 35 cm	nd	-0.5	17.7	gastropod limestone
Drum 15 cm	C	0.4	16.5	gastropod limestone

A = > 97% aragonite (unless otherwise stated) determined by quantiative X-ray diffraction of standard aragonite-calcite mixtures C = calcite; S = siderite; D = dolomite; nd = not done.

of latitude. If 26 °C is accepted as the temperature of equatorial marine waters during the late Aptian to early Albian (Fig. 5 of Spicer and Corfield, 1992), bounding paleotemperatures of 13.4 °C and 17.6°C are calculated at 60° N latitude using the above temperature gradients. The paleotemperature estimate of 14.5°C falls within this wider range of paleotemperatures. Applying the equilibrium fractionation relation in reverse, the isotopic composition of the Moosebar-Clearwater sea could not have been lower than -1.0 ‰ (SMOW), based on an ammonite $\delta^{18}O$ value of 30.8 ‰ and a low temperature estimate of 13.4 °C.

The carbon isotope composition of HCO_3 in modern seawater varies between -4 and +4 ‰ (PDB) (Clayton and Degens, 1959). The two samples of *Beudenticeras* yielded typical marine $\delta^{13}C$ values of 2.5 and 2.6 ‰ (PDB) for the Moosebar sea, similar to a mean value of 3.6 ± 0.1 ‰ reported by McKay and Longstaffe (1993) for the Clearwater sea .

Fresh Waters

If the paleolatitude of a study site is known the $\delta^{18}O$ value of past meteoric waters may be estimated from the observed isotopic dependence of modern precipitation on latitude. For modern coastal areas at 60° N latitude, precipitation has $\delta^{18}O$ value of -8.5 ‰ (SMOW) (Fig. 22 of Yurtserver and Gat, 1981) which corresponds to an equilibrium aragonite $\delta^{18}O$ value of 22.5 ‰ (SMOW) at 14.5°C. At a given paleolatitude the $\delta^{18}O$ value of precipitation decreases towards continental interiors and with increasing altitude. As a mountainous region existed to the west of the Ostracode, Wabasca and McMurray sub-basins, rivers draining high altitude regions should have $\delta^{18}O$ values lower than -8.5‰. This prediction is confirmed by analyses of the aragonitic gastropod *G. multicarinata*, collected from siliciclastic rocks of the upper Mannville Group (General Petroleums unit) which yielded $\delta^{18}O$ values between 16.2 and 17.3‰ with corresponding waters of -14.6 to -13.5‰ at 14.5°C. The McLaren unit (stratigraphically above the General Petroleums unit) has an aragonitic gastropod fauna dominated by *C. ortmanni* which yielded higher $\delta^{18}O$ values between 22.6 and 24.1‰ with corresponding waters of -8.4 to -7.0‰ at 14.5 °C.

The Kootenai limestones, together with the Peterson and Draney lime/dolostones, represent large fresh water lakes which formed along the axis of the foreland basin drainage system in the early Cretaceous (McGookey et al., 1972). Four recrystallized shells of the pelecypod *Unio,* collected from varicolored shales of the Kootenai formation near Harlowton, Montana (Yen, 1951) have $\delta^{18}O$ values between 19.0 and 20.7‰. Corresponding waters are -11.3 to -9.7‰ at 14.5°C. Near Drummond, Montana, a 10 meter thick gastropod limestone gave whole-rock $\delta^{18}O$ values between 13 and 17‰ (Fig. 5-4), with a mean value of 16.6 ±1.3‰ (1σ; n=13). Corresponding waters range from -17.1 to -13.2‰ at 14.5 °C.

Further south along the axis of the foreland basin drainage system, the slightly older Peterson lime/dolostone, Wyoming, shows metre-scale variation in $\delta^{18}O$ and micritic dolomite abundance interpreted to reflect episodic lake level fluctuation in response to regional climate change (Drummond et al., 1989). During periods of relative aridity the lake was hydrologically closed to fluviatile throughflow with evaporation exceeding river inflow. Evaporation increases the $\delta^{18}O$ value of lake water because $H_2{}^{16}O$ has a higher vapor pressure than $H_2{}^{18}O$ and is therefore preferentially incorporated into vapor leaving the lake. Drummond et al. (1993) argued on the basis of textural, geochemical

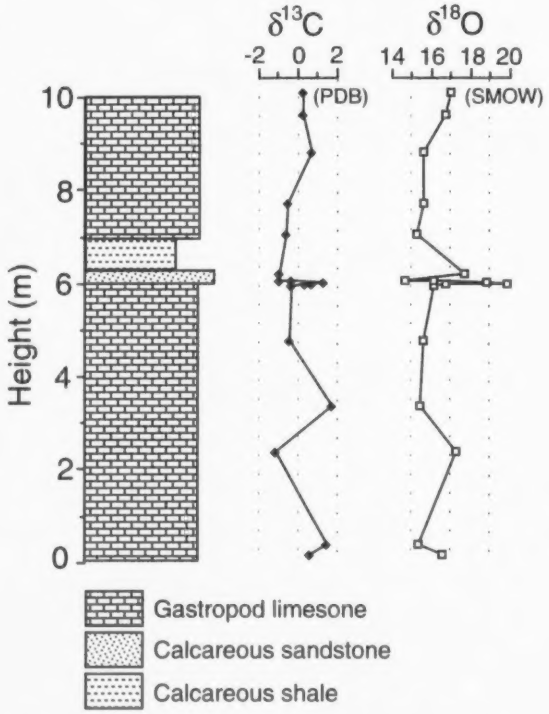

FIGURE. 5-4 C and O isotope profile of lacustrine limestones of the Kootenai Formation, Drummond, Montana. The fairly constant profiles over 10 metres of section indicate relatively long-lived stability of the lake's water balance.

and isotopic evidence that the fine grained Peterson lime/dolostone evolved predominantly in a closed diagenetic system and that the $\delta^{18}O$ values of the original sediments could be recovered. During periods of relative humidity and aridity, the original lake sediments attained values as low as 19.0‰ and as high as 26.1‰ (SMOW), respectively (Fig. 6 of Drummond et al., 1993). Corresponding waters range between -11.3 and -4.4‰ (SMOW) at 14.5°C.

It is difficult to evaluate the degree of isotopic resetting that the Kootenai and Peterson limestones may have experienced as a result of their post-depositional recrystallization histories. Because these are lacustrine carbonates, the isotopic composition of diagenetic fluids may have been higher or lower in $\delta^{18}O$ value than waters from which the original limestones were precipitated. Although Drummond et al. (1993) argued for closed system diagenesis of the Peterson carbonate micrite, no attempt was made to determine the diagenetic history of the Kootenai limestones. It is noted, however, that the Kootenai limestones and primary aragonitic fossils of the General Petroleums unit have identical mean $\delta^{18}O$ values of 16.7‰, suggesting that the water isotopic compositions indicated by the Kootenai limestones are broadly representative of early Cretaceous foreland basin fresh waters.

Additional estimates of early Cretaceous meteoric waters comes from hydrogen isotope data on lower Mannville coal and Cretaceous-Tertiary fluid inclusion waters from quartz veins of the Canadian Cordillera. Coal from the Athabasca tar sands deposit yielded δD values of -150, -156, and -157‰ (SMOW) (J. Steer, unpublished data). Applying a bulk H isotopic fractionation factor between plants and local meteoric waters of +40‰ (Smith et al., 1983), freshwaters with a mean δD value of -114 ±4 ‰ (1σ) are indicated, which may be converted to an equivalent $\delta^{18}O$ value of -15.5 ‰ (SMOW) using the meteoric water line (Craig, 1961). Quartz veins which cross-cut the Canadian Cordillera reflect pathways of crustal fluid flow operating during Cordilleran orogenesis. Much of the thrusting and associated metamorphism is late Cretaceous and Tertiary, and many of the quartz veins and ore deposits probably date to this age (Nesbitt and Muehlenbachs, 1989). Hydrogen isotope values for inclusion waters extracted from these veins range between -120 to -160 ‰ (SMOW) (Nesbitt and Muehlenbachs, 1989). The low δD values indicate these waters were sourced

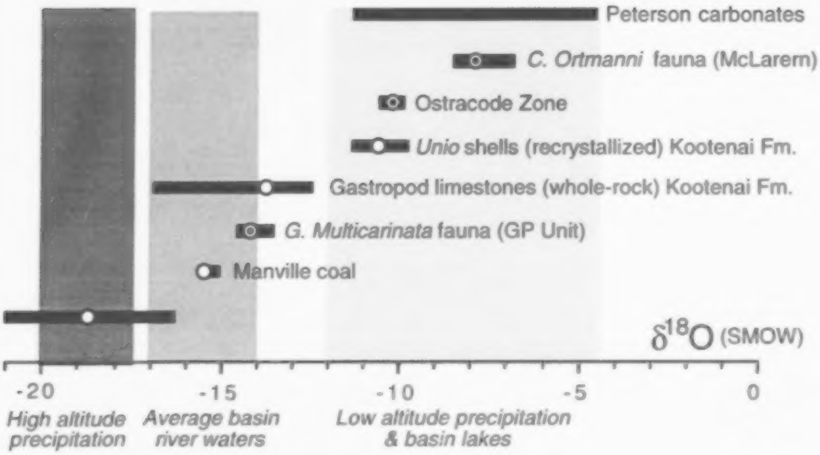

FIGURE 5-5 Range in $\delta^{18}O$ values for Early Cretaceous meteoric waters of the foreland basin drainage system. Two dominant sources are evident: (1) high altitude ^{18}O-depleted meteoric waters with moisture sources from the Pacific ocean, and (2) low altitude, relatively ^{18}O-enriched meteoric waters with moisture sources from the Moosebar-Clearwater sea. The primary isotopic composition of early Cretaceous foreland basin river waters, unaffected by evaporation, is estimated at –14 to –17‰ (SMOW). Open symbols are analyses based on aragonite. White-filled symbols are other materials.

from surface meteoric waters, thus providing an estimate of high altitude Cretaceous meteoric waters. From the meteoric water line corresponding $\delta^{18}O$ values are -16.5 to -21‰ (SMOW), more ^{18}O-depleted than most estimates of meteoric waters from the foreland basin.

The total range in early Cretaceous meteoric waters is -5 to -21 ‰ (SMOW) (Fig. 5-5). Such a wide range of values reflects the physiography and climate of the foreland basin setting. The isotopically lightest meteoric waters were produced over the western Cordillera from moist Pacific air masses moving eastward by the prevailing winds (Glancy et al., 1993). Moist air masses from the southern reaches of the Moosebar-Clearwater sea may have constituted a second more ^{18}O-enriched source of meteoric waters (-8.5‰) within the foreland basin. Mixing of high and low altitude waters and evaporation during residence in foreland basin lakes probably accounts for the wide range of isotopic compositions observed (Fig. 5-5). It is desirable, however, to estimate the average isotopic composition of fluviatile waters of the foreland basin drainage system unaffected by lake storage. Since the majority of waters transported by foreland basin rivers probably originated in the Cordillera, relatively ^{18}O-depleted values of -14 to -17‰ (SMOW) appear to best characterize the

$\delta^{18}O$ value of primary runoff.

Fresh water shells and whole-rock limestones have also been measured for their C isotope compositions. Whole-rock limestones are generally considered to have preserved their original $\delta^{13}C$ signatures because their large C contents buffer them against diagenetic exchange effects. The isotopic composition of C in fresh waters is controlled by various factors: (1) relative rates of decomposition and burial of ^{13}C-depleted organic matter (-16 to -30 ‰), (2) the weathering of marine limestones (-2 to +4‰), (3) exchange of CO_2 with the atmosphere, (4) changes in biological productivity, and (5) mixing of waters with different C isotopic compositions (Sackett and Moore, 1966).

In general it is observed that marine waters have much higher $\delta^{13}C$ values than fresh waters and this difference has been proposed as a method of distinguishing marine and fresh water environments (Clayton and Degens, 1959). Limitations arise when the fresh water C budget is dominated by equilibrium isotope exchange reactions with atmospheric CO_2, or by the weathering of older

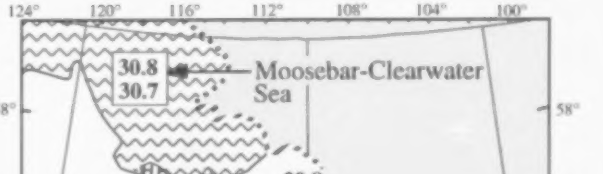
124°
120°
116°
112°
108°
104°
100°
58°
56°
54°
52°
50°
48°
122°
118°
114°
110°
106°
102°
98°
30.8
30.7
Moosebar-Clearwater Sea
20.8
22.6
20.8
22.5
20.4
21.1
22.8
McLaren
16.8
General Petroleums
?
22.5
Alberta
Saskatchewan
Montana
Kootenai limestone 16.6
Peterson limestone 19 to 26
Paleotopographic Highs
Upper Mississippian Carbonates
Upper Devonian Carbonates
Triassic Sandstones
Mountainous Hinterland (schematic)
Ersosional Limit of Early Cretaceous Sediments

FIGURE 5-6 Location of sampled sites within the Ostracode, Wabasca and McMurray sub-basins and their mean O isotopic compositions. Analyses and locations for Upper Mannville fresh water gastropod faunas from the McLaren and General Petroleums Unit are also shown. Bolded data are based on the analysis of aragonite. Figure modified from Leckie and Smith (1992).

marine limestones. Both processes result in isotopic compositions of fresh water HCO_3^- that are indistinguishable from oceanic sources. In their compilation of C isotope data from marine and fresh water molluscs, Keith et al., (1964) demonstrated that considerable overlap exists. Generally, if the limestone whole-rock $\delta^{13}C$ values are < -4 ‰, a predominantly fresh water source is indicated, however, the opposite can not be assumed, i.e., +4‰ carbonates are not necessarily of marine origin.

Mean $\delta^{13}C$ values the *G. multicarinata* (GP unit) and *C. ortmanni* faunas are 0.7 ± 0.4‰ (1σ; n=6) and 0.4 ± 0.4‰ (1σ; n=7), respectively. Gastropod limestones from Drummond, Montana, are similar averaging 0.8 ±0.8‰ (1σ; n=13) and carbonates from the Peterson limestone have slightly lower $\delta^{13}C$ values of -2 to -4 ‰ (Drummond et al., 1993). Overall, these marine-like $\delta^{13}C$ values indicate CO_2 sourced directly from the Cretaceous atmosphere, or weathering of older marine carbonates in the watershed. More typical fresh water signatures of -4.3 to -6.2‰ are recorded in recrystallized shells of the pelecypod *Unio* collected from Kootenai shales near Harlowton, Montana.

Ostracode , Wabasca and McMurray Waters

The $\delta^{18}O$ values of mostly aragonitic fossil material from the Ostracode, McMurray and Wabasca sub-basins is on average 10‰ depleted in ^{18}O relative to the marine ammonites of the Moosebar-Clearwater sea, clearly distinguishing Ostracode and equivalent waters from those of the contemporaneous Moosebar-Clearwater sea (Fig. 5-6). From the Ostracode sub-basin, 11 shell analyses yielded a mean $\delta^{18}O$ value of 20.8 ±0.7 ‰ (1σ). From the McMurray sub-basin, 27 analyses of fossil material from outcrops at Hangingstone River yielded a mean $\delta^{18}O$ value of 20.8 ±0.6 ‰ (1σ), and 2 shell analyses from the Wabasca sub-basin yielded a mean $\delta^{18}O$ value of 21.7 ±1.2‰ (1σ). The uniformity in $\delta^{18}O$ values within and between sampling sites is significant considering the stratigraphic uncertainties and complex facies relations of the Ostracode Zone (Banerjee, 1990), and that shell $\delta^{18}O$ values reflect a variable temperature component. Seasonal variation on the order of 10 °C by itself would translate to a range 2‰ in shell $\delta^{18}O$ values, slightly in excess of the total

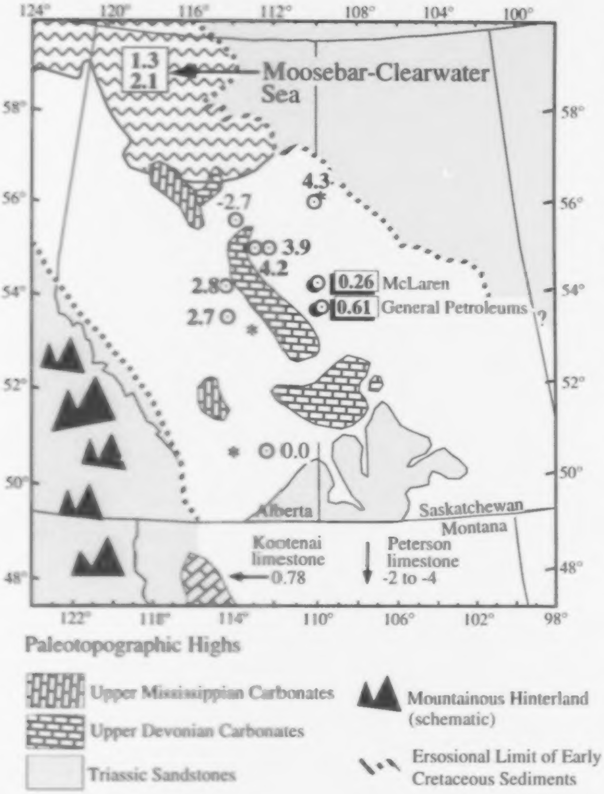
124°
120°
116°
112°
108°
104°
100°
1.3
2.1
Moosebar-Clearwater Sea
58°
56°
54°
52°
50°
48°
4.3
-2.7
3.9
4.2
2.8
2.7
0.26 McLaren
0.61 General Petroleums
?
0.0
Alberta
Saskatchewan
Montana
Kootenai limestone
0.78
Peterson limestone
-2 to -4
122°
118°
114°
110°
106°
102°
98°
Paleotopographic Highs
Upper Mississippian Carbonates
Upper Devonian Carbonates
Triassic Sandstones
Mountainous Hinterland (schematic)
Ersosional Limit of Early Cretaceous Sediments

Figure 5-7 Location of sampled sites within the Ostracode, Wabasca and McMurray sub-basins and their mean C isotopic compositions. Analyses and locations for Upper Mannville fresh water gastropod faunas from the McLaren and General Petroleums Unit are also shown. Bolded data are based on the analysis of aragonite. Figure modified from Leckie and Smith (1992).

variation observed. Consequently, the waters of the Ostracode, McMurray and Wabasca sub-basins can be expected to vary regionally and temporally by not more than ±1‰ for $\delta^{18}O$. The mean $\delta^{18}O$ value for all 3 sites is 20.9 ± 0.7‰ corresponding to an equilibrium $\delta^{18}O$ value for Ostracode, Hangingstone and Wabasca waters of -10.1 ‰ at 14.5 °C. It is evident from these data that a similar bulk O isotope paleohydrology characterized all 3 sub-basins.

In contrast to the low $\delta^{18}O$ values, carbon isotopic compositions for Ostracode, Wabasca and McMurray waters are marine-like (Fig. 5-7). There are also isotopic differences between the sub-basins not seen for O isotopes. The mean $\delta^{13}C$ values for the McMurray (4.3 ±0.6‰;1σ n=27) and Wabasca (4.0 ±0.14‰;1σ n=4) sub-basins are similar (excluding 7-11-82-25W4), but differ from the Ostracode Zone (2.5 ±0.6;1σ n=11), suggesting either diachronous deposition between Ostracode and Wabasca-McMurray sub-basins, or restricted mixing of contemporaneous waters by the Wainwright Ridge.

THE OXYGEN ISOTOPE BALANCE

Many recent studies of the Ostracode Zone have concluded that it was deposited under brackish waters (Wanklyn, 1985; Banerjee, 1990; Banerjee and Kidwell, 1991; Mattison, 1987), possibly in an estuarine paleoenvironment (Finger, 1983; McPhee, 1994). Modern estuarine waters have variable $\delta^{18}O$ values reflecting the contrasting isotopic compositions of marine and fresh water sources (Mook, 1970). Although the isotopic contrast between marine and fresh waters of the early Cretaceous foreland basin was between 14 and 17‰, Ostracode and equivalent waters vary by less than 1‰. Only the oceans and large well mixed lakes are known to homogenize the $\delta^{18}O$ value of their waters to such a remarkable degree. Accordingly, the O isotope data support a lacustrine paleoenvironment. The isotope balance in lake waters is controlled by: (1) the volume and $\delta^{18}O$ value of precipitation and in-flowing river and ground waters, (2) the rate of evaporation, and (3) the residence time of the water (Gat, 1981). The last two factors work to increase the $\delta^{18}O$ value of lake waters because long water residence times enables proportionately greater amounts of $H_2{}^{16}O$ to leave the lake by evaporation. If the Ostracode Zone and equivalent strata record deposition in a

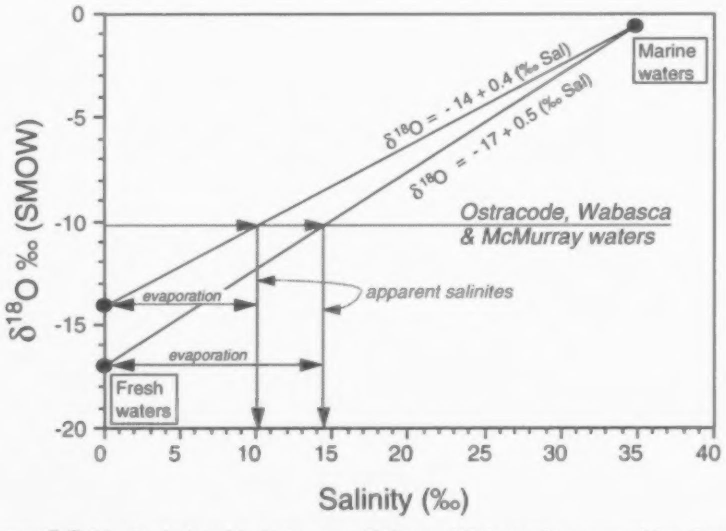

FIGURE 5-8 Ideal relationship between salinity and O isotopic composition for 2 component mixtures of marine and fresh waters. Although apparent salinities of 10-15‰ are indicated from the mixing relations, the very uniform $\delta^{18}O$ values of the Ostracode, Wabasca and McMurray waters indicates long water residence times and an increased probability of evaporation induced isotope effects. Significant evaporation of the mixed waters renders salinities calculated in this manner unreliable.

large lake, the O isotope budget requires that lake waters are between 4 and 7‰ more ^{18}O-enriched than in-flowing river waters, indicating long lake water residence times and disrupted flow of foreland basin waters to the sea. In a lake setting, the marine-like $\delta^{13}C$ values exhibited by Ostracode, McMurray and Wabasca waters could be a result of chemical weathering (Oana and Deevey, 1960) of older Devonian and Mississippian carbonates of the Wainwright Ridge, rather than direct contributions from the Moosebar-Clearwater sea.

Although the depositional environment of the Ostracode Zone most resembles a lake (from our paleohydrological perspective), it is conceivable that a small marine contribution could be mixed uniformly throughout the greater extent of the three basins by wind generated currents and storms. It is also possible that sites close to marine and fresh water inputs were not sampled which may explain the absence of even a small salinity-controlled north-south gradient in $\delta^{18}O$. The equation describing two-component mixtures of seawater and freshwater with differing O isotope compositions is

$$(1) \qquad \delta^{18}O_{Brackish} = \chi\, \delta^{18}O_{Marine} + (1-\chi)\, \delta^{18}O_{Fresh}$$

$$(2) \qquad \text{Proxy salinity (‰)} = 35\, \chi,$$

where χ is the mixing parameter accounting for the fraction of marine waters in the brackish water mixture. Assuming end-member salinities of 35‰ and 0‰ for the marine and fresh water end-members, respectively, χ can be converted to proxy salinities using equation (2). The mixing trajectories defined by the O isotope paleohydrology give model salinities of 10 to 15‰ for the Ostracode, McMurray and Wabasca waters (Fig. 5-8). Even if a small marine contribution is assumed in the Ostracode water balance, these salinities are misleading because the Ostracode waters likely had their ^{18}O contents increased through evaporation. Significant evaporation of mixed waters induces non-conservative effects which invalidates the mixing model and its application to paleosalinity determinations. The mixing lines do provide a useful representation of the O isotope balance and may be applied to more classic estuarine deposits (i.e., those with short water residence times) elsewhere in the Western Canada Sedimentary Basin. For example, if evaporation effects account for 4‰ of the observed 4-7‰ ^{18}O-enrichment in the Ostracode waters relative to fluviatile waters, calculated salinities drop to between 0‰ and 6‰ (depending on which mixing line is used).

The difference between a brackish sea and a lake is a non-trivial distinction. To obtain better constraints on the paleosalinity of the Ostracode waters a tracer unaffected by evaporation or temperature effects is required. Dissolved Sr has been shown to behave conservatively within the seawater-freshwater mixing zone (Ingram and Sloan, 1992; Andersson et al., 1992), its isotopic systematics in natural waters is very well understood (Wadleigh and Veizer, 1985; Goldstein and Jacobsen, 1987), and the relative mass differences between the isotopes of Sr are too small to be affected by evaporation or temperature effects during Sr partitioning in carbonate. Recent studies have highlighted the utility of Sr isotope variations in modern estuaries as a proxy measure of salinity (Ingram and Sloan, 1992; Andersson et al., 1992), and Ingram and DePaolo (1993) have determined paleosalinities from $^{87}Sr/^{86}Sr$ analyses of fossil mollusc shells in near recent sediments of San Francisco Bay estuary. To determine Sr isotope paloesalinities for depositional waters of the Cretaceous Ostracode Zone it is necessary to reconstruct the regional, early Cretaceous, Sr isotope paleohydrology.

STRONTIUM ISOTOPE PALEOHYDROLOGY

Isotopic Composition of Sr in Marine and Fresh Waters

Seawater has a uniform $^{87}Sr/^{86}Sr$ ratio at any given time because the residence time of Sr in seawater (5×10^6 yrs) is longer than the oceanic mixing time (~1000 yrs). This timescale difference effectively homogenizes Sr derived from three principal, isotopically distinct sources: (1) old continental crust ($^{87}Sr/^{86}Sr > 0.712$), (2) young volcanic rocks (< 0.706), and (3) Phanerozoic carbonates (0.7067-0.7091) (Faure, 1986). Old crustal sources have much higher $^{87}Sr/^{86}Sr$ ratios than younger crustal sources due to the decay of ^{87}Rb which increases the relative abundance of ^{87}Sr in a rock over time. Phanerozoic carbonates have intermediate $^{87}Sr/^{86}Sr$ ratios and are an important

Table 5-2 Correlated O and Sr isotopic compositions for Group 1 and Group 2 fresh waters for fossil mollusc shells of the Mannville Group

Samples		δ^{18}O (SMOW)	^{87}Sr/^{86}Sr
Group 1 Fresh Waters			
McLaren Unit			
C. ortmani 1		22.9	0.708791 (12)
C. ortmani 2		22.6	0.708733 (08)
C. ortmani 3		23.1	0.708804 (10)
L. bituminous		22.6	0.708839 (10)
	average	22.8	0.708792
Kootenai Limestone			
Drum 335		17.6	0.708740 (14)
Drum 620		15.4	0.708594 (14)
Drum 770		17.5	0.708633 (13)
	average	16.8	0.708656
Group 1 Average			0.70873
Group 2 Fresh Waters			
General Petroleums Unit			
G. multicarinata 4		16.2	0.707495 (11)
G. multicarinata 5		17.3	0.707550 (09)
G. multicarinata 7		17.2	0.707595 (10)
G. multicarinata 9		16.4	0.707600 (10)
	average	16.8	0.707560
Peterson Limestone			
A-2		nd	0.707586 (16)
A-6		nd	0.707619 (14)
A-15		nd	0.707954 (13)
	average		0.707720
Group 2 average			0.70763

source of unradiogenic Sr to the oceans because they are easily weathered and have relatively high Sr contents (Brass, 1976). Changes in the proportions of these principal rock types exposed to weathering on the continents and in the ocean basins causes the ^{87}Sr/^{86}Sr ratio of seawater to change over time. The changes are recorded in marine carbonates which have been analyzed in detail by Burke et al. (1982) to construct the seawater ^{87}Sr/^{86}Sr age curve for the Phanerozoic era.

In constructing Sr isotope paleohydrologies the seawater ^{87}Sr/^{86}Sr curve can be used to estimate the isotopic composition of marine waters. During the late Aptian to early Albian the marine ^{87}Sr/^{86}Sr ratio fluctuated between 0.70737 and 0.70753 (Ingram et al., 1994). Marine ammonites from this study fall within this range yielding mean ^{87}Sr/^{86}Sr ratios of 0.70745 ($\pm$0.00002; 2σ, n=2) and 0.70750 ($\pm$0.00006 2σ, n=2). The isotopic difference between specimens is insignificant at the 2σ level of uncertainty and so the mean value of 0.70748 is taken as the best estimate of the marine ^{87}Sr/^{86}Sr ratio during Mannville time.

The $^{87}Sr/^{86}Sr$ ratio of modern river waters is a weighted average of the Sr isotopic compositions and concentrations of the bedrock types in the catchment. The average world riverine$^{87}Sr/^{86}Sr$ ratio is 0.7119 (Palmer and Edmond, 1989). The $^{87}Sr/^{86}Sr$ ratios for fresh waters of the foreland basin drainage system are listed in Table 5-2. They had lower $^{87}Sr/^{86}Sr$ ratios than the world average, probably reflecting an abundance of young volcanic arc protoliths in the emerging Cordillera (Samson and Patchett, 1991) and widespread exposure of Paleozoic carbonates. The fresh water data define two groups: Group 1 includes the *C. ortmanni* fauna and the Kootenai limestones (0.70873 ±0.00009; 1σ), and Group 2 includes the *G. multicarinata* fauna and the Peterson Limestone (0.70763 ±0.00015; 1σ) (Table 5-2). The mean $^{87}Sr/^{86}Sr$ ratio of Group 2 is very close to that determined for contemporaneous marine waters (0.70748), one sample is within analytical uncertainty. However a marine influence is unlikely since the Peterson lime/dolostone is >500 kms further south of the southerly limit of the Ostracode Zone (Alberta/Montana border). Although the *C. ortmanni* fossils (stratigraphically above the Ostracode Zone) were much closer to contemporaneous marine sources (Fig. 5-3), they have some of the lowest $\delta^{18}O$ values measured in this part of the Western Interior Sedimentary Basin (Fig. 5-5). It is therefore concluded that the paleohydrology of the Ostracode, Wabasca and McMurray sub-basins involved two isotopically distinct fresh water sources, and that isotopic similarity between Group 2 waters and contemporaneous marine waters is probably fortuitous.

Sr Isotope Paleosalinities

Two component mixtures of marine and fresh waters with differing $^{87}Sr/^{86}Sr$ ratios and Sr concentrations define hyperbolic mixing curves on plots of $^{87}Sr/^{86}Sr$ *vs.* Sr (ppm). The degree of hyperbolic curvature is a function of the end-member isotopic and elemental abundances. Once the hyperbola is determined for a specific hydrological setting, proxy salinities can be calculated for any given $^{87}Sr/^{86}Srr$ ratio assumed to have formed by seawater-freshwater mixing. The mathematical relations describing the isotopic systematics are given in *Chapter 6*.

The proxy salinities are only as precise as the estimates or measurements of the end-mem-

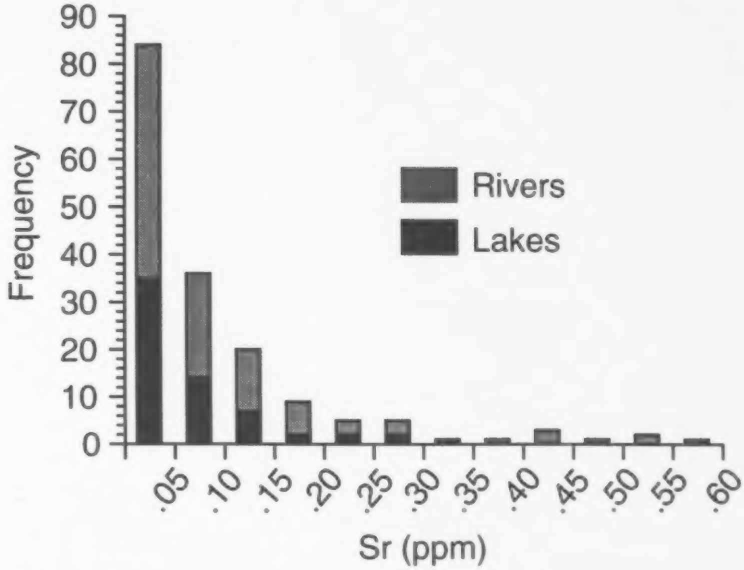

FIGURE 5-9 Histogram of river and lake Sr contents (Alexander et al., 1954; Eastin and Faure, 1970; Faure et al. 1967; Feulner and Hubble, 1960; Goldstein and Jacobsen, 1987; Odum, 1955b; Rosenthal and Katz, 1989; Skougstad and Horr, 1963; Wadleigh et al., 1985). The weighted mean for large rivers is 0.078 ppm (Palmer and Edmond, 1989), accounting for 47% of total world runoff to the oceans.

ber $^{87}Sr/^{86}Sr$ ratios and Sr concentrations are accurate. Determining the $^{87}Sr/^{86}Sr$ ratios of contemporaneous marine and fresh waters is relatively straightforward if the appropriate fossils are available, however, the Sr concentrations of the original waters must also be estimated. The Sr content of Cretaceous seawater is assumed to be uniform and the same as the value today, 7.7 ppm (De Villiers et al., 1994). The average Sr content for world rivers is 0.078 ppm (Palmer and Edmond, 1989) but the specific value for a river depends on the Sr contents of the various rock types in the watershed, and their susceptibility to weathering (see also, Chapter 6). A histogram of world river and lake water Sr concentrations shows a skewed distribution of dissolved Sr contents from near 0 ppm to a near maximum of 0.5 ppm (Fig. 5-9). Paleosalinities are determined from 2 bounding curves: one constructed using the average Sr concentration in rivers and the other using a high Sr concentration of 0.5 ppm. The high concentration curve maximizes the calculated salinities for a given set of hydrological parameters ($^{87}Sr/^{86}Sr$ ratios and Sr contents), thus enabling an evaluation of the impact of the uncertainty in river water Sr concentrations on the calculated salinities.

A composite sample of aragonitic shell fragments from the Ostracode Zone gave a $^{87}Sr/$

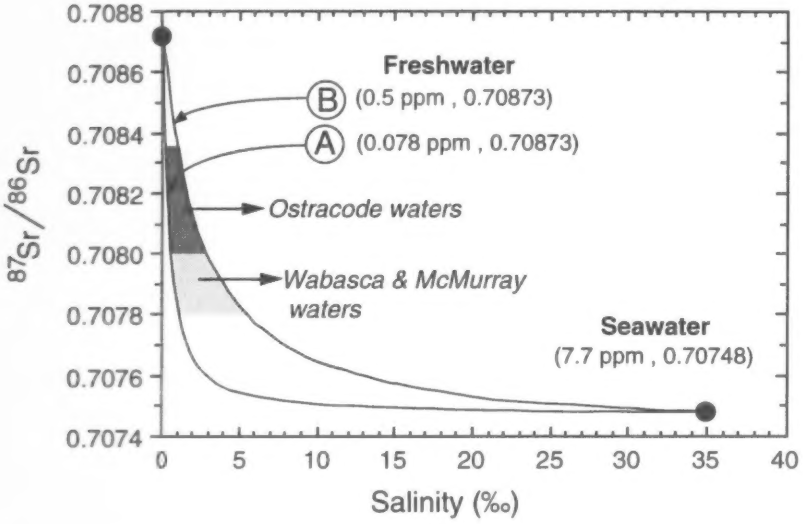

FIGURE 5-10 Relationship between $^{87}Sr/^{86}Sr$ abundance and salinity for waters assumed to have formed by 2 component mixing between marine waters of the Moosebar-Clearwater sea and group 1 fresh waters of the foreland basin drainage system. Even when the Sr content of the fresh water end-member is maximized the $^{87}Sr/^{86}Sr$ ratios in Ostracode waters are less than 3‰. If Group 2 fresh waters contributed 50% of fresh waters to these basins, the salinities represented would be almost halved.

^{86}Sr ratio of 0.70835. Shell fragments from the Wabasca and McMurray sub-basins gave less radiogenic ratios of 0.70798 and 0.70784, respectively. Waters from all three sub-basins have Sr isotopic compositions intermediate between contemporaneous marine (0.70748) and Group 1 fresh waters (0.70873); an observation necessary to the brackish water hypothesis. It is impossible, however, to form the Ostracode, Wabasca and McMurray waters by mixing marine and Group 2 fresh waters (0.70763). Therefore, if the Ostracode and equivalent waters were genuinely brackish, Group 1 fresh waters must have dominated fluviatile inputs.

Two mixing hyperbolas differing only in their riverine Sr concentration are shown in Figure 5-10. Hyberbola-A, using the average Sr content of river water, gives salinities of 1‰ for the Ostracode waters and 1.5‰ for the Wabasca-McMurray waters. If the Sr concentration is increased nearly an order of magnitude (hyperbola-B), salinities ≤3‰ are indicated for the Ostracode waters and ≤4‰ for the Wabasca and McMurray waters. These are the salinities that would result if the range in $^{87}Sr/^{86}Sr$ ratios for Ostracode, Wabasca and McMurray waters (0.70784 - 0.70835) were

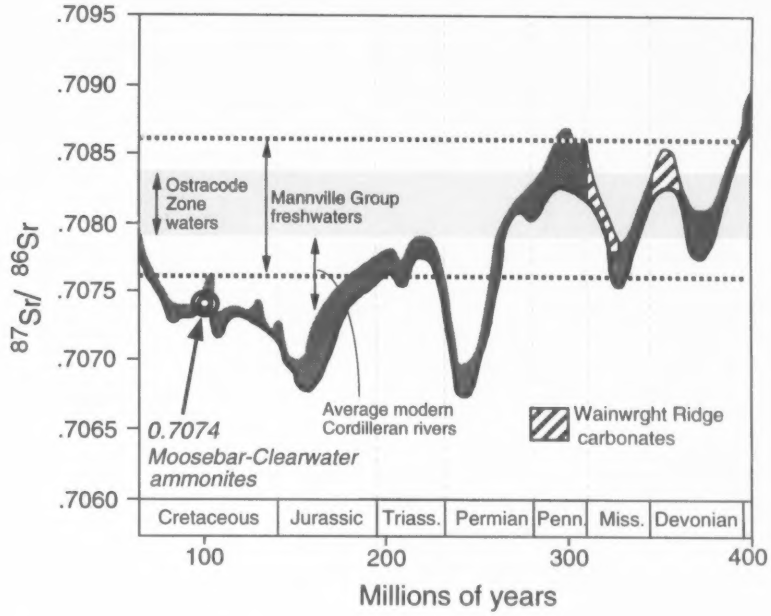

Figure 5-11 The ^{87}Sr/^{86}Sr curve for Cretaceous to Devonian seawater (modified from Burke et al., 1982). The range of ^{87}Sr/^{86}Sr ratios in Ostracode, Wabasca and McMurray fossils may be accounted for by mixing between two freshwater sources. Freshwaters discharging from the Wainwright Ridge carrying Devonian marine Sr can account for the ^{87}Sr/^{86}Sr of Group 1 freshwaters (0.70873), whereas the ^{87}Sr/^{86}Sr of Group 2 freshwaters (0.70764) likely originated from freshwaters draining the early Cretaceous Cordillera (~0.7077; see Table 6-3 *Chapter 6*), and additional contributions from locally abundant Mississippian carbonates (Fig. 5-2).

due solely to mixing between marine waters and Group 1 fresh waters. This range of ^{87}Sr/^{86}Sr ratios is equally well explained by mixing of Group 1 (0.70873) and Group 2 (0.70763) fresh waters. The calculated salinities (when marine contributions are assumed) are so low that a wholly lacustrine paleoenvironment seems likely. In fact, the total range of non-marine ^{87}Sr/^{86}Sr ratios (0.7087 to 0.7078) overlaps ^{87}Sr/^{86}Sr ratios characterizing upper Mississippian and Devonian seawater (Fig. 5-11), suggesting the ^{87}Sr/^{86}Sr ratios for the Ostracode and equivalent waters may have been controlled by chemical weathering of upper Mississippian and upper Devonian carbonates of the Wainwright Ridge. Alternatively, the non-radiogenic ^{87}Sr/^{86}Sr ratio for Group 2 fresh waters may reflect primary runoff from the western Cordillera. Rivers discharging from the present day Cordillera have low ^{87}Sr/^{86}Sr ratios (~0.7077; Wadleigh et al., 1985; Goldstein and Jacobsen, 1987;

Ingram and Sloan, 1992) due to weathering of young juvenile crust in Cordilleran terranes (see Table 6-3, *Chapter 6*) (Samson and Patchett, 1991). Therefore, Group 2 freshwaters were probably more widely distributed within the foreland basin than those of Group 1.

Depositional Environment of the Ostracode Zone

Carbonate occurrences within the Ostracode Zone, and stratigraphically equivalent sediments of the Wabasca and McMurray sub-basins, are constrained by their Sr isotope paleohydrology to have been deposited in lacustrine depositional settings. With the exceptions of Farshori (1983) and Hayes (1986), this interpretation contrasts with most recent sedimentological and paleontological studies of the Ostracode Zone which advocate brackish water deposition. It is possible that just the carbonates of the Ostracode Zone are lacustrine and that the nonfossiliferous, interlayered clastics were deposited under more saline waters. Indeed, the use of fossils to characterize the isotopic compositions of the Ostracode and equivalent waters may have biased our results due to the salinity tolerances of the original shell producing organisms. Since our paleohydrological methods are not directly applicable to the non-carbonate lithologies of the Ostracode Zone we cannot comment on the salinity of their depositional waters. To our knowledge, however, none of the authors promoting brackish water depositional models have made a similar distinction between the carbonate and non-carbonate lithologies of the Ostracode Zone.

If the non-carbonate lithologies of the Ostracode Zone are assumed to have been deposited under brackish waters then a connection to the marine is implied and flooding intervals documented in Ostracode strata (e.g., Banerjee and Kidwell, 1991) may be related to transgression of the Moosebar-Clearwater sea. Presumably, the extent of the lacustrine system represented by carbonate deposition would increase and decrease with water shallowing and deepening, respectively. Alternatively, if all lithologies within the Ostracode Zone were deposited in fresh waters (hydrologically closed to the marine), then flooding events may be related to changing climate conditions (wet and dry periods) which affected rates of fluvial inflow to the lake.

It is possible, however, that both tectonic/eustatic and climatic controls influenced the depositional history and salinity of the Ostracode waters. A possible modern analog is Lake Maracaibo, of the Maracaibo basin, Venezuela (Fig. 5-11). Lake Maracaibo is a large, shallow (<35m) subsiding intermontane lake (12,500 km^2). A 35 km open connection with the sea exists through the Straits of Maracaibo (Hyne et al., 1979) but a sand bar at the southern end of the straits keeps lake waters relatively fresh. Before dredging in 1956, water depths were 2 m over the bar and lake salinities ranged from 0.7 to 2.0‰ (Redfield, 1961). Today, the sill depth is 7-12 m and lake salinities average 3.3‰ (Hyne et al., 1979). The lake maintains a small tidal range of 22 cm in the north, decreasing to 6 cm in the south (Redfield, 1961) and is well mixed by a counter-clockwise current (Battelle Memorial Institute, 1974). Surrounded by mountains, climatic conditions within the Maracaibo basin vary widely. The north eastern part of the lake is arid whereas a tropical rainforest characterizes the mountainous region west and south of the lake. Rainfall is high in the summer and low in the winter, a cycle reflected in lake salinities (Gessner, 1953).

The H isotope hydrology of Lake Maracaibo was investigated by Friedman et al. (1956), representing one of the first applications of stable isotopes in hydrology. To aid comparison with this study, δD data for river water and seawater are converted to equivalent $\delta^{18}O$ values using the meteoric water line which has a slope of 8 (Craig, 1961). Due to evaporation effects, Lake Maracaibo water is converted using a modified meteoric water line of slope 5 (Yurtsever and Gat, 1981). The O isotope budget for Lake Maracaibo is displayed on Fig. 5-12. Despite the open connection to the sea, $\delta^{18}O$ values for Maracaibo lake are very uniform ranging from -5.6 to -7.8‰ with a mean of -6.3 ±0.6‰ (n=22). The Straits of Maracaibo have a mean $\delta^{18}O$ value of -3.1‰ (n=8), the Gulf of Venezuela is -2.6‰ (n=10) and the Caribbean Sea is -2.1 ‰ (n=5). The $\delta^{18}O$ value for average river waters draining into the lake is -9‰, whereas higher altitude rivers (4000m) are typically around -14‰.

Maracaibo lake waters are ~3‰ enriched in ^{18}O over the fresh water inflow. This is due to a combination of evaporation effects resulting from the long water residence time of ~10 years (Friedman et al., 1956), and mixing with marine waters. The magnitude of the evaporation effect may be calculated for differing salinities. At a salinity of 3.3‰, evaporation accounts for ~2‰ of the

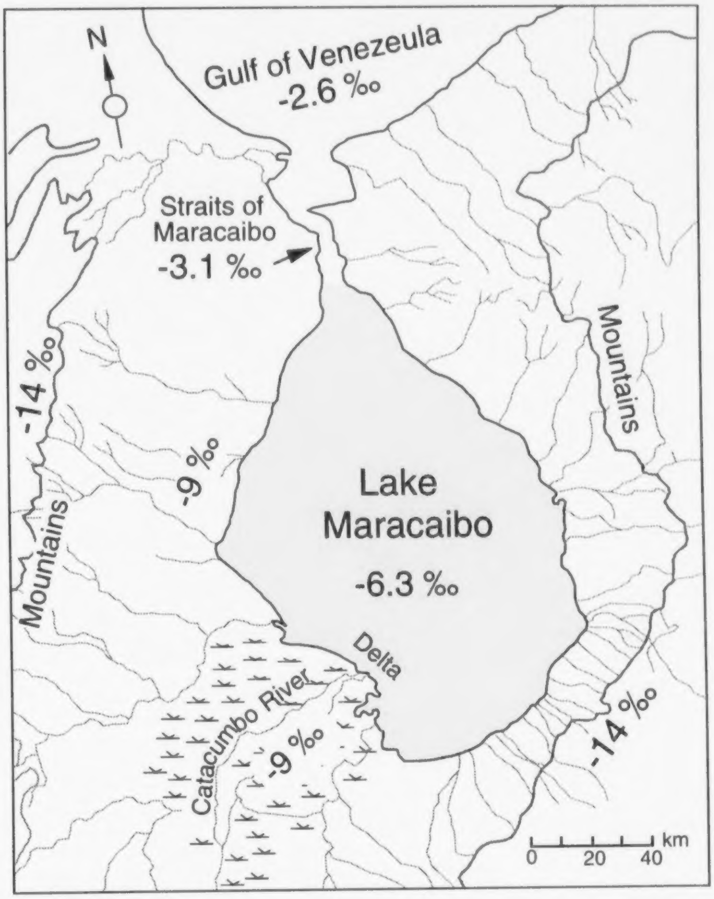
N
Gulf of Venezeula
-2.6 ‰
Straits of
Maracaibo
-3.1 ‰
-14 ‰
Mountains
-9 ‰
Lake
Maracaibo
-6.3 ‰
Mountains
Delta
Catacumbo River
-9 ‰
-14 ‰
0
20
40
km

FIGURE 12 Map showing physiography and deuterium isotope balance of modern Lake Maracaibo which is presented as a modern analogue for the paleohydrology of the early Cretaceous Ostracode Zone. Figure modified from Davey (1949).

total 3‰ ^{18}O-enrichment. If salinities were less than 1‰, >95% of the ^{18}O-enrichment would be the result of evaporation. For Ostracode lake waters, the ^{18}O contributed from possible mixing of marine waters at these low salinities is negligible due to the magnitude of ^{18}O-depletion in foreland basin fluviatile waters. Consequently, the greatest uncertainty in estimating the magnitude of the evaporation effect for Ostracode waters lies in knowing the true δ^{18}O value for the fluviatile in-flow. Overall, the comparison of O isotope balances between Ostracode and Lake Maracaibo waters reinforces the conclusion that water residence times for the Ostracode waters were long and that evaporation may have been enhanced by relatively drier conditions in the foreland basin (rain shadow) than in the foothills and mountains.

The dominantly fresh water paleohydrology of 'Lake Ostracode' may be reconciled with marine indicators like dinoflagellates if a relatively narrow silled connection to the Moosebar-Clearwater sea is postulated. Therefore, the relatively short-lived Ostracode flooding event may represent an alliance between marine transgression, fluvial transport and an early Cretaceous physiography dominated by incised valleys. The Early Cretaceous incised valleys of central Alberta (Edmonton, Spirit River or McMurray channel systems) were significant topographical features with several 100 meters of relief (Ranger et al., 1994) through which foreland basin drainage was funneled on its path to the sea. As the Moosebar-Clearwater sea advanced up these channels, the rise in base level reduced fluvial discharge rates, and the excess foreland basin drainage was backed up into a large lake or series of hydrologically connected lakes. The isotopic similarity between carbonates of the Ostracode Zone and Kootenai formation suggest that both areas were part of the same lake system which reached as far south as central Montana. The enormous size of the lake probably reflects the large volumes of water carried by the foreland basin drainage system, which also helps to explain why fresh waters dominated the paleohydrology. Only when the sea had transgressed to near the top of the valley systems was Lake Ostracode destroyed, and true estuarine conditions widely developed.

Conclusions

A method of paleosalinity determination in ancient brackish water systems has been demonstrated. The greater than 2 orders of magnitude difference in Sr concentration between marine and fresh waters makes Sr isotopes well suited to assessing the degree of marine influence in fresh to brackish water depositional systems. The O, C and Sr isotope variations in fossils from the Ostracode, Wabasca and McMurray sub-basins are consistent with an entirely lacustrine depositional environment, based on their respective isotopic paleohydrologies. Nevertheless, an inclusive depositional model is developed for deposition of the Ostracode Zone based on the hydrology of modern Lake Maracaibo, Venezuela, which is predominantly controlled by fresh water inputs but maintains a connection to the sea.

Paleosalinities calculated by the O isotope method are subject to significant uncertainties because of evaporation effects that are difficult to quantify. However, the O isotope systematics of natural waters is well understood and provides a paleohydrological framework within which to interpret the Sr isotope paleohydrology. With correlated Sr and O isotopes it is not necessary to rely on prevailing wisdom concerning the salinity tolerances of the various organisms used. In addition, correlated oxygen isotopes are useful where the contrast in $^{87}Sr/^{86}Sr$ ratio is small between contemporaneous marine and fresh waters, as between early Albian seawater and group 2 fresh waters.

Oxygen isotopes can also provide valuable information on the regional hydrology and climate. The very uniform $\delta^{18}O$ values for fossils of the Ostracode, Wabasca and McMurray subbasins indicate the depositional waters were maintained in steady-state isotopic equilibrium with fluviatile inputs, outputs and evaporation. Long water residence times are indicated by the 4-7‰ ^{18}O-enrichment of Lake Ostracode waters relative to inflowing rivers. The extremely ^{18}O depleted signature for meteoric waters is surprising given the warmer Cretaceous paleoclimate (14.5°C) and suggests that parts of the emerging North American Cordillera had already achieved or surpassed present-day altitudes as early as the Albian. The relatively enriched ammonite $\delta^{18}O$ values indicate the Moosebar-Clearwater sea was fully marine and so the northern Interior Seaway had not yet experienced the restrictions to mixing with open ocean waters that would occur over much of its subsequent history.

REFERENCES

Alexander G.V., Nusbaum R.E., and MacDonald N.S. (1954) Strontium and calcium in municipal water supplies. *American Water Works Association Journal* **46,** 643-654.

Andersson P.S., Wasserburg G.J. and Ingri J. (1992) The sources of Sr and Nd isotopes in the Baltic Sea. *Earth and Planetary Science Letters* **113,** 459-472.

Banerjee I. and Davies E.H. (1988) An integrated lithostratigraphic and palynostratigraphic study of the Ostracode zone and adjacent strata in the Edmonton Embayment, Central Alberta. In *Sequences, Stratigraphy, Sedimentology: Surface and Subsurface* (ed. D.P. James and D.A. Leckie) , pp. 261-274. Canadian Society of Petroleum Geologists Memoir 15.

Banerjee I. (1990) Some aspects of Lower Mannville sedimentation in southeastern Alberta. *Geological Survey of Canada Paper* **90-11**.

Banerjee I. and Kidwell S.M. (1991) Significance of molluscan shell beds in sequence stratigraphy: an example from the Lower Cretaceous Mannville Group of Canada. *Sedimentology* **38,** 913-934.

Barron E.J. (1983) A warm equable Cretaceous: the nature of the problem. *Earth Science Reviews* **19,** 305-338.

Barron E.J., Arthur M.A. and Kauffman E.G. (1985) Cretaceous rhythmic bedding sequences: a plausible link between orbital variations and climate. *Earth and Planetary Science Letters* **72,** 327-340.

Battelle Memorial Institute (1974) Study of the effects of oil discharges and domestic and industrial wastewaters on the fisheries of Lake Maracaibo, Venezuela.Richland, Washington Pacific Northwest Lab, v. 1.

Brass G.W. (1976) The variation in the marine ^{87}Sr/^{86}Sr ratio during Phanerozoic time: interpretation using a flux model. *Geochimica et Cosmochimica Acta* **40,** 721-730.

Burke W.H., Denison E.A., Hetherington R.B., Koepnick R.B. Nelson H.F. and Otto J.B. (1982) Variation of seawater ^{87}Sr/^{86}Sr ratio throughout Phanerozoic time. *Geology* **10,** 516-519.

Clayton R.N. and Degens E.T. (1959) Use of carbon isotope analyses of carbonates for differentiating freshwater and marine sediments. *American Association of Petroleum Geologists Bulletin* **43,** 890-897.

Craig H. (1961) Isotopic variations in meteoric waters. *Science* **133,** 1702-1703.

Dansgaard W. and Tauber H. (1969) Glacier oxygen-18 content and Pleistocene ocean temperatures. *Science* **166,** 499-502.

Davey J.C. (1949) The Maracaibo Basin. *Mining Magazine* **81,** 9-16.

De Villiers S., Shen G.T., Nelson B.K. (1994) The Sr/Ca-temperature relationship in coralline aragonite: Influence of variability in (Sr/Ca)$_{seawater}$ and skeletal growth parameters. *Geochimica et Cosmochimica Acta* **58,** 197-208.

Drummond C.N., Wilkinson B.H. and Lohmann KC. (1989) Lacustrine carbonate record of Cretaceous climatic variation in the Wyoming-Idaho overthrust belt. Geological Society of America Abstracts with Programs **21,** 126 (abstract).

Drummond C.N., Wilkinson B.H. and Lohmann KC. (1993) Rock-dominated diagenesis of lacustrine magnesian calcite micrite. *Carbonates and Evaporites* **8,** 214-223.

Eastin R. and Faure G. (1970) Seasonal variation of the solute content and the $^{87}Sr/^{86}Sr$ ratio of the Olentangy and Scioto Rivers at Columbus, Ohio. *The Ohio Journal of Science* **70,** 170-179.

Faure G. (1986) *Principles of Isotope Geology.* John Wiley and Sons.

Faure G., Crocket J.H. and Hurley P.M. (1967) Some aspects of the geochemistry of strontium and calcium in Hudson Bay and the Great Lakes. *Geochimica et Cosmochimica Acta* **31,** 451-461.

Farshori M.Z. (1983) Depositional environment of Ostracode beds in southern Alberta. In *The Mesozoic of Middle North America* (eds. D.F. Stott and D.J. Glass), Canadian Society of Petroleum Geology Memoir **9,** 568.

Feulner A.J. and Hubble J.H. (1960) Occurrence of strontium in the surface and ground waters of Champaign County. *Ohio Economic Geology* **55,** 176-186.

Finger K.L. (1983) Observations on the lower Cretaceous Ostracode zone of Alberta. *Bulletin of Canadian Petroleum Geology* **31,** 326-337.

Friedman I., Norton D.R., Carter D.B., and Redfield A.C. (1956) The deuterium balance of Lake Maracaibo. *Limnology and Oceanography* **1,** 239-246.

Gat J.R. (1981) Lakes. In *Stable Isotope Hydrology, Deuterium and Oxygen-18 in the water cycle* (eds. J.R. Gat and R. Gonfiantini), pp. 203-221. Technical Reports Series No. 210. International Atomic Energy Agency, Vienna.

Gessner, F. (1953) Investigaciones hidrograficas en al Lago de Maracaibo. Acta Cientifica *Venezolana* **4,** 173-177.

Glancy T.J., Arthur M.A., Barron E.J. and Kauffman E.G. (1993) A paleoclimate model for the North American Cretaceous (Cenomanian-Turonian) Epicontinental sea. In *Evolution of the Western Interior Basin* (Ed. W.G.E. Caldwell and E.G. Kauffman), Geological Association of Canada Special Paper **39,** 219-241.

Glaister, R.P. (1959) Lower Cretaceous of southern Alberta and adjacent areas. *American Association of Petroleum Geologists Bulletin* **43,** 590-640.

Goldstein S.J. and Jacobsen S.B. (1987) The Nd and Sr isotopic systematics of river water dissolved material: implications for the sources of Nd and Sr in seawater. *Chemical Geology* **66,** 245-272.

Gregory R.T. and Taylor H.P. Jr. (1981) *Journal of Geophysical Research* **86,** 2737-2755.

Hayes B.J.R. (1986) Stratigraphy of the Basal Cretaceous Lower Mannville Formation, Southern Alberta and North-Central Montana. *Bulletin of Canadian Petroleum Geology* **34,** 30-48.

Hayes B.J.R., Christopher J.E., Rosenthal L., Lus G., McKercher B., Minker D., Trembley Y.M. and Fennell J. (1994) The Mannville Group. In *Geological Atlas of the Western Canada Sedimentary Basin* (Ed. G.D. Mossop and I. Shetsen), pp. 317-334. Canadian Society of Petroleum Geologists.

Hopkins J.C. (1985) Channel-fill deposits formed by aggradation in deeply scoured, superimposed distributaries of the lower Kootenai formation (Cretaceous). *Journal of Sedimentary Petrology* **55**, 42-52.

Hunt C.W. (1950) Preliminary report on Whitemud oil field, Alberta, Canada. *American Association of Petro-*

leum Geologists Bulletin **34,** 1795-1801.

Hyne N.J., Cooper W.A. and Dickey P.A. (1979) Stratigraphy of intermontane, lacustrine delta, Catacumbo River, Lake Maracaibo, Venezuela. *American Association of Petroleum Geologists Bulletin* **61,** 2042-2057.

Ingram B.L. and Sloan D. (1992) Strontium isotopic composition of estuarine sediments as paleosalinity-paleoclimate indicator. *Science* **255,** 68-72.

Ingram B.L. and DePaolo D.J. (1993) A 4300 year strontium isotope record of estuarine paleosalinity in San Francisco Bay, California. *Earth and Planetary Science Letters* **119,** 103-119.

Irving E., Wynne P.J. and Globerman B.R. (1993) Cretaceous paleolatitudes and overprints of the North American Craton. In *Evolution of the Western Interior Basin* (Ed. W.G.E. Caldwell and E.G. Kauffman), Geological Association of Canada Special Paper **39,** 91-96.

Jackson P.C. (1984) Paleogeography of the lower Cretaceous Mannville Group pf western Canada. In *Elmworth–acase study of a deep basin gasfield* (ed. A. Masters), pp. 49-77. American Association of Petroleum Geologists Memoir **38**.

Kauffman E.G. (1984) Paleobiogeography and evolutionary response dynamic in the Cretaceous Western Interior Seaway of North America. In *Jurassic-Cretaceous biochronology and paleogeography of North America* (ed. G.E.G. Westermann), Geological Association of Canada Special Paper **27,** 273-306.

Keith M.L., Anderson G.M. and Eichler R. (1964) Carbon and oxygen isotopic composition of mollusk shells from marine and fresh-water environments. *Geochimica et Cosmochimica Acta* **28,** 1757-1786.

Koke K.R. and Stelck C.R. (1984) Foraminifera of the *Stelckiceras* Zone, basal Hasler Formation (Albian), Northeastern British Columbia. In *The Mesozoic of Middle North America* (ed. D.F. Stott and D.J. Glass), Canadian Society of Petroleum Geologists Memoir **9,** 271-279.

Kramers J.W. (1973) Road Log, Ft. McMurray to Ft. McKay. In *Guide to the Athabasca oil sands area* (ed. M.A. Carrigy and J.W. Krammers), pp. 188-212. Canadian Society of Petroleum Geologists Oils Sands Symposium.

Kyser T.K., Caldwell W.G.E., Whittaker S.G. and Cadrin A.J. (1993) Paleoenvironment and geochemistry of the northern portion of the Western Interior Seaway during late Cretaceous time. In *Evolution of the Western Interior Basin* (Ed. W.G.E. Caldwell and E.G. Kauffman), Geological Association of Canada Special Paper **39,** 355-378.

Leckie D.A. and Smith D.G. (1992) Regional setting, evolution, and depositional cycles of the Western Canada Foreland Basin. In *Foreland Basins and Foldbelts* (ed. R.W. McQueen and D.A. Leckie), *American Association of Petroleum GeologistsMemoir* **55,** 9-46.

Loranger, D.M. (1951) Useful Blairmore microfossil zone in central and southern Alberta, Canada. *American Association of Petroleum Geologists Bulletin* **35,** 2348-2367.

Mattison B.W. (1987) Ichnology and paleontology of the McMurray Formation. M.Sc. dissertation Univ. of Alberta.

Mattison B.W. (1991) Stratigraphic and paleoenvironmental analysis of the upper and middle Mannville subgroups: Cold Lake Oil Sands area, east central Alberta. Ph.D. dissertation Univ. of Alberta.

McCrea J.M. (1950) On the isotopic chemistry of carbonates and a paleotemperature scale. *Journal of Chemical Physics* **18,** 849-857.

McGookey D.P., Haun J.D., Hale L.A., Goodell H.G., McCubbin D.G., Weimer R.J. and Wulf G.R., 1972. Cretaceous System. In *Geological Atlas of the Rocky Mountains* (ed. W.W. Mallory), pp. 190-228. Denver, Rocky Mountain Association of Geologists.

McKay J.L. and Longstaffe F.J. (1993) Diagenesis of the lower Cretaceous Clearwater Formation (excluding the Wabiska member) Primrose area, northeastern, Alberta. Canadian Society of Economic Geologists and Petroleum Geologists Joint Annual Meeting, 305-306 (abstract).

McLean J.R. and Wall J.H. (1981) The early Cretaceous Moosebar Sea in Alberta. *Bulletin of Canadian Petroleum Geology* **29,** 334-377.

McPhee D. (1994) Sequence stratigraphy of the lower Cretaceous Mannville Group of east-central Alberta. M.Sc. dissertation Univ. of Alberta.

Mook W.G. (1970) Paleotemperatures and chlorinities from stable carbon and oxygen isotopes in shell carbonate. *Paleoceanography, Paleoclimatology, Paleoecology* **9,** 245-263.

Nesbitt B.E. and Muehlenbachs K. (1989) Origins and movement of fluids during deformation and metamorphism in the Canadian Cordillera. *Science* **245,** 733-736.

Oana S. and Deevey E.S. (1960) Carbon 13 in lake waters, and its possible bearing on paleolimnology. *American Journal of Science* **258-A,** 253-272.

Odum H.T. (1955) Strontium in natural waters. Institute of Marine *Science* **4,** 22-37.

O'Neil J.R., Clayton, R.N. and Mayeda, T.K. (1969) Oxygen isotope fractionation in divalent metal carbonates. *Journal of Chemical Physics* **51,** 5547-5558.

Palmer M.R. and Edmond J.M. (1989) The strontium isotope budget of the modern ocean. *Earth and Planetary Science Letters* **92,** 11-26.

Pocock S.A.J. (1980) The Aptian-Albian boundary in Canada. *Proceedings of the 4th International Palynology Conference, Lucknow, 1976-77* **2,** 419-424.

Pratt L.M. (1993) Paleoceanographic cycles and events during the late Cretaceous in the Western Interior Seaway of North America. In *Evolution of the Western Interior Basin* (eds. W.G.E. Caldwell and E.G. Kauffman), pp. 333-353. Geological Association of Canada Special Paper, **39**.

Ranger M.J., McPhee D., Pemberton S.G. and Zaitlan B. (1994) Basins and sub-basins: Controls on sedimentation and stratigraphy of the Mannville Group. Canadian Society of Economic Geologists and Petroleum Geologists Joint Annual Meeting, 24-25 (abstract).

Redfield A.C. (1961) The tidal system of Lake Maracaibo, Venezuela. *Limnology and Paleoceanography* **1,** 1-12.

Rosenthal Y. and Katz A. (1989) The applicability of trace elements in freshwater shells for paleogeochemical studies. *Chemical Geology* **78,** 65-76.

Russell L.S. (1932) Mollusca from the McMurray Formation of Northern Alberta. *Proceedings and Transactions of the Royal Society of Canada* **27,** 37-42.

Sackett W.M. and Moore W.S. (1966) Isotopic variations of dissolved inorganic carbon. *Chemical Geology* **1,** 323-328.

Samson S.D. and Patchett P.J. (1991) The Canadian Cordillera as a modern analogue of Proterozoic crustal growth. *Australian Journal of Earth Science* **38,** 595-611.

Skougstad M.W. and Horr C.A. (1963) Occurrence and distribution of strontium in natural water. Geological Survey Water-Supply Paper **1496-D,** 55-97.

Smith J.W., Rigby D., Schmidt P.W. and Clark D.A. (1983) D/H ratios of coals and their paleolatitude of deposition. *Nature* **302,** 322-323.

Spicer R.A. and Corfield R.M. (1992) A review of terrestrial and marine climates in the Cretaceous with implications for modeling the 'Greenhouse Earth'. *Geological Magazine* **129,** 169-180.

Tarutani T. , Clayton R.N. and Mayeda T.K. (1969) The effect of polymorphism and magnesium substitution on oxygen isotope fractionation between calcium carbonate and water. *Geochimica et Cosmochimica Acta* **33,** 987-996.

Wadleigh M.A, Veizer J. and Brooks C. (1985) Strontium and its isotopes in Canadian rivers. *Geochimica et Cosmochimica Acta* **49,** 1727-1736.

Wanklyn R.P. (1985) Stratigraphy and depositional environments of the Ostracode member of the McMurray formation (Lower Cretaceous; Late Aptian-Early Albian) in west-central Alberta. M.Sc. dissertation Univ. of Colorado.

Williams G.D.C. (1960) The Mannville Group, Central Alberta. Ph.D. dissertation Univ. of Alberta.

Wright E.K. (1987) Stratification and paleocirculation of the late Cretaceous Western Interior Seaway of North America. *Geological Society of America Bulletin* **99,** 480-490.

Yen T.C. (1951) Fresh water molluscs of Cretaceous age from Montana and Wyoming, Part 1: A fluviatile fauna from the Kootenai formation near Harlowton, Montana. Geological Survey Professional Paper **233-A,** 1-20.

Yurtsever Y. and Gat J.R. (1981) Atmospheric waters. In *Stable Isotope Hydrology, Deuterium and Oxygen-18 in the Water Cycle* (Ed. J.R. Gat and R. Gonfiantini), pp. 103-142. Technical Reports Series No. 210. International Atomic Energy Agency, Vienna.

Chapter 6

PALEOSALINITIES IN ANCIENT BRACKISH WATER SYSTEMS DETERMINED BY ^{87}SR/^{86}SR RATIOS IN CARBONATE FOSSILS[1]

A CASE STUDY FROM THE WESTERN CANADA SEDIMENTARY BASIN

Introduction

Determining the salinities of ancient water masses is a classic geochemical problem which has traditionally received less attention than paleotemperature as a desirable paleoceanographic quantity. In ancient epeiric seas, where water masses were shallow and proximity to freshwater sources high, the magnitude of salinity variation may have been greater than temperature. This is indeed the case for estuarine and estuarine-like systems which in times of past continental inundation should have been more widely distributed than today (Zaitlin et al., 1994). Brackish water systems are difficult to recognize in the sedimentary rock record because sedimentological and paleontological techniques are relatively insensitive to salinity reduction. Sedimentologists use a wide variety of indicators to substantiate a brackish water hypothesis including: (1) inferences on the ecological affinities of various macrofauna or microfauna (Pickerill and Brenchley, 1991), (2) palynology (Banerjee and Davies 1988), (3) ichnology (Pemberton and Wightman, 1992), (4) identification of syneresis cracks (Plummer and Gostin, 1981), (5) basin geometry (Zaitlin et al., 1994), and (6) presence of tidal structures (Howard and Frey, 1973; Thomas et al., 1987). Faunal evidence can be particularly misleading because the brackish water fauna is largely a subset of the local marine fauna (Remane, 1934; Barnes, 1989). Even when a package of sediments is identified as being of brackish water origin all that may be confidently stated is that the neither fully marine nor fully fresh water conditions prevailed during sediment deposition. Estimating the magnitude of any salinity reduction is beyond the capacity of sedimentological and paleontological techniques (Barnes, 1989).

---

[1] A version of this chapter has been submitted to *Geochimica et Cosmochimica Acta* 08/ '95 coauthored by R.A. Creaser and K. Muehlenbachs

Potentially, dissolved chemical constituents (and their isotopes) that are conservative with salinity can be used to determine paleosalinity differences in ancient water masses. In this paper we describe a geochemical method for determining accurate and precise paleosalinities in ancient estuarine and estuarine-like systems based on the isotope paleohydrology of Sr in carbonate fossils and limestones. Using examples from the early Cretaceous Mannville Group of the Western Canada Sedimentary Basin, strategies for reconstructing the Sr isotope paleohydrology are evaluated and paleosalinities determined. The paleohydrological (salinity) perspective adds a new dimension to traditional paleoenvironmental analysis and a methodology that emphasizes spatial rather than temporal resolution of an important paleoenvironmental parameter.

The conservative behavior of dissolved Sr and its isotopic variation with salinity has been demonstrated in modern estuarine systems (Ingram and Sloan, 1992; Andersson et al., 1992). The Sr content of brackish waters, formed by mixing of high-Sr marine waters (7.7 ppm) with low-Sr freshwaters (~0.071 ppm), varies linearly with salinity (fractional degree of dilution of seawater by freshwater). The $^{87}Sr/^{86}Sr$ ratio of dissolved Sr varies with salinity because seawater and freshwaters generally have contrasting isotopic signatures. For example, river water $^{87}Sr/^{86}Sr$ is highly variable, reflecting the isotopic composition of the bedrock and sediment over which rivers flow (Wadleigh and Veizer, 1985; Goldstein and Jacobsen, 1987; Palmer and Edmond, 1992). Seawater has a uniform $^{87}Sr/^{86}Sr$ because the residence time of Sr in the oceans (5×10^6 years; Taylor and McLennan, 1985) is longer than the oceanic mixing time of ~1000 years (Broecker, 1963). This difference in time scales homogenizes the isotopic composition of Sr derived from weathering of the isotopically heterogeneous continental crust, so that seawater $^{87}Sr/^{86}Sr$ at any time reflects the rate of weathering and relative proportions of exposed: (1) older continental crust (>0.712), (2) younger mantle-derived volcanic rocks (0.703), and (3) Phanerozoic carbonates (0.7067-0.7091) (Brass, 1976; Palmer and Edmond, 1989). Rb-enriched, old sialic crust has very radiogenic $^{87}Sr/$

^{86}Sr due to *in situ* decay of ^{87}Rb. Younger crust and mantle-derived juvenile rocks have lower ^{87}Sr/^{86}Sr reflecting long term Rb-depletion in the upper mantle. Weathering of Phanerozoic carbonates buffers changes in seawater ^{87}Sr/^{86}Sr because these rocks are easily weathered, have high Sr contents, and define a relatively narrow isotopic range.

Previous attempts to distinguish marine and freshwater sediments involved elemental B and the isotopes of C and O. As with Sr, dissolved B is conservative in the seawater-freshwater mixing zone and marine and continentally-derived fresh waters have contrasting B concentrations (Liddicoat, 1983). Early work showed that variation in the B content of shales correlated with differences in salinity of depositional waters (Frederickson and Reynolds, 1959; Landergren, 1963). Subsequent work showed that additional factors influence B uptake by clay minerals, compromising its reliability as paleosalinity proxy (Harder, 1970). The generally contrasting δ^{18}O signatures between marine and continental fresh waters, and differences in δ^{13}C values for dissolved marine and freshwater carbon, is the basis for distinguishing marine and freshwaters sediments through stable isotope analysis of carbonate fossils and limestones (Clayton and Degens, 1959; Keith et al., 1964; Keith and Weber, 1964). Several authors investigated an extension of this approach to cover transitional brackish waters (Mook and Vogel, 1967; Eisma et al., 1976), demonstrating the approximately conservative behavior of O and C isotopes in the mixing zone. Several factors limit the widespread application of O and C isotopes as proxy measures of paleosalinity: (1) δ^{18}O values for marine and fresh waters can be similar in low latitude tropical settings, or reversed in sign for regions characterized by net evaporation, (2) precision is limited by differences in original water temperature for different parts of the estuarine system, translating to a blanket uncertainty of 1-2‰ on carbonate-based water δ^{18}O values, (3) evaporation can induce non-conservative effects in the mixing zone by increasing δ^{18}O of estuarine waters if the climate is dry or the water residence time long, (4) fresh waters can have marine-like δ^{13}C values if older marine carbonates constitute a significant part of the watershed, or if the residence time of lake waters is long allowing partial equilibration with atmospheric CO_2 , or (5) local differences in biological productivity or rates of organic C oxidation/burial can induce non-conservative effects in brackish water δ^{13}C values. Accordingly, there have been few attempts to use O and C isotopes in paleosalinity studies (Lloyd, 1965; Weber et al. 1965; Dodd and Stanton, 1975; Holmden et al., submitted).

The Sr isotope system has several advantages over previous methods. Unlike O and C isotopes, there is no measurable temperature or kinetic isotope effect associated with Sr partitioning in carbonate, so that carbonate fossils record $^{87}Sr/^{86}Sr$ of past waters directly. Natural variations in $^{87}Sr/^{86}Sr$ result only from the *in situ* decay of ^{87}Rb to ^{87}Sr and mixing of isotopically distinct components. This fact, coupled with the relatively unreactive nature of dissolved aqueous Sr (which follows Ca), enables continental freshwaters to maintain $^{87}Sr/^{86}Sr$ values that reflect contributions from bedrock sources and mixing with other isotopically distinct waters. For paleo-freshwaters mixing with paleo-marine waters, the mixing proportions may be deduced from the measured $^{87}Sr/^{86}Sr$ in brackish water carbonate fossils and paleosalinities determined with knowledge of $^{87}Sr/^{86}Sr$ and Sr concentrations in contemporaneous marine and fluvial waters. Ingram and DePaolo (1993) determined paleosalinities of San Francisco Bay waters over the past 4300 years by comparing $^{87}Sr/^{86}Sr$ ratios in estuarine mollusc shells with the modern isotope paleohydrology. In this paper we evaluate two strategies for determining paleosalinities in older brackish water systems. The first requires reconstructing the Sr isotope paleohydrology of a depositional basin using contemporaneous marine and freshwater fossils. The isotope paleohydrology defines the mixing curve which is used to convert $^{87}Sr/^{86}Sr$ ratios in potentially brackish water shells to proxy salinities. The second is a graphical technique using shell Sr/Ca and $^{87}Sr/^{86}Sr$ ratios. The advantage of this approach is that the mixing line defines the mixing hyperbola. If contemporaneous seawater constitutes the high Sr/Ca end-member on the corresponding water mixing line, than shells defining that line inhabited brackish waters. To calculate paleosalinities, knowledge of the Sr isotope paleohydrology is still required.

THE MANNVILLE GROUP

The early Cretaceous Mannville Group comprises some of the earliest clastic sediments deposited within the Western Canada Sedimentary Basin in Alberta (Hayes et al., 1994). Accretion

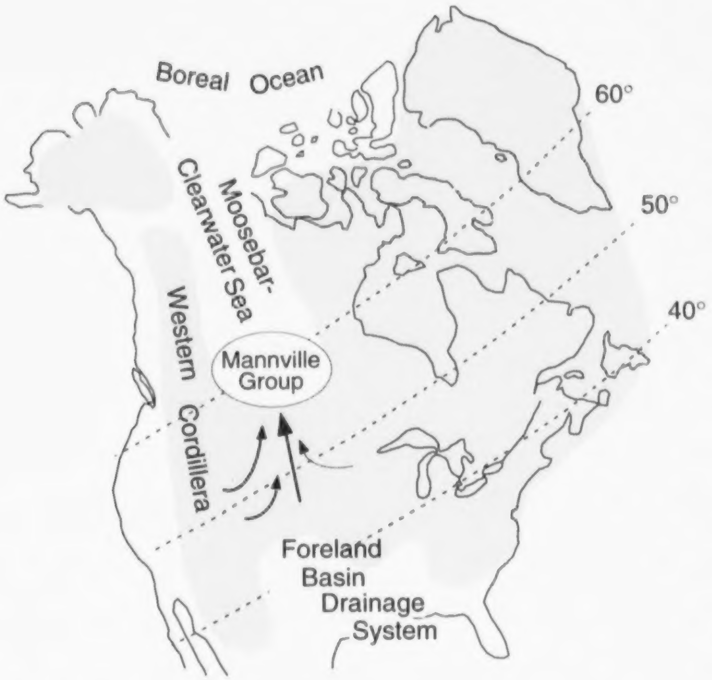

FIGURE 6-1 Paleogeographic map of early Cretaceous North America showing brackish water systems of the Mannville Group, the extent of the Albian Moosebar-Clearwater transgression (Koke and Stelck, 1984) and the foreland basin drainage system. Figure modified from Kauffman (1984) and paleolatitudes from Irving et al. (1993).

within the Intermontane belt and concomitant tectonic loading of the western North American continental margin initiated development of the foreland basin by the late Jurassic (Monger, 1989). By the early Cretaceous, the Western Interior Seaway had begun to form and water masses of the northern Boreal ocean transgressed into northern Alberta (Koke and Stelck, 1984; Leckie and Smith, 1992). The southern reaches of the foreland basin hosted a major north-flowing fluvial system that drained the highlands of the emerging western Cordillera and interior regions to the east (McGookey, 1972; Jackson, 1984; Hayes et al., 1994; Ranger et al., 1994). The Cretaceous Mannville Group contains examples of fresh, brackish and marine depositional environments, having formed in a complex hydrological interface between northerly flowing rivers of the foreland basin drainage system and southerly transgressing waters of the Moosebar-Clearwater epicontinental sea (Fig. 6-1).

Mannville Group thickness maps show sedimentation occupying a number of paleovalleys incised into underlying Paleozoic carbonates and early Mesozoic clastics during the previous lowstand of sea level (Jackson, 1984; Hayes et al., 199; Ranger et al., 1994). These paleovalleys are, in some cases, outlined by paleohighs, ridges of dominantly Devonian carbonates. The Wainwright Ridge is a major paleotopographic feature (Fig. 6-2) and existed as a hydrological barrier throughout most of

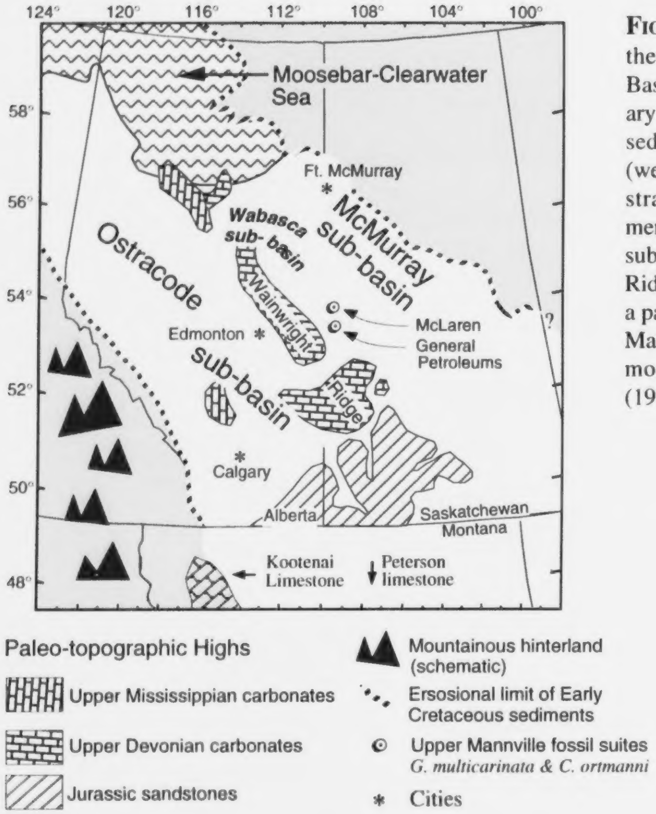
124°
120°
116°
112°
108°
104°
100°
58°
56°
54°
52°
50°
48°
Moosebar-Clearwater Sea
Ft. McMurray
Wabasca sub-basin
McMurray sub-basin
Ostracode sub-basin
Wainwright Ridge
McLaren
General Petroleums
Edmonton
Calgary
Alberta
Saskatchewan
Montana
Kootenai Limestone
Peterson limestone
?
Paleo-topographic Highs
Upper Mississippian carbonates
Upper Devonian carbonates
Jurassic sandstones
Mountainous hinterland (schematic)
Ersosional limit of Early Cretaceous sediments
Upper Mannville fossil suites
G. multicarinata & C. ortmanni
Cities

Figure 6-2 Paleogeographic map of the Western Canada Sedimentary Basin at the Aptian–Albian boundary showing sub-basins containing sediments of the Ostracode Zone (west of the Wainwright Ridge) and stratigraphically equivalent sediments of the Wabasca and McMurray sub-basins (east of the Wainwright Ridge). The Wainwright Ridge was a paleotopographic high throughout Mannville Group deposition. Figure modified from Leckie and Smith (1992).

Mannville Group deposition. At the top of the lower Mannville Group, a 15m interval known informally as the Ostracode Zone or Calcareous Member records a shift to finer-grained lithologies comprising pyritic dark shales, thin carbonates and coquinas of gastropods and pelecypods (Banerjee, 1990). Sediments of the Ostracode Zone are restricted to west of the Wainwright Ridge an area referred to here as the Ostracode sub-basin (Fig. 6-2). Accumulations of shells are also found within stratigraphically equivalent sections of the Wabasca sub-basin (developed in a pocket of the Wainwright Ridge) and the McMurray sub-basin east of the Wainwright Ridge (Ranger et al., 1994). The flooding event responsible for deposition of the Ostracode Zone and equivalent strata has been linked to a transgressive pulse of the Moosebar-Clearwater sea which encroached southwards along the incised valley systems (Banerjee, 1990), but there is little agreement among sedimentologists and paleontologists whether seawater or freshwater dominated the depositional paleohydrology.

Although the earliest studies favoured a predominantly lacustrine paleoenvironment based on the occurrence of fossil ostracodes, charophytes and fresh water gastropods (Loranger, 1951; Glaister, 1959; McLean and Wall, 1981), more recent studies document an increasing number of marine indicators in Ostracode strata, including bioturbation (Wanklyn, 1985; Banerjee, 1990), echinoid spines (Banerjee, 1990), syneresis cracks and dinoflagellates (Banerjee and Davies, 1988), and tidal structures (Wanklyn, 1985; Banerjee and Kidwell, 1991). Other workers have developed or supported brackish water depositional models based primarily on the assumption that the fossil molluscs constitute a mixed assemblage of fresh and brackish water types (Finger, 1983; Mattison, 1987; McPhee, 1994). Interpretations of the Ostracode Zone paleoenvironment include brackish bay (Wanklyn, 1985; Mattison, 1987; McPhee, 1994), calcareous sea (James, 1985), lagoon (Wanklyn, 1985), estuary (Finger, 1983; Wanklyn, 1985), lagoon/tidal-flat to open marine (Banerjee and Davies, 1988), or lacustrine (Farshori, 1983; Hayes, 1986).

SAMPLING AND ANALYTICAL TECHNIQUES

Aragonitic fossils were analyzed wherever possible to minimize diagenetic effects. Ostracode Zone fossils were collected from two subsurface cores in central Alberta (Williams, 1960). Aragonitic fossils from the McMurray sub-basin comprising a single gastropod species (*Lioplacodes bituminous*) were collected from outcrops of the upper McMurray Formation along the Hangingstone River near Ft. McMurray, Alberta (Russell, 1932; Kramers 1971). Aragonitic shells from upper McMurray deposits of the Wabasca sub-basin were collected from two subsurface cores (M. Ranger, unpublished core descriptions). Two marine ammonites (*Beudenticeras*) of the Loon River Formation were analyzed to constrain the marine end-member. The freshwater end-member was constrained using presumed freshwater limestones of the Kootenai Formation, Montana (Hopkins, 1985), the Peterson Limestone, Wyoming (Glass and Wilkinson, 1980) and aragonitic gastropods of the General Petroleums and McLaren units of the upper Mannville Group, central Alberta (Mattison, 1991).

Most strontium and oxygen isotope analyses were determined on different shell fractions from the same handsample. For whole-rock samples and the marine ammonites, all analyses were conducted on the same powder. Aragonite mineralogy was confirmed for many of the samples analyzed for stable isotopes and all samples analyzed for Sr isotopes by x-ray diffraction. Shell material was prepared by physically removing adhering detritus and diagenetic overgrowths, followed by brief sonication in ultradistilled water or ethanol. The shells were powdered in an agate mortar. Samples for stable isotope analysis were bleached for >1 week to remove organic matter and rinsed and dried prior to sample digestion in 100% phosphoric acid (McCrea, 1950). The CO_2 was cryogenically purified and analyzed on a VG 602D mass spectrometer. Oxygen and carbon isotope data are reported relative to Standard Mean Ocean Water (SMOW) and Pee Dee Belemnite (PDB), respectively, in delta (δ) notation defined as $(R_{sample}/R_{standard} - 1)1000$, where $R={}^{18}O/{}^{16}O$ or ${}^{13}C/{}^{12}C$. Stable isotope analyses were monitored using internal and international standards with a reproducibility on replicate $\delta^{18}O$ of ± 0.3‰ and $\delta^{13}C$ of 0.2‰.

Separate aliquots of powder were weighed for Sr isotope dilution and isotopic ratio analysis and dissolved in 0.25M HCl for 8-14 hrs, with the exception of the Peterson lime/dolostone which was dissolved in 0.4M HCl. A weighed amount of mixed ${}^{87}Rb$-${}^{84}Sr$ spike was added to the isotope dilution aliquot and left overnight to equilibrate. Any residues were removed by centrifugation and the supernatant evaporated to dryness. Rb and Sr were separated and purified by standard cation exchange chromatography and loaded onto the side filament of a double rhenium filament assembly for mass spectrometric analysis. Isotope dilution analyses were performed using a single-collector Micromass 30 instrument and ${}^{87}Sr/{}^{86}Sr$ ratio determinations were performed on a VG 354 5-collector mass spectrometer by multidynamic peak-hopping using VG software. All analyses are normalized for variable mass-dependent isotope fractionation to ${}^{86}Sr/{}^{88}Sr = 0.1194$. Rubidium contents were checked in several samples and were predictably low (2–4 ppm) so no corrections were applied to the measured ${}^{87}Sr/{}^{86}Sr$ ratio due to decay of *in situ* ${}^{87}Rb$ as this effect is covered by the analytical uncertainty. Repeat analyses of National Bureau of Standards SRM 987 over the course of this work yielded 0.71028 ± 0.00001 ($2\sigma_m$,) with an external reproducibility of ± 0.00002 (2σ).

General Mixing Relationships

An equation describing two component mixing between seawater and freshwater with different Sr concentrations is given by

$$\mathrm{Sr}_{BW} = \mathrm{Sr}_{SW}\chi + \mathrm{Sr}_{FW}(1-\chi) \tag{1}$$

where Sr_{BW}, Sr_{SW}, and Sr_{FW} represent the Sr concentrations in brackish water, seawater and freshwater, respectively. The fraction of seawater in the brackish water mixture is denoted χ. The systematic variation in brackish water $^{87}\mathrm{Sr}/^{86}\mathrm{Sr}$ is given by

$$\mathrm{Sr}_{BW}\left(\frac{^{87}\mathrm{Sr}}{^{86}\mathrm{Sr}}\right)_{BW} = \mathrm{Sr}_{SW}\left(\frac{^{87}\mathrm{Sr}}{^{86}\mathrm{Sr}}\right)_{SW}\chi + \mathrm{Sr}_{FW}\left(\frac{^{87}\mathrm{Sr}}{^{86}\mathrm{Sr}}\right)_{FW}(1-\chi) \tag{2}$$

where seawater and freshwater are assumed to have contrasting isotopic signatures. Combining equations (1) and (2) through the elimination of χ yields

$$\left(\frac{^{87}\mathrm{Sr}}{^{86}\mathrm{Sr}}\right)_{BW} = \frac{\mathrm{Sr}_{SW}\mathrm{Sr}_{FW}\left[\left(\frac{^{87}\mathrm{Sr}}{^{86}\mathrm{Sr}}\right)_{FW} - \left(\frac{^{87}\mathrm{Sr}}{^{86}\mathrm{Sr}}\right)_{SW}\right]}{\mathrm{Sr}_{BW}(\mathrm{Sr}_{SW} - \mathrm{Sr}_{FW})} + \frac{\mathrm{Sr}_{SW}\left(\frac{^{87}\mathrm{Sr}}{^{86}\mathrm{Sr}}\right)_{SW} - \mathrm{Sr}_{FW}\left(\frac{^{87}\mathrm{Sr}}{^{86}\mathrm{Sr}}\right)_{FW}}{\mathrm{Sr}_{SW} - \mathrm{Sr}_{FW}} \tag{3}$$

which is hyperbolic in coordinates of $(^{87}\mathrm{Sr}/^{86}\mathrm{Sr})_{BW}$ and Sr_{BW}. Since Sr is conservative in the seawater-freshwater mixing zone, salinity (S_{BW}) may be substituted for Sr_{BW} by substituting S_{BW} / 35‰ for χ in (1) and combining the resulting expression with (3) to yield

$$\frac{S_{BW}}{35‰} = \frac{\mathrm{Sr}_{FW}\left(\frac{^{87}\mathrm{Sr}}{^{86}\mathrm{Sr}}\right)_{FW} - \mathrm{Sr}_{FW}\left(\frac{^{87}\mathrm{Sr}}{^{86}\mathrm{Sr}}\right)_{BW}}{\left(\frac{^{87}\mathrm{Sr}}{^{86}\mathrm{Sr}}\right)_{BW}(\mathrm{Sr}_{SW} - \mathrm{Sr}_{FW}) - \left[\mathrm{Sr}_{SW}\left(\frac{^{87}\mathrm{Sr}}{^{86}\mathrm{Sr}}\right)_{SW} - \mathrm{Sr}_{FW}\left(\frac{^{87}\mathrm{Sr}}{^{86}\mathrm{Sr}}\right)_{FW}\right]} \tag{4}$$

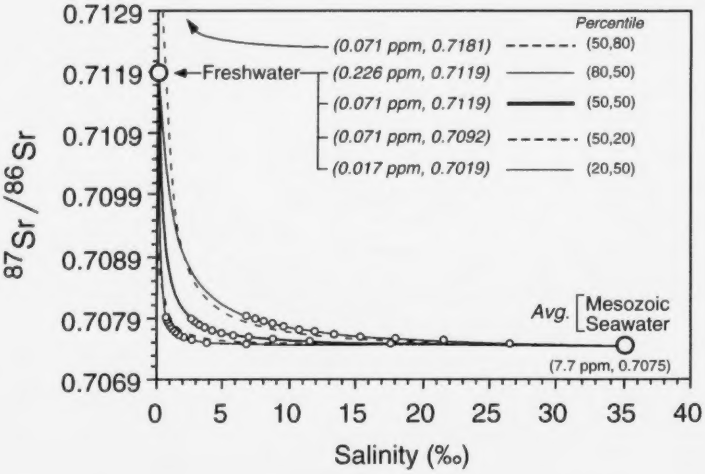

FIGURE 6-3 Shown are hyperbolic mixing curves between average Mesozoic seawater, and freshwaters with differing Sr concentrations and ^{87}Sr/^{86}Sr ratios. Symbols on mixing lines represent the potential for each curve to uniquely resolve paleosalinities within the stated analytical uncertainty of ±0.00002 (2σ). The hyperbolic form of the mixing curve results in greater uncertainties for paleosalinities along the seawater asymptote. The Sr concentration and ^{87}Sr/^{86}Sr ratio in the freshwater end-member largely determines the range of resolvable palesalinities. Paleosalinities <15‰ are the most likely to be resolved. Distinguishing paleosalinities >20‰ is possible if the freshwater ^{87}Sr/^{86}Sr ratio or Sr concentration is higher than the median.

where the salinity of seawater and freshwater are assumed to be 35 and 0‰, respectively.

The most prominent feature of the seawater-freshwater mixing hyperbola is the high degree of curvature exhibited (Fig. 6-3) which reflects the nearly 100-fold difference in Sr concentration between seawater and the median value for continental freshwaters. We use median rather than average so that world river and lake water Sr concentrations and ^{87}Sr/^{86}Sr ratios can be discussed in terms of percentiles, which enables comparison of modelled parameters to the range of possible

Table 6-1 Percentiles for Sr, Ca, Sr/Ca and ^{87}Sr/^{86}Sr ratios in world rivers and lakes (sources in Fig. 6-4)

Percentile	^{87}Sr/^{86}Sr	Sr (ppm)	Ca (ppm)	1000Sr/Ca (atom)
0 th	0.70452	0.001	0.2	0.46
10 th	0.70711	0.010	1.72	0.99
20 th	0.70920	0.017	3.44	1.34
30 th	0.70979	0.031	7.96	1.69
40 th	0.71095	0.051	14.57	1.93
50 th	0.71190	0.071	19.65	2.31
60 th	0.71396	0.096	25.02	2.66
70 th	0.71565	0.135	32.08	3.13
80 th	0.71808	0.226	42.48	3.68
90 th	0.72707	0.429	57.18	4.77
100 th	0.73844	0.949	91.03	8.12

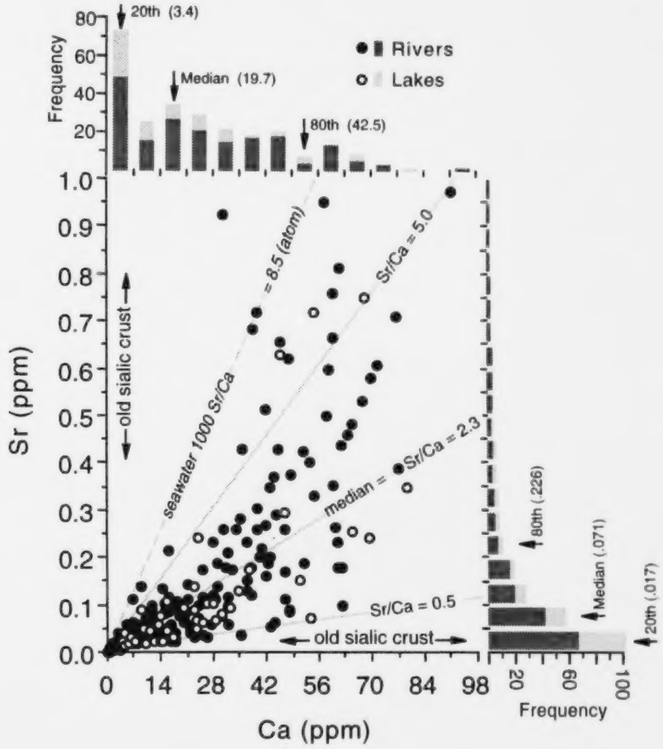

Figure 6-4 The relationship between Sr and Ca, and 1000Sr/Ca (atom) ratio is shown using 253 analyses from world rivers (●) and lakes (○). The histograms for dissolved Sr and Ca are also shown. Rivers and lakes show similar distributions of Sr and Ca. The Sr distribution is skewed with a median value of 0.071 ppm (Table 1) similar to the weighted average of 0.078 ppm reported by Palmer and Edmond (1989). The Ca distribution is broadly skewed with a maxima between 14 and 21 ppm and a median at 19.7 ppm. River and lake water Sr/Ca ratios range between 0.5 and 5.0 (in agreement with Odum (1955b)). Few continental waters attain a Sr/Ca ratio greater than seawater (8.5). The median river and lake water Sr/Ca ratio is 2.3 (Table 6-1). Data compiled from Alexander et al. (1954); Odum (1955b); Feulner and Hubble (1960); Skougstad and Horr (1963); Faure et al. (1967); Wadleigh et al. (1985); Goldstein and Jacobsen (1987); Palmer and Edmond (1989) and Rosenthal and Katz (1989). Rivers and lakes with Sr and Ca concentrations greater than 1.0 and 98 ppm, respectively, were omitted from the compilation.

choices. Percentiles for Sr, Ca, Sr/Ca and $^{87}Sr/^{86}Sr$ in world rivers and lakes are listed in Table 6-1 and plotted in Figures 6-4 and 6-5. The median values reported here are similar to weighted averages reported by Wadleigh and Veizer (1985), Goldstein and Jacobsen (1987) and Palmer et al. (1989), weighted for river flux.

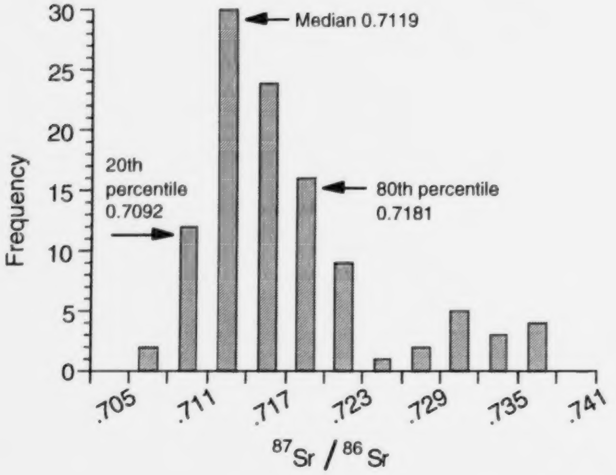

Figure 6-5 Histogram of $^{87}Sr/^{86}Sr$ ratios for dissolved river water Sr. The median value (0.7119) is identical to the weighted average given by Palmer and Edmond (1989). Data compiled from Wadleigh and Veizer (1985), Goldstein and Jacobsen (1987) and Palmer and Edmond (1989).

The asymptotic character of the mixing curve causes a systematic variation in the uncertainty of paleosalinity determinations which increase with increasing salinity. Salinities below ~15‰ are the most precisely determined. To resolve salinities >15‰ the contrast in $^{87}Sr/^{86}Sr$ and Sr concentration between contemporaneous seawater and freshwater must be larger and smaller, respectively. Since seawater has a uniform $^{87}Sr/^{86}Sr$ at any time (and we assume a constant seawater Sr concentration), the Sr concentration and $^{87}Sr/^{86}Sr$ in freshwater controls the shape of the mixing curve and therefore the range over which paleosalinities can be resolved. The impact of changing the freshwater inputs on paleosalinities is assessed by plotting points on these curves that are resolvable within the stated analytical uncertainty of ± 0.00002 (Fig. 6-3). Relative to an average Mesozoic seawater value of 0.70745, the medial mixing curve has a first resolvable paleosalinity (0.70749) at 18.5‰. Decreasing either the freshwater Sr concentration or $^{87}Sr/^{86}Sr$ to the 20th percentile (Table 6-1) in each of their respective distributions lowers the first resolvable paleosalinity to ~8‰. Increasing the freshwater $^{87}Sr/^{86}Sr$ or Sr concentration to 80th percentile (Table 6-1) values increases the first resolvable paleosalinity to 26‰ and 29‰, respectively.

Since the most accurate paleosalinities are determined at the low end of the salinity spectrum, uncertainty in the Sr concentration of the freshwater end-member has a greater impact on the accuracy of paleosalinity determinations than does a similar uncertainty in the marine Sr concentration. Therefore a modern day seawater concentration of 7.7 ppm is assumed. This is probably a valid assumption because Sr has a long residence time in the oceans and is therefore buffered against extreme changes. Nevertheless, changes in the steady-state cycling of Sr in ancient oceans (for example, due to changes in the proportions of organisms secreting carbonate shells or changes in carbonate shell mineralogy) will affect the Sr concentration of seawater. The only data on this issue are from Graham et al., (1982) who attributed a 10% lowering of Sr/Ca ratios in 6 Ma planktonic foraminifera to changes in Ca cycling at mid-ocean ridges. Using the median model mixing curve (Fig. 6-3), a ±10% difference in the Sr concentration of past seawater translates to an uncertainty of only ±0.9‰ for a salinity of 15‰. Relative paleosalinities remain unaffected.

Although seawater $^{87}Sr/^{86}Sr$ and Sr concentration are constant for all depositional basins of the same age, the $^{87}Sr/^{86}Sr$ and Sr concentration for freshwaters is basin-specific and cannot be predicted. Strategies for reconstructing the Sr isotope paleohydrology are developed in the following section.

ISOTOPE PALEOHYDROLOGY OF THE CRETACEOUS MANNVILLE GROUP

The Sr isotope paleohydrology can be reconstructed using contemporaneous marine and freshwater fossils. Since it is our aim to develop a geochemical method of determining paleosalinities that is as independent as possible of paleontological or sedimentological considerations, carbonate $\delta^{18}O$ analyses are also used to help place the $^{87}Sr/^{86}Sr$ analyses within a regional paleohydrological framework because in contrast to Sr isotopes, $\delta^{18}O$ variations in natural waters reflect participation in the meteorological cycle (Yurtsever and Gat, 1981). Although carbon isotopes may also be useful for this purpose (Clayton and Degens, 1959), the fossils of this study yielded generally marine-like $\delta^{13}C$ values (Table 6-2) indicating a source of C derived primarily from weathering of older marine carbonates (Holmden et al., submitted).

Marine end-member

Pocock (1980) assigned a late Aptian to early Albian age for the Mannville Group based on palynomorph biostratigraphy, which corresponds to seawater $^{87}Sr/^{86}Sr$ between 0.7074 and 0.7075

Table 6–2. Strontium oxygen and carbon isotope data from carbonate fossils and whole-rocks

Sample	Phase	*Sr/Ca (atom)	Sr (ppm)	$^{87}Sr/^{86}Sr$ (measured)	$\delta^{18}O_{Shell}$ (‰SMOW)	$^{+}\delta^{18}O_{Water}$ (‰SMOW)	$\delta^{13}C$ (PDB)	Remarks
MARINE AMMONITES (*Beudenticeras*)								
1. BEUD 38081 (1)	A	2.61	2284	0.707458 (14)	30.7	-0.6	2.1	thick fragment, nacreous lustre
2. BEUD 38081 (2)	A	----	----	0.707447 (11)	----	----	----	thick fragment, nacreous lustre
3. BEUD 20-46-34F (1)	A	2.85	2494	0.707508 (18)	30.8	-0.5	1.3	thin flakes, nacreous lustre
repeat				0.707525 (16)				
4. BEUD 20-46-34F (2)	A	----	----	0.707476 (13)	----	----	----	thin flakes, nacreous lustre
TRANSITIONAL ENVIRONMENTS (?)								
Ostracode sub-basin								
5. 7-21-56-27W4 (1154.1m)	A	----	nd	0.708347 (17)	21.1	-9.9	2.5	shell composite^
6. 10-12-25-20W4 (1421.3m)	C	----	nd	0.708273 (11)	23.2	-7.2	1.5	recrystallized shell composite^
Wabasca sub-basin								
7. 6-17-76-23W4 (795.8m)	A	2.61	2290	0.708095 (14)	22.5	-8.5	4.1	shell composite^
Ft. McMurray sub-basin								
8. FM 120 1-gast	A	2.31	2022	0.707707 (11)	21.1	-9.9	4.3	single gastropod shell^
9. FM 70 1-gast	A	2.02	1768	0.707825 (11)	----	----	----	single gastropod shell
10. FM 70	A	2.16	1888	0.707807 (16)	20.7	-10.3	3.5	shell composite^
repeat				0.707799 (10)				
11. FM 205-1	A	1.47	1290	0.708000 (17)	21.6	-9.4	4.4	shell composite^
12. FM 205-2	A	1.44	1263	0.708002 (17)	----	----	----	shell composite
13. FM 185	A	2.03	1778	0.707812 (09)	----	----	----	
repeat				0.707806 (11)	----	----	----	
14. HS-B	A	1.81	1588	0.707836 (21)	20.4	-10.3	4.5	shell composite^
repeat				0.707856 (08)				
15. HS-D 1-gast	A	1.83	1601	0.707880 (09)	20.7	-10.3	4.7	single gastropod shell^
16. FMP-0	A	1.77	1549	0.708155 (11)	22.3	-8.7	5.3	shell composite^
FRESH WATER ENVIRONMENTS (FLUVIAL AND LACUSTRINE)								
Group 1 freshwaters								
McLaren Unit (Core 13-1-65-4W4; 383-386 m)								
17. *C. ortmanni* 1	A	1.52	1333	0.708791 (12)	22.9	-8.1	0.54	single gastropod shell^
18. *C. ortmanni* 2	A	1.50	1312	0.708733 (08)	22.6	-8.4	0.19	single gastropod shell ^
19. *C. ortmanni* 3	A	1.52	1331	0.708804 (10)	23.1	-7.9	0.08	single gastropod shell^
20. *L. bituminous*	A	1.82	1591	0.708839 (10)	22.6	-8.4	0.21	single gastropod shell ^
Kootenai Limestones (Montana)								
21. Drum 335	C	—	nd	0.708740 (14)	17.6	-12.7	-0.8	whole-rock limestone
22. Drum 620	C	0.470	414.0	0.708594 (14)	15.4	-14.8	0.6	whole-rock limestone
23. Drum 770	C	—	nd	0.708633 (13)	17.5	-12.8	1.5	whole-rock limestone
		Average	*0.70873*	*±0.00009*				
Group 2 freshwaters								
General Petroleums Unit (Core 16-13-58-5W4; 505 m)								
24. *G. multicarinata* #4	A	1.38	1208	0.707495 (11)	16.2	-14.6	0.9	single gastropod shell ^
25. *G. multicarinata* #5	A	1.67	1459	0.707550 (09)	17.3	-13.6	0.5	single gastropod shell ^
26. *G. multicarinata* #7	A	1.23	1077	0.707595 (10)	17.2	-13.7	1.0	single gastropod shell ^
27. *G. multicarinata* #9	A	1.44	1261	0.707600 (10)	16.4	-14.4	0.1	single gastropod shell ^
Peterson Limestone (Wyoming)								
28. A-2	C/D	—	483.1	0.707586 (16)	nd	----	----	whole-rock lime/dolostone
29. A-6	C/D	—	547.1	0.707619 (14)	nd	----	----	whole-rock lime/dolostone
30. A-15	C/D	—	318.1	0.707954 (13)	nd	—	—	whole-rock lime/dolostone
			Average	*0.70763 ±0.00015 (1σ)*				
WAINWRIGHT RIDGE (DEVONIAN DOLOSTONES)								
31. 3-34-86-20W4 (391 m)	D	—	67.25	0.708175 (12)	27.3	—	-1.4	whole-rock dolostone
32. UGM-3	D	—	nd	0.708353 (11)	24.3	—	-3.3	whole-rock dolostone
33. 6-34-81-19W4	D	—	66.38	0.709260 (20)	26.2	—	0.7	whole-rock dolostone

+ Water $\delta^{18}O$ values calculated using the temperature dependent calcite-water equilibrium fractionation relation of (O'Neil et al.., 1969), a +0.6‰ correction for the aragonite-calcite fractionation (Tarutani et al., 1969) and a temperature of 14.5°C

* Calculated assuming 40 wt.% Ca

^ stable and radiogenic isotope analyses done on different shells from the same handsample

(Koepnick et al., 1985). Two samples of the ammonite *Beudenticeras* from the Moosebar-Clearwater epicontinental sea gave $^{87}Sr/^{86}Sr$ of 0.70745 and 0.70750 (Table 6-2) for the Mannville depositional interval, consistent with that predicted from the seawater $^{87}Sr/^{86}Sr$ curve.

To obtain the most accurate paleosalinities it is necessary to consider possible salinity reductions in brackish water systems developed adjacent to epicontinental seas like the Moosebar-Clearwater sea, because the paleosalinity of shallow epicontinental seas may have been lower than 35‰ by dilution with fresh waters. Outside of the equatorial belt, $\delta^{18}O$ yields qualitative information on a possible salinity reduction. The two samples of *Beudenticeras* have $\delta^{18}O$ values of 30.7‰ and 30.6 ‰ (SMOW), consistent with a temperature between 14 and 16°C and water $\delta^{18}O$ values between 0 and -1‰ (see *Chapter 5*). The *Beudenticeras* results overlap values from fossil molluscs collected from Deep Sea Drilling Project cores (Douglas and Savin, 1975) indicating the combination of temperature and water $\delta^{18}O$ values was similar between deep and shallow marine settings at this time and that fully marine conditions (35‰ salinity) prevailed. However, in slightly younger Interior Seaway sediments, Cenomanian and Turonian ammonites have aragonite $\delta^{18}O$ values that are significantly lower, averaging 26‰ (SMOW) (Kyser et al. 1993). If lowering of Cenomanian and Turonian ammonite $\delta^{18}O$ values results from mixing with ^{18}O-depleted river waters from the Cordillera (-17‰ ; see *Chapter 5*), salinities for Interior Seaway waters may have averaged 28‰ based on simple two-component mixing. The putative shift in $^{87}Sr/^{86}Sr$ resulting from this salinity reduction is not resolvable from 35‰ salinity (see above). For example, to distinguish a difference

Table 6-3 $^{87}Sr/^{86}Sr$, Sr, Ca and Sr/Ca for present day rivers draining the Western North American Cordillera

River	$^{87}Sr/^{86}Sr$	Sr (ppm)	Ca (ppm)	1000Sr/Ca (atom)	Literature Source
Skeena	0.70460	0.071	10.0	3.25	Wadleigh et al. (1985)
Nass	0.70540	0.097	12.0	3.70	Wadleigh et al. (1985)
Stikine	0.70542	0.058	17.0	1.56	Wadleigh et al. (1985)
Sacremento	0.70556	0.088	-----	-----	Ingram and Sloan (1992)
Feather	0.70566	0.056	-----	-----	Ingram and Sloan (1992)
San Joaquin	0.70734	0.094	-----	-----	Ingram and Sloan (1992)
Merced	0.70774	0.017	1.35	5.76	Goldstein and Jacobsen (1987)
Tuolumne	0.70785	0.019	-----	-----	Ingram and Sloan (1992)
Bruneau	0.70927	0.041	14.2	1.32	Goldstein and Jacobsen (1987)
Snake	0.70986	0.101	15.4	3.00	Goldstein and Jacobsen (1987)
Fraser	0.71195	0.080	15.0	2.44	Wadleigh et al. (1985)
Columbia	0.71210	0.074	19.0	1.78	Goldstein and Jacobsen (1987)
Average	0.7077	0.066	13.0	2.85	
Deviation (1 σ)	± 0.026	±0.029	± 5.5	±1.5	

of 0.00004 in ammonite $^{87}Sr/^{86}Sr$ at 28‰ salinity would require freshwaters with Sr concentrations and $^{87}Sr/^{86}Sr$ ratios ≥90th percentile values for world rivers. The average Sr concentration (0.066) and $^{87}Sr/^{86}Sr$ ratio (0.7077) for rivers draining the North American Cordillera today (Table 6-3) represent approximately the 45th and 15th percentiles, respectively (Table 6-1); too low to have had a measurable impact on Interior Seaway $^{87}Sr/^{86}Sr$ as originally concluded by McArthur et al. (1994).

Freshwater end-member

Presumed freshwater aragonitic gastropods from the McLaren Unit (*C. ortmanni* suite) and the General Petroleums Unit (*G. multicarinata* suite), which stratigraphically overlie the Ostracode Zone (Fig. 6-2; Mattison, 1991), gave contrasting $^{87}Sr/^{86}Sr$ results. The *C. ortmanni* suite gave $^{87}Sr/^{86}Sr$ ratios of 0.7087–0.7089, whereas the *G. multicarinata* suite gave 0.7075–0.7076, similar to the contemporaneous marine signature (Table 6-2). This latter result is somewhat surprising in that the *G. multicarinata* suite have the lower $\delta^{18}O$ values, consistent with equilibrium waters between -13.6 and -14.6‰ (SMOW), at 14.5 °C (see *Chapter 5*). Two explanations are possible: (1) the *G. multicarinata* suite occupied brackish, not fresh, waters or, (2) the similarity of $^{87}Sr/^{86}Sr$ to the contemporaneous marine value is fortuitous.

If the first explanation is correct it is possible to place first order constraints on the possible paleosalinity using the O isotope paleohydrology reconstructed in *Chapter 5*. If the paleolatitude of a study site is known, the $\delta^{18}O$ value for meteoric waters can be predicted from the known relation between the isotopic composition of precipitation and latitude (Yurtsever and Gat, 1981). However, the O isotope paleohydrology of the Mannville Group is complicated by an altitude effect in the western Cordillera which caused very significant ^{18}O-depletion of east-flowing paleo-Pacific airmasses (Glancy et al., 1993). In *Chapter 5* it was estimated that early Cretaceous drainage from the Cordillera imparted a very low O isotope signature (-14 to -17‰ SMOW) to foreland basin rivers, similar to meteoric water values in Alberta today (Yurtsever and Gat, 1981), and strong evidence that the early Cretaceous Cordillera had achieved altitudes comparable to the present day

Rockies. If foreland basin rivers were -17‰, then by simple two-component mixing, it is possible that the -14‰ waters calculated for the *G. multicarinata* suite (Table 6-2) are a mixture containing 20% seawater with a $\delta^{18}O$ value of -1‰; the resulting paleosalinity is 6‰.

Alternatively, the isotopic similarity to the marine $^{87}Sr/^{86}Sr$ may be fortuitous. If this is the case, other freshwater carbonates should show analogous marine-like values. Indeed, $^{87}Sr/^{86}Sr$ ratios for lacustrine carbonates of the Peterson Limestone (Glass and Wilkinson, 1980; Drummond et al., 1989; 1993) have $^{87}Sr/^{86}Sr$ ratios of 0.7076–0.7080 (Table 6-2). Located 500 km further south along the axis of the foreland basin, there is no evidence that marine waters ever influenced the hydrology of this lake. Furthermore, a relatively nonradiogenic $^{87}Sr/^{86}Sr$ for foreland rivers is consistent with the isotopic composition of rivers discharging from the Cordillera today (0.7077; Table 6-3) which reflects the relatively juvenile character of the Cordilleran crust (Samson and Patchett, 1991). Based on these arguments it is tentatively concluded that the *G. multicarinata* suite inhabited freshwaters, but this issue is discussed further in a latter section.

The 0.7087–0.7089 signature of the *C. ortmanni* suite is also regionally expressed. Presumed lacustrine carbonates of the Kootenai formation, Montana, have $^{87}Sr/^{86}Sr$ ratios of 0.7086–0.7087. The Kootenai limestones (Hopkins, 1985; Hayes, 1986) are located 500 km south of the *C. ortmanni* collection site (Fig. 6-2) and are considered stratigraphically equivalent to the Mannville Group of Alberta.

In summary, two sources of freshwater characterized the paleohydrology of the foreland basin setting, a more radiogenic source with an average $^{87}Sr/^{86}Sr$ ratio of 0.70873 ±0.00009 (1σ) herein referred to as Group 1 freshwaters, and a less radiogenic source averaging 0.70763 ±0.00015 (1σ) referred to as Group 2 freshwaters (Table 6-2).

Strontium isotope paleosalinities for Ostracode, Wabasca and McMurray fossils

Aragonitic shell fragments from the Ostracode Zone yielded $^{87}Sr/^{86}Sr$ of 0.70835 and from another location (~300 km away) a composite of recrystallized calcitic needles (formerly aragonite)

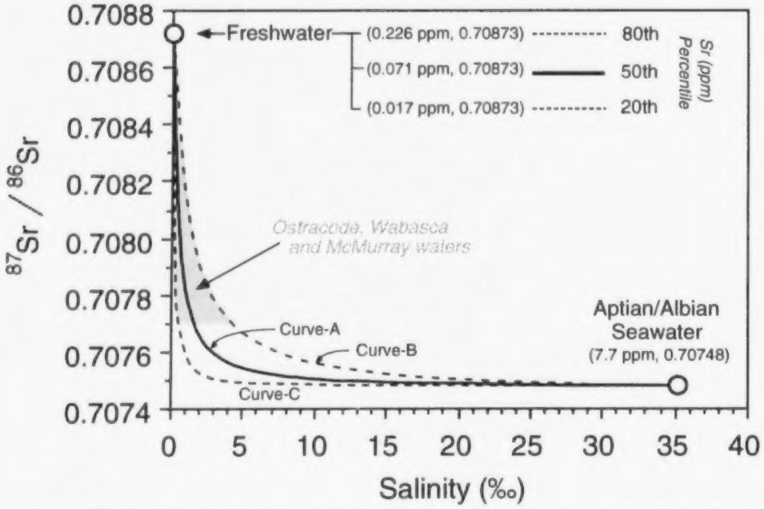

FIGURE 6-6 Seawater-freshwater mixing curves for the early Cretaceous Mannville Group based on the Sr isotope paleohydrology. The solid curve-A assumes the median value for freshwater Sr concentration, whereas the dashed curves are constructed using 20th (curve-C) and 80th (curve-B) percentile values. Paleosalinities for carbonate fossils of the Ostracode, Wabasca and McMurray sub-basins vary between values <0.5‰ (50th) and 4‰ (80th percentile).

yielded 0.70827. A sample of aragonitic shells from the Wabasca sub-basin yielded 0.70809 and nine composite shell analyses and 3 single shell analyses from the Ft. McMurray sub-basin yielded $^{87}Sr/^{86}Sr$ between 0.70771 and 0.70816. To satisfy the brackish water hypothesis for the depositional environment of the Ostracode, McMurray and Wabasca sub-basins, Group 1 fresh waters (0.70873) must have dominated the fluviatile inputs as it is impossible to mix marine and Group 2 fresh waters (0.70763) and obtain the $^{87}Sr/^{86}Sr$ observed. Using the median value of 0.071 ppm (Table 6-1) for the Sr concentration of Group 1 freshwaters yields paleosalinities of ≤1‰ for fossils from all three sub-basins (Curve-A, Fig. 6-6). To maximize potential salinities and the impact of assumed values for the Sr concentration of the freshwater end-member, mixing curve-B (Fig. 6-6) is constructed using a Sr concentration of 0.226 ppm (80th percentile for world rivers and lakes). This treatment results in paleosalinities ≤6‰. Considering that Group 2 freshwaters also contributed to the Ostracode, Wabasca and McMurray waters, true paleosalinities were even lower.

If the fossils analyzed are representative of the depositional conditions under which the bulk of the Ostracode, Wabasca and McMurray sediments were deposited, the inferred paleosalinities are so low that a wholly lacustrine paleoenvironment is possible. Potentially, mixing between a major north-flowing foreland river with $^{87}Sr/^{86}Sr$ similar to average Cordilleran rivers today (0.7077), and Devonian marine Sr derived from weathering of carbonates comprising the Wainwright Ridge (0.7082–0.7092; Table 6-2) could account for all of the variation in $^{87}Sr/^{86}Sr$ observed; seawater input is not required.

APPLICATION OF SR/CA RATIOS IN SR ISOTOPE PALEOHYDROLOGY

The maximum potential of the Sr isotope paleosalinity method lies in reintegrating the Sr mass balance which may be partly accomplished using shell Sr/Ca ratios. The main factor that controls shell Sr/Ca is the water Sr/Ca from which the shell precipitated (Kulp et al., 1952). Molluscs discriminate against the incorporation of Sr relative to Ca, such that shell Sr/Ca is lower than that in ambient waters. The magnitude of this effect varies between species (Thompson and Chow, 1955; Turekian and Armstrong, 1960), but is uniform within a single species so that a distribution coefficient (K_d), expressed as

$$\left(\frac{\mathrm{Sr}}{\mathrm{Ca}}\right)_{Shell} = K_d\left(\frac{\mathrm{Sr}}{\mathrm{Ca}}\right)_{Water} \tag{5}$$

may be applied to shell data to obtain water Sr/Ca . Well-determined K_d values for Sr in freshwater biogenic aragonite are 0.24 (*Limnaea stagnalis*; Buchardt and Fritz, 1978), 0.26 (*Lampsilis*; Faure et al. 1967), 0.29 (*Physa*; Odum, 1951), and 0.31 (*M. tuberculata*; Rosenthal and Katz, 1989). These values are also assumed to apply to aragonite secreting marine molluscs. An expression describing the mixing between seawater and freshwater with different Sr/Ca is

$$\left(\frac{\mathrm{Sr}}{\mathrm{Ca}}\right)_{BW} = \frac{\mathrm{Sr}_{SW}\chi + \mathrm{Sr}_{FW}(1-\chi)}{\mathrm{Ca}_{SW}\chi + \mathrm{Ca}_{FW}(1-\chi)} = \frac{\mathrm{Sr}_{BW}}{\mathrm{Ca}_{SW}\chi + \mathrm{Ca}_{FW}(1-\chi)} \tag{6}$$

Combining (6)and (2) yields

$$\left(\frac{^{87}\mathrm{Sr}}{^{86}\mathrm{Sr}}\right)_{BW} = \frac{\mathrm{Sr}_{SW}\mathrm{Sr}_{FW}\left[\left(\frac{^{87}\mathrm{Sr}}{^{86}\mathrm{Sr}}\right)_{FW} - \left(\frac{^{87}\mathrm{Sr}}{^{86}\mathrm{Sr}}\right)_{SW}\right]}{\left(\frac{\mathrm{Sr}}{\mathrm{Ca}}\right)_{BW}\left(\mathrm{Sr}_{SW}\mathrm{Ca}_{FW} - \mathrm{Sr}_{FW}\mathrm{Ca}_{SW}\right)} + \frac{\mathrm{Sr}_{SW}\mathrm{Ca}_{FW}\left(\frac{^{87}\mathrm{Sr}}{^{86}\mathrm{Sr}}\right)_{FW} - \mathrm{Sr}_{FW}\mathrm{Ca}_{SW}\left(\frac{^{87}\mathrm{Sr}}{^{86}\mathrm{Sr}}\right)_{SW}}{\mathrm{Sr}_{SW}\mathrm{Ca}_{FW} - \mathrm{Sr}_{FW}\mathrm{Ca}_{SW}} \qquad (7)$$

which is hyperbolic in coordinates of $(^{87}\mathrm{Sr}/^{86}\mathrm{Sr})_{BW}$ and $(\mathrm{Sr/Ca})_{BW}$ ratios.

A property of the hyperbolic mixing relation (eq. 7) is that two-component mixtures are linearly correlated on an inverse plot of $^{87}\mathrm{Sr}/^{86}\mathrm{Sr}$ *vs.* Ca/Sr, referred to as the companion plot (Langmuir et al., 1978). This allows the two-component mixing hypothesis to be tested graphically. The quantity Ca/Sr is used rather than 1/Sr because ultimately it is desirable to convert shell Sr/Ca to water Sr/Ca using an appropriate K_d so that a large database on the Sr/Ca variations in natural waters can be used (Fig. 6-4) (e.g., Odum, 1955a; 1955b).

Seawater has a 1000Sr/Ca atom ratio of 8.5 (De Villiers et al., 1993) whereas freshwaters typically have 1000Sr/Ca ratios between 0.5 and 5.0 (Odum, 1955b), with a median value of 2.3 (Table 6-1). Odum (1955b) studied Sr/Ca in natural waters and concluded: (1) Sr/Ca of rivers and lakes broadly reflect Sr/Ca of local bedrock sources, (2) the lower limit of Sr/Ca is set by the congruent weathering of Phanerozoic limestones, (3) although rivers draining limestone terrains have low Sr/Ca ratios their absolute Sr and Ca abundances are high, (4) rivers with Sr/Ca above the 50th percentile are found in regions of volcanic drainage, drainage of carbonate rocks with associated evaporites, and arid climate regions, (5) rivers from humid regions have low Sr/Ca, and (6) hydrologically closed basins can develop higher Sr/Ca than their input waters due to $\mathrm{CaCO_3}$ precipitation (Fig. 6-4).

Application to the L. bituminous suite (McMurray sub-basin)

Twelve analyses of *L. bituminous* shells from the Ft. McMurray sub-basin are linearly correlated on the $^{87}Sr/^{86}Sr$–Ca/Sr plot (r^2=0.96) satisfying the criteria for two-component mixing (Fig. 6-7a). Shell Sr concentrations are converted to Sr/Ca assuming ideal Ca-stoichiometry for aragonite (40.0 wt.%). This assumption was found to be reliable through electron microprobe analyses of several *L. bituminous* shell fragments which gave elemental Ca contents of 39.3, 39.2, 38.9, 38.8 and 38.3 wt.%. The lowest Ca measured yields Sr/Ca ratios only 3% higher than stoichiometry; a negligible difference compared to the variation in the data (Table 6-2). In addition to the *L. bituminous* shell trend, mixing lines for waters calculated using K_ds of 0.25 and 0.31 are also shown on Fig. 6-7a.

Sr/Ca$_{water}$ values for the *L. bituminous* shells do not fall on a mixing line that includes

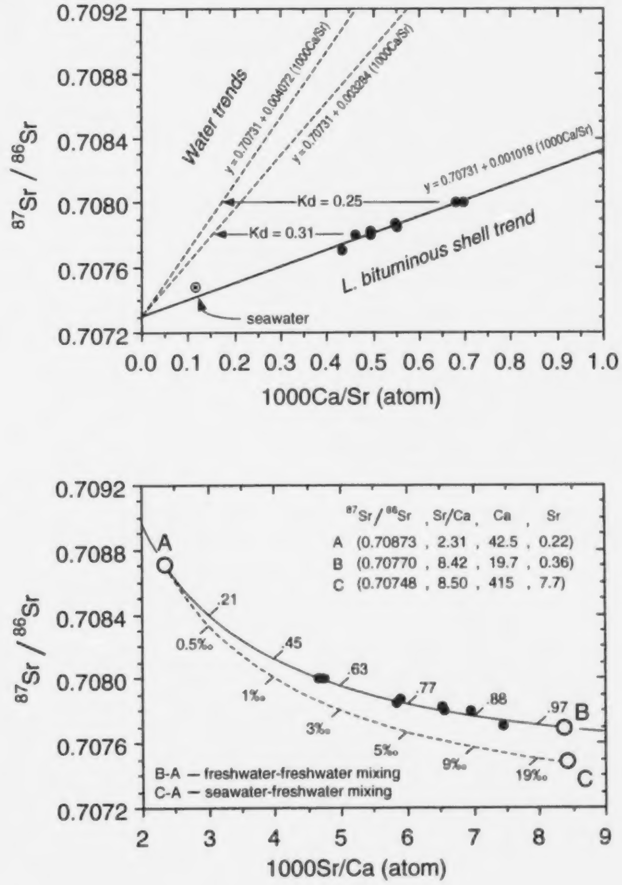

FIGURE 6-7 (a) $^{87}Sr/^{86}Sr$ – Ca/Sr mixing line for *L. bituminous* shells of the McMurray sub-basin (r^2=0.96). Shell mixing lines are transformed to water mixing lines using K_ds of 0.25 and 0.31. Seawater does not fall on or between either mixing line indicating that the mixing is between two freshwater sources. **(b)** The hyperbolic form of the freshwater mixing curve (A-B) is constructed using $^{87}Sr/^{86}Sr$ ratios determined from the isotope paleohydrology and corresponding Sr/Ca ratios from the equation of the water mixing line (K_d=0.31; Fig 6-7a). Sr and Ca concentrations for the freshwater end-member reflect bedrock types in the watershed which may be inferred from Sr/Ca and $^{87}Sr/^{86}Sr$ ratios. The fraction of each freshwater source contributing to the mixture is shown on the curve. The potential seawater-freshwater mixing curves is shown for comparison.

Aptian-Albian seawater as one of the points, whether K_ds of 0.31 or 0.25 are used (Fig. 6-7b). An unrealistic K_d of 0.66 is required to place seawater on the mixing line indicating mixing between two non-marine sources. Using the $^{87}Sr/^{86}Sr$ – Sr/Ca plot, it is possible to asymptotically derive the $^{87}Sr/^{86}Sr$ ratio of the end-member with the highest Sr/Ca ratio. Although the curvature of the mixing line is too shallow to be very accurate, a $^{87}Sr/^{86}Sr$ ratio between 0.7076 and 0.7078 is indicated and consistent with the isotopic composition of Group 2 freshwaters previously determined from the isotope paleohydrology (0.70764; Table 6-2), and those discharging from the modern Cordilleran today (0.7077; Table 6-3). For comparison, hypothetical mixing lines between Aptian-Albian seawater and Group 1 and 2 freshwaters are also plotted.

To quantify the fraction of each freshwater source in the mixture, or paleosalinities in the case of seawater mixing with freshwater, the Sr and Ca concentrations in the end-member waters must be approximated. As before, Sr concentrations will govern the mass balance, but rather than assuming quantities for these parameters, Ca concentrations are chosen and the Sr concentrations determined from the Sr/Ca ratio. Unlike Sr, the distribution of Ca in fresh waters has a maxima between 12 and 18 ppm (Fig. 6-4), which is close to the equilibrium Ca concentration of 20 ppm for the system $CaO–CO_2–H_2O$ in equilibrium with atmospheric ρCO_2 (Table 5.3 in Stumm and Morgan, 1981). This is consistent with the median value for world rivers and lakes (Table 6-1), but freshwater Ca contents can be higher or lower indicating significant disequilibrium (Fig.6-4). A sensitivity analysis based on increasing Ca contents can be undertaken to test the impact of the assumed Ca concentration on the resulting salinity with the additional constraint that the Sr/Ca ratio places some limits on the possible range of Sr concentrations. For the case of seawater-freshwater mixing, the present day marine Sr/Ca ratio of 8.5 and Sr concentration of 7.7 ppm is used.

For the freshwater end-member, the Ca concentration depends on the type of terrane being weathered, for which the freshwater Sr/Ca and $^{87}Sr/^{86}Sr$ ratios provide constraints. For example weathering of Precambrian crust yields very radiogenic $^{87}Sr/^{86}Sr$ approximately median Sr/Ca ratios and below median Ca concentrations (Wadleigh et al., 1985). Weathering of carbonates yields lower than median $^{87}Sr/^{86}Sr$ (0.7065-0.7092), Sr/Ca of ~0.5 and higher than median Ca concentrations (Odum, 1955b). A Ca concentration in the 80th percentile is chosen for Group 1 waters (Table 6-1) based on the carbonate source of Sr. A median value for the Ca concentration of Group 2 waters is chosen because the high Sr/Ca ratio is interpreted to reflect the weathering of juvenile volcanic rocks in the early Cretaceous Cordillera and an intermittently dry foreland basin climate (Drummond and Wilkinson, 1989; Holmden et al., submitted), factors linked with high Sr/Ca in modern rivers (Odum, 1955b; Skougstad and Horr, 1963). The mixing proportions can be determined from equation 8 which is expressed in terms of seawater-freshwater mixing as

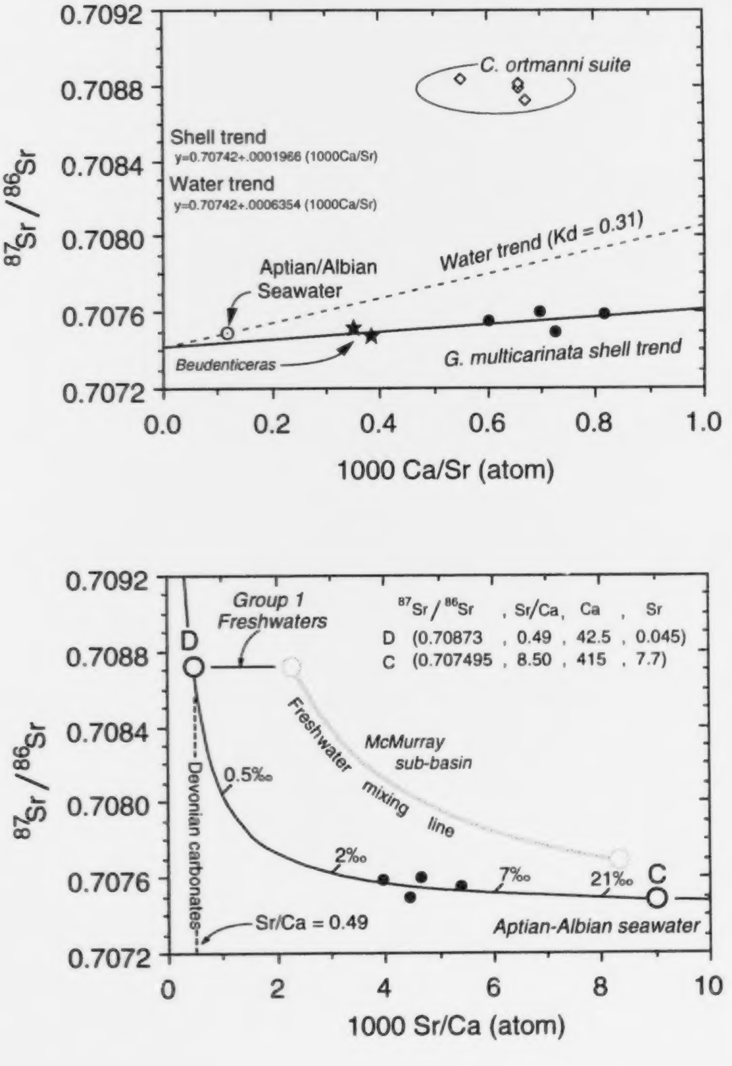

FIGURE 6-8 (**a**) Presumed freshwater fossils of the *G. multicarinata* suite fall on a seawater–freshwater mixing line (r^2=0.43) that includes the two marine ammonites (*Beudenticeras*), strongly inferring a brackish water habitat for *G. multicarinata*. The shell mixing line is transformed to a corresponding water mixing line using equation (9). The K_d is fixed by the requirement that the mixing line must pass through Aptian-Albian seawater. The freshwater *C. ortmanni* suite is shown for reference. (**b**) The hyperbolic form of the mixing curve constructed from the equation of the water mixing line in Figure7-7a using Group 1 freshwaters (Table 6-2). Paleosalinities between 2 and 5‰ are consistent with the $\delta^{18}O$ constraints.

$$\chi = \frac{\mathrm{Sr}_{FW} - \mathrm{Ca}_{FW}\left(\frac{\mathrm{Sr}}{\mathrm{Ca}}\right)_{BW}}{\left(\frac{\mathrm{Sr}}{\mathrm{Ca}}\right)_{BW}\left(\mathrm{Ca}_{SW} - \mathrm{Ca}_{FW}\right) + \mathrm{Sr}_{FW} - \mathrm{Sr}_{SW}} \qquad (8)$$

Paleosalinities (S_{BW}) are determined by multiplication of χ by 35‰.

The data presented above indicates that the paleohydrology of the Ft. McMurray sub-basin was dominated by Group 2 freshwaters, which contributed 60–100% of the water mass (Fig. 6-7b).

Application to the G. multicarinata suite (Group 2 freshwaters)

Fossils of the *G. multicarinata* suite also show significant variations in Sr/Ca correlated with ^{87}Sr/^{86}Sr (Fig. 6-8a). The δ^{18}O values for these shells allow up to 20% mixing with marine waters (see above). If the apparent mixing line of Figure 6-8a is between seawater and freshwater, the specific K_d necessary to transform shell Sr/Ca to corresponding water Sr/Ca is fixed by the condition that seawater must fall on the mixing line. The K_d may be determined from equation 9

$$\left(\frac{^{87}\mathrm{Sr}}{^{86}\mathrm{Sr}}\right)_{SW} = \left(\frac{^{87}\mathrm{Sr}}{^{86}\mathrm{Sr}}\right)_{X=0} + \frac{m}{K_d}\left[1000\left(\frac{\mathrm{Ca}}{\mathrm{Sr}}\right)_{SW}\right] \qquad (9)$$

where m and (^{87}Sr/^{86}Sr)$_{X=0}$ is the slope and Y intercept of the shell mixing line, respectively. Substituting ^{87}Sr/^{86}Sr (0.70748) and Ca/Sr (0.1176) for Aptian-Albian seawater yields a K_d of 0.39 which is slightly higher than modern estimates. However, K_ds determined in this manner are very sensitive to the value of the marine ^{87}Sr/^{86}Sr, and to a lesser degree Sr/Ca. For example, a marine ^{87}Sr/^{86}Sr of 0.70749 yields a K_d value of 0.33, and 0.70750 yields a value of 0.29. Changing the marine Sr/Ca by only 10% and maintaining constant ^{87}Sr/^{86}Sr yields K_ds of 0.35 and 0.43, for Sr/Ca of 9.35 and 7.65, respectively. Since the slope of the mixing line is not well constrained in the present example (Fig. 6-8a, r^2=0.43), a K_d = 0.31 and a seawater Sr/Ca = 8.5 are assumed, which yields a seawater ^{87}Sr/^{86}Sr of 0.707495. This result is within the analytical uncertainty of our measured *Beudenticeras* values (Table 6-2) and consistent with the *G. multicarinata* fossils inhabiting brackish waters. Paleosalinites are determined by choosing a freshwater end-member. Group I freshwaters (0.70783) are chosen because the low Sr/Ca (0.49) determined from the mixing line is consistent with weathering of carbonates comprising the Wainwright Ridge. Paleosalinities ≤6‰ result if a Ca concentration in the 80th percentile of world rivers and lakes is assumed (Fig. 6-8b). Lower salinities result if lower Ca concentrations are considered.

IMPLICATIONS FOR THE DEPOSITIONAL ENVIRONMENT OF THE OSTRACODE, WABASCA AND MCMURRAY SUB-BASINS

Carbonate occurrences within the Ostracode Zone, and stratigraphically equivalent sediments of the Wabasca and McMurray sub-basins, are constrained by their Sr isotope paleosalinities to have been deposited in predominantly lacustrine paleoenvironments. The Sr isotope paleohydrology revealed two freshwater sources; a relatively nonradiogenic source (0.7076 ±0.0002) with high Sr/Ca, interpreted as the signature of a major north flowing foreland basin river, and a more radiogenic signature (0.7087) with low Sr/Ca reflecting freshwater drainage from the Wainwright Ridge. With the exception of Farshori (1983) and Hayes (1986), this interpretation conflicts with most recent studies of the Ostracode Zone using paleontology and sedimentology (e.g., Finger, 1983; James, 1985; Wanklyn, 1985; Mattison, 1987; Banerjee and Davies, 1988; Banerjee, 1990; McPhee, 1994). It is possible that only the carbonate lithologies are lacustrine and that the nonfossiliferous interlayered clastic lithologies were deposited in more saline waters. Alternatively, the pattern of interlayered carbonates and clastics may be due to diagenetic (early shell dissolution) or taphonomic effects (shell destruction prior to burial). Elucidating the relationship between fossil shells and their enclosing sediment is an old problem in paleoecology which may be overcome by analyzing rare *in situ* fossils. What we have shown is that the habitat paleosalinities of these shells can be deduced.

To our knowledge, however, none of the authors supporting brackish water deposition have made a similar distinction between the carbonate and non-carbonate lithologies of the Ostracode Zone. The fact that the limestones and coquinas are a characteristic feature of the Ostracode Zone suggests that any marine connection was restricted to enable frequent oscillation between fresh and potential brackish water hydrologies. Limestone deposition in the Ostracode Zone may be linked to shifting regional precipitation patterns which induced changes in the flux of freshwaters carried by foreland basin rivers, or relative sea level change with lacustrine conditions dominating during relative lowstands of sea level.

A modern analog for the paleohydrology of the Ostracode Zone is Lake Maracaibo, Venezuela, a large (12,500 km^2), shallow (<35m) intermontane lake with a long narrow connection to the sea. A 7-12 m sill at the entrance to the lake helps to maintain low stable salinities of about 3.3‰ (Hyne et al., 1979). Rainfall is high in the summer and low in the winter and this cycle is reflected in lake salinities (Gessner, 1953). The H isotopic composition of lake waters is very uniform (–21.6± 6‰, SMOW) and about 40‰ enriched over the δD of mean river inputs (–62.4‰) (Friedman et al., 1956). Only 4‰ of the 40‰ difference between lake and river δD values is attributed to mixing with Caribbean seawater (δD=–20‰), the remainder is caused by evaporation due to the long lake water residence time of ~10 years (Friedman et al., 1956). The average $\delta^{18}O$ value for equilibrium waters of the Ostracode, Wabasca and McMurray sub-basins are also very uniform (–10.1 ±0.7‰ n=40 shells) and enriched in ^{18}O relative to primary meteoric waters (–14 and –17‰; *Chapter 5*) suggesting that these fossils inhabited lakes rather than rivers. Lakes with long water residence times can explain the relatively high Sr/Ca (2.31) determined from the *L. bituminous* mixing line (Fig. 6-7a,b) for Group 1 freshwaters, which is higher than expected for congruous weathering of Devonian dolostone. Chemical weathering of the Wainwright Ridge dolostone would initially yield low Sr/Ca (<0.2; Table 6-2). If runoff was to a lake, input Sr/Ca would increase through biogenic production and sedimentation of $CaCO_3$ in lake waters (Odum, 1955b). Accordingly, the *L. bituminous* line (Fig. 6-7a) may record mixing of lake waters with similar $\delta^{18}O$ but different $^{87}Sr/^{86}Sr$ and Sr/Ca across the Wainwright Ridge.

CONCLUSIONS

Strontium isotope ratios in fossil shells may be used to determine paleosalinities in ancient brackish water systems. Two different approaches were investigated for reconstructing the Sr isotope paleohydrology, the framework upon which accurate paleosalinity estimates depend. The first method utilized $^{87}Sr/^{86}Sr$ in contemporaneous seawater and freshwater fossils to construct the Sr isotope mixing hyperbola. Oxygen isotope analyses were useful in providing increased confidence that the $^{87}Sr/^{86}Sr$ results fit within a rational paleohydrological framework. Paleosalinities for potential brackish water fossils are determined by comparing their $^{87}Sr/^{86}Sr$ ratios to the mixing hyperbola. The most critical unknown is the Sr concentration of the freshwater end-member which can significantly affect the accuracy of any paleosalinity determinations, but not their relative magnitude.

A second approach utilized potential brackish water fossils directly and deduced from their variations in $^{87}Sr/^{86}Sr$ and Sr/Ca what the end-member compositions were. This approach allows the brackish water affinity of the fossils to be tested graphically on a plot of $^{87}Sr/^{86}Sr$ *vs.* Ca/Sr. If the data correlate linearly, this constitutes primary evidence that the original waters are mixtures of two sources. If one source is seawater, the choice of K_d (necessary to convert shell Sr/Ca to water Sr/

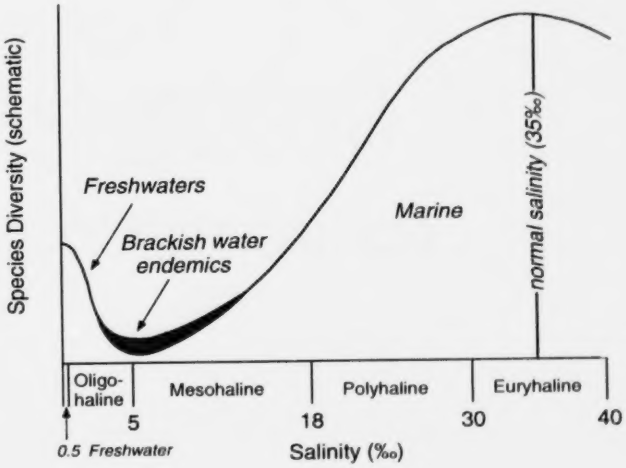

FIGURE 6-9 A schematic version of the Remane plot showing the relationship between species diversity and salinity in the Baltic Sea (Remane, 1934). The species minimum between 5 and 8‰ is the most prominent feature. Provided there is sufficient isotopic contrast between marine and freshwaters, Sr isotope paleosalinities can always be resolved in the diversity minimum zone and will often be resolvable in the 10–20‰ range where faunal criteria are more ambiguous. Very few depositional basins will have the combined characteristics of high freshwater $^{87}Sr/^{86}Sr$ and Sr content necessary for resolution of paleosalinities >20‰. Modified from Hudson (1990).

Ca) is fixed by the condition the seawater (with an Ca/Sr of ~0.1176) is one of the points on the mixing line. The K_d determined should be comparable to modern K_ds for Sr partitioning in biogenic carbonates.

Applying these techniques to fossils collected from suggested brackish water deposits of early Cretaceous Ostracode Zone, and stratigraphically equivalent deposits in the Wabasca and McMurray sub-basins yielded consistent results. Although brackish water depositional conditions have been widely proposed, a lacustrine setting is deduced for the carbonates and shell containing clastic sediments thus demonstrating the importance of paleohydrological techniques in paleoenvironment analysis.

Present-day brackish waters are dominated by pelecypods, gastropods, ostracodes and small benthic foraminifera (Pickerill and Brenchley, 1991). Relative to marine and freshwater environments, brackish waters are characterized by lower species diversities which is graphically displayed on the modified Remane plot (Remane, 1934) (Fig. 6-9). The most prominent feature is the diversity minimum between 5 and 8‰ salinity. This is likely the region where combined sedimentological and paleontological indicators are the most unambiguous regarding a salinity reduction. Due to the nature of the mixing relations between seawater and freshwater, and provided there is resolvable isotopic contrast, Sr isotope paleosalinities can always be determined across this diversity minimum (salinities 0 - 10‰). The intermediate range (10 - 20‰) is also resolvable in many cases but with higher uncertainty. Salinities from 20-30 ‰ will be resolvable in very few depositional settings. Even though it is feasible to reduce the analytical uncertainty on $^{87}Sr/^{86}Sr$ (Ingram and DePaolo, 1993) geological uncertainties remain that will influence accuracy, but not relative precision, of the paleosalinity determinations. The methods presented here have applications beyond the estimation of paleosalinity and may be used to identify sources and mixing of waters in sedimentary basins, aquifers, lakes, and those accompanying carbonate diagenesis.

REFERENCES

Alexander G.V., Nusbaum R.E. and Macdonald, N.S. (1954) Strontium and calcium in municipal water supplies. *American Water Works Association Journal* **46,** 643-654.

Andersson Per S., Wasserburg G.J. and Ingri, J. (1992) The sources of Sr and Nd isotopes in the Baltic Sea. *Earth and Planetary Science Letters* **113,** 459-472.

Banerjee I. (1990) Some aspects of Lower Mannville sedimentation in southeastern Alberta. *Geological Survey of Canada Paper* **90-11,** 40 p.

Banerjee I. and Davies E.H. (1988) An integrated lithostratigraphic and palynostratigraphic study of the Ostracode zone and adjacent strata in the Edmonton Embayment, Central Alberta. In *Sequences, Stratigraphy, Sedimentology:Surface and Subsurface* (ed. D.P. James and D.A. Leckie), *Canadian Society of Petroleum Geologists Memoir* **15,** 261-274.

Banerjee I. and Kidwell S.M. (1991) Significance of molluscan shell beds in sequence stratigraphy: an example from the Lower Cretaceous Mannville Group of Canada. *Sedimentology* **38,** 913-934.

Barnes R.S.K. (1989) What, if anything, is a brackish water fauna? *Transactions of the Royal Society of Edinburgh* **80,** 235-240.

Brass G.W. (1976) The variation of the marine $^{87}Sr/^{86}Sr$ ratio during Phanerozoic time: interpretation using a flux model. *Geochimica et Cosmochimica Acta* **40,** 721-730.

Broecker W. (1963) Radioisotopes and large-scale oceanic mixing. In *The Sea* (ed. M.N. Hill), pp. 88-108. Interscience.

Buchardt B. and Fritz P. (1978) Strontium uptake in shell aragonite from the freshwater gastropod Limnaea stagnalis. *Science* **199,** 291-292.

Clayton R.N. and Degens E.T. (1959) Use of carbon isotope analyses of carbonates for differentiating freshwater and marine sediments. *American Association of Petroleum Geologists Bulletin* **43,** 890-897.

De Villers S., Shen G.T., Nelson B.K. (1993) The Sr/Ca-temperature relationship in coralline aragonite: Influence of variability in $(Sr/Ca)_{seawater}$ and skeletal growth parameters. *Geochimica et Cosmochimica Acta* **58,** 197-208.

Dodd J.R. and Stanton R.J. (1975) Paleosalinities within a Pliocene bay, Rettleman Hills, California: a study of the resolving power of isotope and faunal techniques. *Geological Society of America Bulletin* **86,** 51-64.

Douglas R.G. and Savin S.M. 1975. Oxygen and carbon isotope analyses of Tertiary abd Cretaceous microfossils from Shatsky Rise and other sites in the north Pacific ocean. In *Initial Reports of the Deep Sea Drilling Project 32* (Ed. R.L. Larson, R. Moberly), pp. 509-520. United States Government Printing Office, Washington, DC.

Drummond C.N., Wilkinson B.H. and Lohmann KC. (1989) Lacustrine carbonate record of Cretaceous climatic variation in the Wyoming-Idaho overthrust belt. *Geological Society of America Abstracts with Programs* **21,** 126 (abstr).

Drummond C.N., Wilkinson B.H. and Lohmann KC. (1993) Rock-dominated diagenesis of lacustrine magnesian calcite micrite. *Carbonates and Evaporites.* **8,** 214-223.

Eisma D., Mook W.G. and Das H.A. (1976) Shell characteristics, isotopic composition and trace-element contents of some euryhaline molluscs as indicators of salinity. *Paleogeography, Paleoclimatology, Paleoecolology* **19,** 39-62.

Faure G., Crocket J.H. and Hurley P.M. (1967) Some aspects of the geochemistry of strontium and calcium in Hudson Bay and the Great Lakes. *Geochimica et Cosmochimica Acta* **31,** 451-461.

Farshori M.Z. (1983) Depositional environment of Ostracode beds in southern Alberta. In *The Mesozoic of Middle North America* (eds. D.F. Stott and D.J. Glass), *Canadian Society of Petroleum Geologists Memoir* **9,** 568.

Feulner A.J. and Hubble J.H. (1960) Occurrence of strontium in the surface and ground waters of Champaign County. *Ohio Economic Geology* **55,** 176-186.

Finger K.L. (1983) Observations on the lower Cretaceous Ostracode zone of Alberta. *Bulletin of Canadian Petroleum Geology* **31,** 326-337.

Frederickson A.F. and Reynolds R.C., Jr. (1959) Geochemical method for determining paleosalinity in clays and clay minerals. *Proceedings of the 8th National Conference on Clays and Clay Minerals* pp. 203-213. Pemagon Press.

Friedman, I., Norton, D.R., Carter, D.B. and Redfield, A.C. (1956) The deuterium balance of Lake Maracaibo. *Limn. Ocean.* **1,** 239-246.

Gessner, F. (1953) Investigaciones hidrograficas en al Lago de Maracaibo. *Acta Cientifica Venezolana* **4,** 173-177.

Glancy T.J., Arthur M.A., Barron E.J. and Kauffman E.G. (1993) A paleoclimate model for the North American Cretaceous (Cenomanian-Turonian) Epicontinental sea. In *Evolution of the Western Interior Basin* (Ed. W.G.E. Caldwell and E.G. Kauffman), *Geological Association of Canada Special Paper* **39,** 219-241.

Glass S.W. and Wilkinson B.H. (1980) The Peterson Limestone–early Cretaceous carbonate deposition in western Wyoming and southeastern Idaho. *Sedimentary Geology* **27,** 143-160.

Glaister, R.P. (1959) Lower Cretaceous of southern Alberta and adjacent areas. *American Association of Petroleum Geologists Bulletin* **43,** 590-640.

Goldstein S.J. and Jacobsen S.B. (1987) The Nd and Sr isotopic systematics of river water dissolved material: implications for the sources of Nd and Sr in seawater. *Chemical Geology* **66,** 245-272.

Graham D.W., Bender M.L., Williams D.F., Keigwin L.D. Jr. (1982) Srontium-calcium ratios in Cenozoic planktonic foraminifera. *Geochimica et Cosmochimica Acta* **46,** 1281-1292.

Harder H. (1970) Boron content of sediments as a tool in facies analysis. *Sed. Geol.* **4,** 153-175.

Hayes B.J.R. (1986) Stratigraphy of the Basal Cretaceous Lower Mannville Formation, Southern Alberta and North-Central Montana. *Bulletin of Canadian Petroleum Geology* **34,** 30-48.

Hayes B.J.R., Christopher J.E., Rosenthal L., Lus G., McKercher B., Minker D., Trembley Y.M. and Fennell J. (1994) The Mannville Group. In *Geological Atlas of the Western Canada Sedimentary Basin* (Ed. G.D. Mossop and I. Shetsen), pp. 317-334. Canadian Society of Petroleum Geologists.

Holmden C., Muehlenbachs K. and Creaser R.A. Depositional environment of the early Cretaceous Ostracode Zone: Paleohydrologic Constraints from O, C and Sr Isotopes. *Canadian Society of Petroleum Geologists Memoir* submitted May, 1995.

Hopkins J.C. (1985) Channel-fill deposits formed by aggradation in deeply scoured, superimposed distributaries of the lower Kootenai formation (Cretaceous). *Journal of Sedimentary Petrology* **55**, 42-52.

Howard J.D. and Frey R.W. (1973) Characteristic physical and sedimentary structures in Georgia estuaries. *American Association of Petroleum Geologists Bulletin* **57,** 1169-1184.

Hudson J.D. (1990) Salinity from faunal analysis and geochemistry. In *Paleaobiology, a Synthesis* (Ed. D.E.G. Briggs andP.R. Crowther), pp. 406-410. Blackwell.

Hyne N.J., Cooper W.A. and Dickey P.A. (1979) Stratigraphy of intermontane, lacustrine delta, Catacumbo River, Lake Mracaibo, Venezuela. *American Association of Petroleum Geologists Bulletin* **61,** 2042-2057.

Ingram B.L. and Sloan D. (1992) Strontium isotopic composition of estuarine sediments as paleosalinity-paleoclimate indicator. *Science* **255,** 68-72.

Ingram B.L. and DePaolo D.J. (1993) A 4300 year strontium isotope record of estuarine paleosalinity in San Francisco Bay, California. *Earth and Planetary Science Letters* **119,** 103-119.

Irving E., Wynne P.J. and Globerman B.R. (1993) Cretaceous paleolatitudes and overprints of the North American Craton. In *Evolution of the Western Interior Basin* (Ed. W.G.E. Caldwell and E.G. Kauffman), Geological Association of Canada Special Paper **39,** 91-96.

Jackson P.C. (1984) Paleogeography of the lower Cretaceous Mannville Group pf western Canada. In *Elmworth–acase study of a deep basin gasfield* (ed. A. Masters), pp. 49-77. American Association of Petroleum Geologists Memoir **38**.

James D.P. (1985) Sedimentology, paleogeography and reservoir quality of the Mannville Group, southwestern Alberta: Implications for exploration. *Reservoir* **12,** 2-3.

Kauffman E.G. (1984) Paleobiogeography and evolutionary response dynamic in the Cretaceous Western Interior Seaway of North Amercia. In *Jurassic-Cretaceous biochronology and paleogeography of North America* (ed. G.E.G. Westermann), Geological Association of Canada Special Paper **27,** 273-306.

Keith M.L., Anderson G.M. and Eichler R. (1964) Carbon and oxygen isotopic composition of mollusk shells from marine and fresh-water environments. *Geochimica et Cosmochimica Acta* **28,** 1757-1786.

Keith M.L. and Weber J. N. (1964) Carbon and oxygen isotopic composition of selected limestones and fossils. *Geochimica et Cosmochimica Acta* **28,** 1787-1816.

Koepnick R.B., Burke W.H., Denison R.E., Hetherington E.A., Nelson H.F., Otto J.B. and Waite L.E. (1985). Construction of the seawater ^{87}Sr/^{86}Sr curve for the Cenozoic and Cretaceous: Supporting data. *Chemical Geology* **58,** 55-81.

Koke K.R. and Stelck C.R. (1984) Foraminifera of the *Stelckiceras* Zone, basal Hasler Formation (Albian), Northeastern British Columbia. In *The Mesozoic of Middle North America (*ed. D.F. Stott and D.J. Glass), *Canadian Society of Petroleum Geologists Memoir.* **9,** 271-279.

Kramers J.W. (1971) Road Log, Ft. McMurray to Ft. McKay. In *Guide to the Athabasca oil sands area* (ed. M.A. Carrigy and J.W. Krammers), pp. 188-212. Canadian Society of Petroleum Geologists Oils Sands Symposium.

Kulp J.L., Turekian K. and Boyd D.W. (1952) Strontium content of limestones and fossils. *Bulletin of the Geological Society of America* **63,** 701-716.

Kyser T.K., Caldwell W.G.E., Whittaker S.G. and Cadrin A.J. (1993) Paleoenvironment and geochemistry of the northern portion of the Western Interior Seaway during late Cretaceous time. In *Evolution of the Western Interior Basin* (Ed. W.G.E. Caldwell and E.G. Kauffman), Geological Association of Canada Special Paper **39,** 355-378.

Landergren S. (1963) Borhaltens beroende av salinitet och kornstorlek i marina sediment. *Dansk Geol. Foren,* **15,** 244.

Langmuir C.H., Vocke R.D. Jr., Hanson G.N. (1978) A general mixing equation with applications to icelandic basalts. *Earth and Planetary Science Letters* **37,** 380-392.

Leckie D.A. and Smith D.G. (1992) Regional setting, evolution, and depositional cycles of the Western Canada Foreland Basin. In *Foreland Basins and Foldbelts* (ed. R.W. McQueen and D.A. Leckie), *American Association of Petroleum Geologists Memoir* **55,** 9-46.

Liddicoat M. I., Turner D.R. and Whitfield M. (1983) Conservative behaviour of B in the Tamar Estuary. *Coastal Shelf Science* **17,** 467-472.

Lloyd R.M. (1965) $\delta^{18}O$ and $\delta^{13}C$ variations in molluscs from transitional environments. In *Stable Isotopes in Oceanographic Studies and Paleotemperatures* (ed. E. Tongiorgi), pp. 235-265. Consiglio Nazionale Delle Ricerche, Spoleto.

Loranger, D.M. (1951) Useful Blairmore microfossil zone in central and southern Alberta, Canada. American Association of Petroleum Geologists *Bulletin* **35,** 2348-2367.

Mattison B.W. (1987) Ichnology and paleontology of the McMurray Formation. M.Sc. dissertation Univ. of Alberta.

Mattison B.W. (1991) Stratigraphic and paleoenvironmental analysis of the upper and middle Mannville subgroups: Cold Lake Oil Sands area, east central Alberta. Ph.D. dissertation Univ. of Alberta.

McArthur J.M., Kennedy W.J., Chen M., Thirlwall M.F. and Gale A.S. (1994) Strontium isotope stratigraphy for Late Cretaceous time: Direct numerical calibration of the Sr isotope curve based on the US western Interior. *Palaeogeography, Palaeclimatology, Palaeoecology* **108,** 95-119.

McLean J.R. and Wall J.H. (1981) The early Cretaceous Moosebar Sea in Alberta. *Bulletin of Canadian Petroleum Geology* **29,** 334-377.

McCrea J.M. (1950) On the isotopic chemistry of carbonates and a paleotemperature scale. *Journal of Chemi-*

cal Physics **18,** 849-857.

McGookey D.P., Haun J.D., Hale L.A., Goodell H.G., McCubbin D.G., Weimer R.J. and Wulf G.R., 1972. Cretaceous System. In *Geological Atlas of the Rocky Mountains* (ed. W.W. Mallory), pp. 190-228. Denver, Rocky Mountain Association of Geologists.

McPhee D. (1994) Sequence stratigraphy of the lower Cretaceous Mannville Group of east-central Alberta. M.Sc. dissertation Univ. of Alberta.

Mook W.G. and Vogel J.C. (1967) Isotopic equilibrium between shells and their environment. *Science* **159,** 874-875.

Monger J.W.H., 1989. Overview of Cordilleran geology. In *Western Canada Sedimentary Basin: A case History* (ed. B.D. Ricketts), pp. 9-32. Geological Survey of Canada Institute for Sedimentary and Petroleum Geolog, Canada.

Odum H.T. (1951) The stability of the world Sr cycle. *Science* **114,** 407-411.

Odum H.T. (1955a) Biogeochemical deposition of Strontium. *Institute of Marine Science* **4,** 38-114.

Odum H.T. (1955b) Strontium in natural waters. *Institute of Marine Science* **4,** 22-37.

O'Neil J.R., Clayton, R.N. and Mayeda, T.K. (1969) Oxygen isotope fractionation in divalent metal carbonates. *Journal of Chemical Physics* **51,** 5547-5558.

Palmer M.R. and Edmond J.M. (1989) The strontium isotope budget of the modern ocean. *Earth and Planetary Science Letters* **92,** 11-26.

Palmer M.R. and Edmond J.M. (1992) Controls over the strontium isotope composition of river water. *Geochimica et Cosmochimica Acta* **56,** 2099-2111.

Pemberton S.G. and Wightman D.M. (1992) Ichnological characteristics of brackish water deposits. *Society of Economic Paleontologists and Mineralogists Core Workshop* **17,** 141-167.

Pickerill R.K. and Brenchley P.J. (1991) Benthic macrofossils as paleoenvironmental indicators in marine siliciclastic facies. *Geoscience Canada* **18,** 119-138.

Pocock S.A.J. (1980) The Aptian-Albian boundary in Canada. *Procedings 4th International Palynology Conference Lucknow, 1976-77* **2,** 419-424.

Plummer P.S. and Gostin V.A. (1981) Shrinkage cracks: dessication or synaeresis? *Journal of Sedimentary Geology* **51,** 1147-1156.

Ranger M.J., McPhee D., Pemberton S.G. and Zaitlan B. (1994) Basins and sub-basins: Controls on sedimentation and stratigraphy of the Mannville Group. Canadian Society of Economic Geologists and Petroleum Geologists Joint Annual Meeting, 24-25 (abstract).

Remane A. (1934) Die Brackwasserfauna. *Verh. Dtsch. Zool. Ges.* **36,** 34-74.

Rosenthal Y. and Katz A. (1989) The applicability of trace elements in freshwater shells for paleogeochemical studies. *Chemical Geology* **78,** 65-76.

Russell L.S. (1932) Mollusca from the McMurray Formation of Northern Alberta. *Proceedings and Transactions of the Royal Society of Canada* **27,** 37-42.

Samson S.D. and Patchett P.J. (1991) The Canadian Cordillera as a modern analogue of Proterozoic crustal growth. *Austrailian Journal of Earth Science* **38,** 595-611.

Skougstad M.W. and Horr C.A. (1963) Occurrence and distribution of strontium in natural water. *Geol. Sur. Water-Supply Paper* **1496-D,** 55-97.

Stumm W. and Morgan J.J. (1981) *Aquatic Chemistry.* John Wiley and Sons.

Tarutani T. , Clayton R.N. and Mayeda T.K. (1969) The effect of polymorphism and magnesium substitution on oxygen isotope fractionation between calcium carbonate and water. *Geochimica et Cosmochinica Acta* **33,** 987-996.

Taylor S.R. and McLennan S.M. 1985. *The Continental Crust: its Isotopic Composition and Evolution* . Blackwell Scientific Publications.

Thomas R.G., Smith D.G., Wood J.M., Visser J., Calverly-Range E.A. and Koster E.H. (1987) Inclined heterolithic stratification–terminology, description, interaction and significance. *Sedimentary Geology* **53,** 123-179.

Thompson T.G. and Chow T.J. (1955) The strontium–calcium ratio in carbonate secreting marine organisms. *Deep-Sea Research* **3,** 20-39.

Turekian K.K. and Armstrong L. (1960) Magnesium, strontium and barium concentrations and calcite aragonite ratios of some recent molluscan shells. *Journal of Marine Research* **18,** 133-151.

Wadleigh M.A, Veizer J. and Brooks C. (1985) Strontium and its isotopes in Canadian rivers. *Geochimica et Cosmochimica Acta* **49,** 1727-1736.

Wanklyn R.P. (1985) Stratigraphy and depositional environments of the Ostracode member of the McMurray formation (Lower Cretaceous; Late Aptian-Early Albian) in west-central Alberta. M.Sc. dissertation Univ. of Colorado.

Weber J.N., Williams E.G. and Bergenback R.E. (1965) Stable isotopes of carbon and oxygen in basin analysis. In *Stable isotopes in oceanographic studies and paleotemperatures* (ed. E. Tongiorgi), pp. 285-296. Consiglio Nazionale Delle Ricerche, Spoleto.

Williams G.D.C. (1960) The Mannville Group, Central Alberta. Ph.D. dissertation Univ. of Alberta.

Yurtsever Y. and Gat J.R. (1981) Atmospheric waters. In *Stable Isotope Hydrology, Deuterium and Oxygen-18 in the Water Cycle* (Ed. J.R. Gat and R. Gonfiantini), pp. 103-142. Technical Reports Series No. 210. International Atomic Energy Agency, Vienna.

Zaitlin B.A., Dalrymple R.W., Boyd R. and Leckie D. (1994) The stratigraphic organization of incised valley systems: Implications for hydrocarbon exploration and production. In *Short Course Notes,* Canadian Society of Petroleum Geologists Annual Meeting.

Chapter 7

CONCLUSIONS

Isotopes can be used in a variety of ways to solve very specific problems concerning the origin, mixing and ultimate fate of ancient water masses. As the studies of this dissertation have shown, the isotope systems employed and the proxy materials used can vary widely. Predictably, the use of bentonites as time-planes will have wide application in paleoceanography because *environmental* changes can occur on timescales that are too fine to be resolved by geochronology or biostratigraphy. Sequence stratigraphic methods also show much promise as a means of providing control over regional correlation. Future advances in the paleoceanography of Paleozoic and older systems will likely involve new proxy materials for analysis and controls on the dimension of time.

The main conclusions of this dissertation are summarized in point form,

1. Ancient epeiric seas were restricted from mixing with contemporaneous deep oceans.
   –internal water masses within epeiric seas were restricted from mixing with each other!
2. Secular isotope curves for Nd, C and O may be influenced by factors operating within the epeiric sea environment.
3. The use of bentonites as time planes will have wide application in isotopic paleoceanography as a means of controlling the dimension of time.
4. The Ostracode Sea was lake!
5. The $\delta^{18}O$ of Proterozoic seawater was 0‰!
   –seafloor spreading operated in the Proterozoic.
6. Most biogenic apatites are unreliable recorders of ancient seawater $^{87}Sr/^{86}Sr$.
   –conodont taxa consisting of 100% crown material show much promise as a recorder of seawater $^{87}Sr/^{86}Sr$, especially if a leaching protocol is adopted.
   –all biogenic apatites are potentially reliable recorders of seawater $^{143}Nd/^{144}Nd$.
7. Conodonts are heterogeneous with respect to their trace element distributions.
8. The diagenesis of conodonts is completely analogous with the diagenesis of vertebrate bone and teeth.
9. Paleosalinities may be determined in the ancient seawater-freshwater mixing zone with knowledge of the Sr isotope paleohydrology recorded in carbonate fossils and limestones.
10. Combining $^{87}Sr/^{86}Sr$ with Sr/Ca ratios has wide application in paleohydrology as a tracer of origins and mixing of ancient water masses.